Interim Report For The Upper Mississippi River – Illinois Waterway System Navigation Study

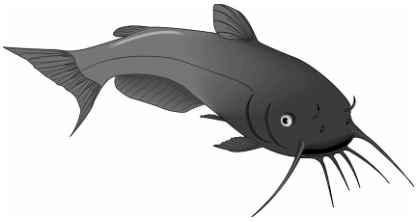

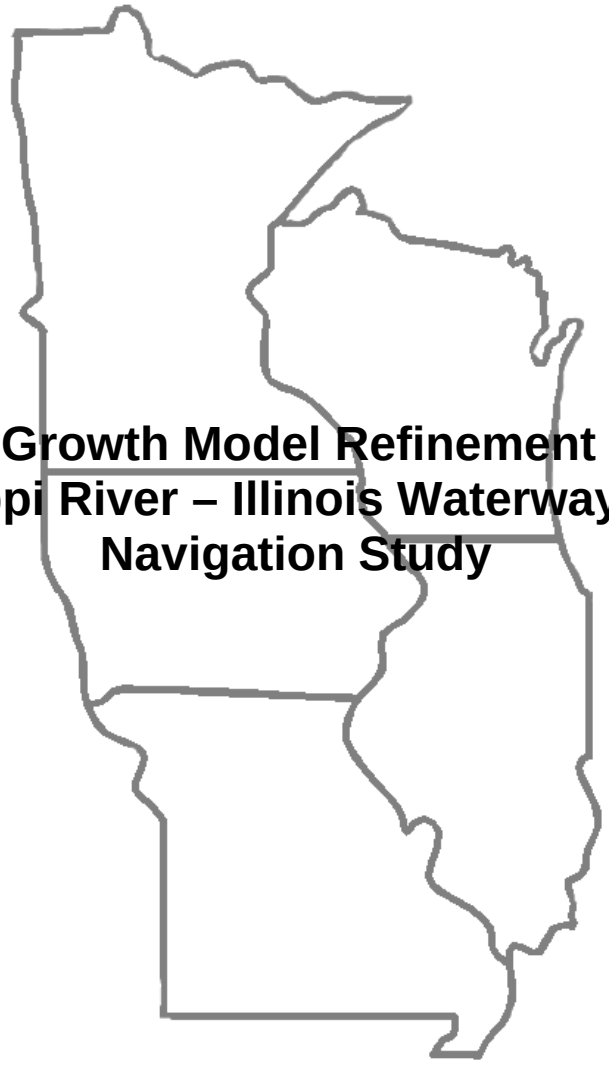

Aquatic Plant Growth Model Refinement for the Upper Mississippi River – Illinois Waterway System Navigation Study

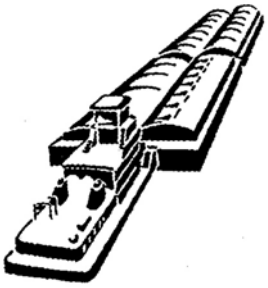

US Army Corps of Engineers®

September 2005

Rock Island District
St. Louis District
St. Paul District

Upper Mississippi River - Illinois Waterway System Navigation Study

ENV Report 51
September 2005

Aquatic Plant Growth Model Refinement for the Upper Mississippi River – Illinois Waterway System Navigation Study

Elly P. H. Best, Gregory A. Kiker, Beth Anne Rycyzyn

Environmental Laboratory
U.S. Army Engineer Research and Development Center
3909 Halls Ferry Road
Vicksburg, MS 39180-6199

Kevin P. Kenow, Jim Fischer

Upper Midwest Environmental Sciences Center, U.S. Geological Survey
2630 Fanta Reed Road
La Crosse, WI 54650

Shyam K. Nair

The Cadmus Group, Inc.
78a Mitchell Road
Oak Ridge, TN 37830

Daniel B. Wilcox

U.S. Army Corps of Engineers, St. Paul District
190 5th Street East
St. Paul, MN 55101

Interim report

Prepared for U.S. Army Engineer District, Rock Island
Rock Island, IL 61204-2004
U.S. Army Engineer District, St. Louis
St. Louis, MO 63103-2833
U.S. Army Engineer District, St. Paul
St. Paul, MN 55101-1638

ABSTRACT: Simulation models have been developed for two submersed plant species that reproduce vegetatively through tubers. These two species, American wildcelery (*Vallisneria americana*), a meadow former, and sago pondweed (*Potamogeton pectinatus*), a canopy former, represent the characteristic life forms of submersed aquatic vegetation in the Upper Mississippi River System (UMRS). The models simulate growth in an established plant bed and are based on carbon flow through the vegetation rooted in meter-squared (m^2) water columns. The models take into account the effects of changes in (1) water depth, (2) shading by seston, (3) self-shading, and (4) temperature on plant biomass formation.

For application to the UMRS, the models were expanded with equations enabling calculation of the effects of current velocity and shading by epiphytes on biomass production. Calibration data for these equations were derived from new field data collected in 2002. The effects of current velocity on plant biomass of American wildcelery were quantified in a study on the Red Cedar River, WI. Potential shading by epiphytes of wildcelery and sago pondweed was quantified using field data collected in UMRS Pools 8 and 13. The self-shading coefficient of sago pondweed beds in the UMRS was measured in Pool 8, was higher than the model default value determined in more clear water, and allowed a higher light capture. A new field data set on shoot biomass of both species and environmental factors, all collected at the same selected sites in UMRS Pools 8 and 13 in 2001 and 2002, was used for model validation.

Output generated by the refined plant growth models agreed with the measured data, in that the model output generated for several sites in Pool 8 was within the range of the measured values. Simulated plant development was slightly delayed compared to local plant development in wildcelery, but matched in sago pondweed. Increased current velocity and shading by epiphytes decrease plant biomass. The combined biomass-decreasing effect is expected to be strongest at sites with a high current velocity. Current velocities $\geq$ 0.94 m s^{-1} prevent growth of both species.

Simulated plant density in established beds of both plant species, to which the default model input values pertain, is relatively constant. In one-year runs, simulated plant biomass was sensitive to initial values of tuber density and size, which may deviate from the default values. Simulated biomass from runs started at the default tuber bank density and tuber size agreed with the measured plant biomass of wildcelery. However, simulated biomass from runs started at default values consistently over-predicted measured plant biomass of sago pondweed, leading us to believe that in UMRS Pool 8 this vegetation starts from a far lower tuber density (in the order of 10 m^{-2}) than default (240 m^{-2}) – possibly because of the high grazing pressure by waterfowl. Comparison of simulated and measured data was greatly impeded by (1) large variability in measured plant biomass data, (2) lack of measured plant growth curves, tuber density and tuber size, and (3) relative scarcity of measured environmental data requiring large-scale interpolation and derivation of values pertaining to other sites within the same water body. The refined models can be used to explore effects of changes in existing river management practices that affect the physical environment for submersed aquatic plants, and to implement operational scenarios aimed at conserving and establishing submersed aquatic vegetation. Grazing can be introduced in the simulations by decreasing the initial tuber bank density and/or removing shoot biomass at various water depths during the growth season.

Contents

List of Figures

List of Tables

Preface

The work reported herein was conducted as part of the Upper Mississippi River – Illinois Waterway (UMR – IWW) Navigation Study. The information generated for this technical report will be used in risk assessment for the effects of increased navigation traffic on aquatic plants in channel borders of the Mississippi River.

The UMR – IWW Navigation Study is being conducted by the U.S. Army Engineer Districts of Rock Island, St. Louis, and St. Paul under the authority of Section 216 of the Flood Control Act of 1970. Commercial navigation traffic is increasing and, in consideration of existing system lock constraints, will result in traffic delays that will grow in the future. The system navigation study scope is to examine the feasibility of navigation improvements to the Upper Mississippi River and Illinois Waterway, to reduce delays to commercial navigation traffic, and to manage a sustainable river ecosystem. The study will determine the location and appropriate sequencing of potential navigation improvements and management actions to protect and restore the river ecosystem through the year 2050. The final product of the System Navigation Study will be a Feasibility Report and Environmental Impact Statement.

The Principal Investigator for this research was Dr. Elly P.H. Best, Environmental Risk Assessment Branch (ERAB), Environmental Processes and Engineering Division (EPED), Environmental Laboratory (EL), U.S Army Engineer Research and Development Center (ERDC), Vicksburg, MS. Dr. Best prepared this report and was responsible for experimental and modeling work. The environmental studies were conducted on the Red Cedar River in Wisconsin and the Upper Mississippi River in Wisconsin and Iowa. Mr. Kevin P. Kenow of the U.S. Geological Survey, Upper Midwest Environmental Science Center (UMESC) contributed to the experimental design and logistics for the experiments. Ms. Beth A. Rycyzyn, ERAB, EPED-EL conducted field and laboratory work. Mr. James Fisher of the Wisconsin Department of Natural Resources, Onalaska, WI, provided water quality and other environmental data.
Dr. Gregory A. Kiker, ERAB, EPED-EL, and Dr. Shyam K. Nair of The Cadmus Group, Inc., Oak Ridge, TN, participated in the evaluation of the plant growth model performance. Mr. Daniel Wilcox of the St. Paul District, Corps of Engineers, served as technical coordinator for the aquatic plants work for the Navigation Study. Drs. David Soballe and Michael Smart, Environmental Processes and Effects Branch (EPEB), EPED, ERDC-Vicksburg; and David Spencer, USDA-ARS, Davis, CA, and Rick Wortelboer, Netherlands Environmental Assessment Agency of the National Institute for Public Health and the

Environment, The Netherlands, provided Technical Reviews of earlier drafts of this report.

This investigation was performed under the direct supervision of Dr. Lance D. Hansen, Chief, ERAB, and the general supervision of Dr. Richard E. Price, Chief, EPED. Dr. Ed Theriot was Director, EL, ERDC. Mr. Robert C. Gunkel, Jr., EL, ERDC, was responsible for coordinating the necessary activities leading to publication.

At the time of publication of this report, COL James R. Rowan, EN, was Commander and Executive Director of ERDC. Dr. James R. Houston was Director.

1 Introduction

The Upper Mississippi-Illinois Waterway System, Navigation Traffic, and Navigation Related Stresses Imposed on Aquatic Plants

The Mississippi River is an integral part of our American heritage, a unique resource, and a good example of a river used for many purposes in the United States. The Mississippi River, with a drainage basin of almost 4 million km^2, is one of the largest and most productive ecosystems in the world (Holland-Bartels et al. 1990). The river above the confluence of the Ohio River is commonly called the Upper Mississippi River (UMR) and includes almost 500,000 km^2 of watershed in five states (Figure 1; Holland-Bartels et al. 1990). The UMR, including the Illinois Waterway (IWW) and several important tributaries (Figure 1), is designated both a nationally significant ecosystem and a nationally significant navigation system; it is the only inland river in the U.S. to have such a designation. Several units of the National Wildlife Refuge System exist along the river corridor. In addition, wetland habitats within the UMR support millions of migratory birds each year during autumn and spring migrations (Wiener et al. 1998).

Navigation on the UMR – IWW System began in the 1820s, when Congress authorized navigation improvements by the Corps of Engineers. These improvements included the removal of snags and other obstructions in several locations of the Mississippi River and the construction of a canal connecting Lake Michigan to the Illinois River (Fremling and Claflin 1984). Several navigation improvement projects, such as the excavation of rocks, closing off sloughs, construction of the 4.5-foot navigation channel, and construction of the 6-foot navigation channel, continued through the early 1900s. Projects creating the current 9-foot navigation channel were authorized in the 1930s, and by 1940, most had been completed by the U.S. Army Corps of Engineers (USACE) (Fremling and Claflin 1984). Twenty-nine locks and dams on the Mississippi River and eight on the Illinois River replaced the rapids and falls with a series of terraced pools for commercial and recreational traffic (Figure 1). Habitats in a typical pool include a braided channel in the upper pool, a lotic area at the head of the pool, and a lentic area above the impounding lock and dam (Van Vooren 1983). Barge traffic transports a wide variety of essential goods on the UMR – IWW System, such as agricultural commodities, petroleum products, and coal.

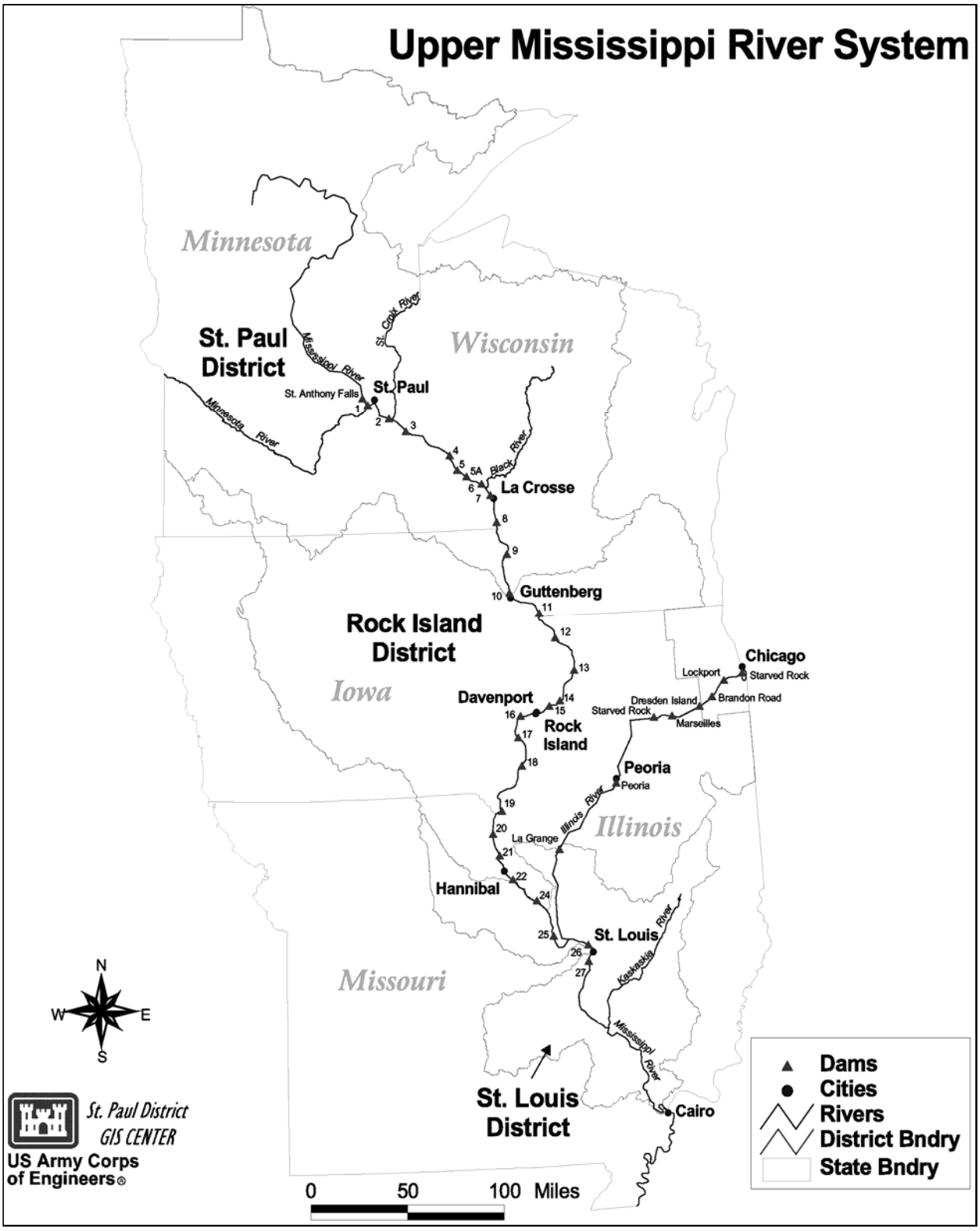

Figure 1. The Upper Mississippi River – Illinois Waterway System. Numbers indicate dams and accompanying pools

Estimates indicate that the transport of commodities (commercial navigation traffic) on the river system could significantly increase in the future (Holland 1986; Holland-Bartels et al. 1990). Direct impacts on submersed aquatic plants that could result from a passing tow include breakage or uprooting of plants due to changes in current velocity and waves produced by the commercial tows as they pass. Possible indirect impacts include the reduction in plant growth and/or vegetative reproduction caused by the decrease in available underwater light because of resuspension of nearshore sediments caused by passing tows throughout the growing season.

Application of Models in Ecological Risk Assessment

A Submersed Aquatic Plant Ecological Risk Assessment is being carried out as part of the Upper Mississippi River System - Illinois Waterway System Navigation Study (Bartell et al. 2000). The purpose of this study is to assess the incremental impact of increased commercial navigation traffic from 2000 to 2050 (in 10-year increments) on submersed aquatic plants on the channel borders of the UMR – IWW System. Backwaters are not included in this risk assessment because of the absence of data on ambient suspended sediment concentrations in backwaters and the difficulty to relate traffic increases to changes in suspended sediment in backwaters. This assessment will meet the technical requirements of the National Environmental Policy Act (NEPA), but is being conducted and organized in a manner consistent with the framework for ecological risk assessment recommended in the Guidelines for Ecological Risk Assessment developed by the United States Environmental Protection Agency (USEPA) (1998). The USEPA framework was developed to promote consistent approaches to ecological risk assessment, identify key issues to be addressed in assessments, and standardize risk assessment terminology (Bartell 1996). The framework identifies three components of an ecological risk assessment process: problem formulation, analysis (characterization of exposure and characterization of ecological effects), and characterization of risk.

In the problem formulation component, the disturbance or stressor is identified, the subject or ecological effects (commonly referred to as endpoints) of the risk assessment are defined, and the scope and scale of the ecological risk assessment are presented. In the characterization of exposure, the frequency, magnitude, extent, and duration of the disturbance are described. In the risk characterization component, the available information and data are integrated, the risks are estimated, and the uncertainties and their assessment implications are identified and estimated (USEPA 1998; Bartell et al. 2000).

In the current ecological risk assessment procedure, the problem formulation entails increased suspended sediments expected to result from increased commercial traffic that can decrease the amount of light available for photosynthesis of submersed aquatic plants, with subsequent decreases in growth and reproduction of these plants. This assessment requires (1) characterizing baseline and increased commercial traffic intensity for specified UMRS sites, (2) relating commercial tows at specified UMRS sites to a time series of suspended sediment

concentrations, (3) translating the increased sediment concentrations to reductions in available light within the water column, and (4) simulating the effects of reduced light availability on submersed plant growth and reproduction. Economic projections of demand for commodity transport and commercial traffic rates on the UMRS are being developed. This same risk assessment approach is also used to assess the effects of recreational boat traffic on submersed aquatic plants on the channel borders of the UMRS. A forecast of recreational boat traffic on the UMRS has been prepared (Carlson et al. 2000).

A rule-based conceptual model was developed to assess the direct physical impacts on submersed aquatic plants caused by currents and waves resulting from commercial navigation. Hydraulic effects resulting from a passing commercial tow were calculated using a physical forces model, NAVEFF (Maynord 1999). These calculations have been used to delineate areas where rules are exceeded within the potential submersed plant habitat coverage in the UMR – IWW System, and where physical forces resulting from a passing commercial tow would prevent the occurrence of submersed aquatic plants.

Two aquatic plant growth simulation models are being used to assess the indirect impacts on submersed plant growth and vegetative reproduction caused by the decrease in available underwater light because of resuspension of nearshore sediments caused by tows throughout the growing season (Bartell et al. 2000; Best et al. 2001). The models pertain to American wildcelery (*Vallisneria americana*) and sago pondweed (*Stuckenia pectinata*) (Best and Boyd 2001a,b; Best and Boyd 2003a,b), both species representing the predominant submersed aquatic plant life forms and widely distributed in the UMR – IWW System (Tyser et al. 2001). Since all literature pertaining to *Stuckenia pectinata* is listed under the plants' name *Potamogeton pectinatus* used up to 2000, *Potamogeton pectinatus* is further used in this report. The models take into account the effects of changes in (1) water depth, (2) shading by seston, (3) self-shading, and (4) temperature on plant biomass formation. For application to the UMRS, the models had to be expanded with equations describing effects of current velocity and shading by epiphytes on biomass production.

Objectives Current Study

The objective of the current study is to assess the requirements for application of two aquatic plant growth simulation models pertaining to American wildcelery and sago pondweed to the UMR, expand and recalibrate the models where needed, and evaluate model application to field sites in the UMR for which both plant biomass and environmental data were collected in 2001 and 2002. The refined models are translated in a Visual Basic framework.

2 Aquatic Plant Growth Models: Initial Performance and Improvements Suggested

Aquatic Plant Growth Models Used

The two simulation models that we developed to predict growth of American wildcelery (VALLA, Version 1.0) and of sago pondweed (POTAM, Version 1.0) are summarized below. These models focus on processes that affect plant carbon gain. Growth limitation by phosphorus and nitrogen has not yet been incorporated into these models due to lack of evidence for growth limitation by these nutrients in the water bodies concerned. Annual average levels of phosphorus and nitrogen in UMR Pool 8 were as follows: total-P 0.13 mg L^{-1} in 2001 and 2002, total-N 2.34 mg L^{-1} in 2001 and 2.59 mg L^{-1} in 2002, (NO_2+NO_3)N 1.67 mg L^{-1} and 1.82 mg L^{-1} in 2002 (Above Dam 8 site, Station M679.5V; LTRMP). Although considerable information on the nutrition of submersed plants is available, it remains difficult to predict submersed plant growth based on sediment nutrient availability alone. It appears that tissue N:P ratios rather than tissue-N or tissue-P concentrations are determinants of submersed plant growth (Best et al. 1996; Spencer and Ksander 2003). The models have been published elsewhere (Best and Boyd 2001a,b; Best and Boyd 2003a,b). The parameter values of these models are presented in Appendix A, Tables 1 and 2.

Both wildcelery and sago pondweed are rooted, tuber-forming, submersed aquatic plants native to North America, and have similar phases in their phenological cycles. The species differ greatly in their geographical distribution, and in their growth habits in terms of the vertical distribution of biomass within the water column. American wildcelery occurs typically in circum-neutral fresh to slightly saline water, with an alkalinity ranging from 0-300 mg L^{-1}, at depths of 0.1 to 7 m, and rooted in a variety of sediment types. It occurs in eastern North America from Nova Scotia to northern parts of Mexico, and in Arizona (Best and Boyd 2001a). Wildcelery has a basal rosette of leaves that may extend to the water surface, with over 60 percent of its biomass distributed in the lower 0.3-m of the water column. Sago pondweed is common in fresh, alkaline to slightly saline water, with a high alkalinity and pH>6, at depths of 0.1 to 7 m, and rooted in sediment types varying from bedrock to mineral bottoms with particle size

ranging from rubble to fine clay (Best and Boyd 2003a). It is cited in the American continent from Quebec and Newfoundland to South America. It is native to the western United States, and was probably introduced into Florida. Its occurrence has also been documented in Western Europe, the Russian Federation, and in subtropical and tropical areas in India. Sago pondweed is a typical canopy-former with over 60 percent of its biomass distributed in the upper portion of the water column.

The models reported here can be used to quantify the impacts of changes in important environmental factors on the dynamics of populations of submersed plant species, distinguished on the basis of their phenology and morphology. The effects of the following environmental factors can be explored using the model Versions 1.0:

a. Climate (site irradiance and air temperature)

b. Water depth

c. Transparency

d. Temperature

e. Wave action (removal of shoot biomass from the water surface to a specified water depth)

f. Grazing (removal of shoot biomass from the water surface to a given water depth, or removal of subterranean tubers)

Each model uses input files that detail plant characteristics and environmental conditions that can be changed by the user. Numeric model output is provided and graphics can be viewed within a user-friendly shell. Executable FORTRAN programs and user manuals are available (Best and Boyd 2001b, Best and Boyd 2003b).

The models simulate growth of a monotypic (single species) submersed plant community, including roots and tubers under ample supply of nitrogen and phosphorus in a pest-, disease- and competitor-free environment under the prevailing weather conditions. At least one plant cohort waxes and wanes each growth season in climates ranging from temperate to tropical. The modeled rate of dry matter accumulation is a function of irradiance, temperature, CO_2 availability, and plant characteristics. Light attenuation by epiphytes was not incorporated in the Versions 1.0. The rate of CO_2 assimilation (photosynthesis) of the plant community depends on the radiant energy absorbed by the canopy, which is a function of incoming radiation; reflection at the water surface and attenuation by the water column; attenuation by the plant material; and leaf area of the community. The daily rate of gross CO_2 assimilation of the community is calculated from the absorbed radiation, the photosynthetic characteristics of individual shoot tips, and the pH-determined CO_2 availability.

A fraction of the carbohydrates produced is used to maintain the existing plant biomass. The remaining carbohydrates are converted into structural dry matter (plant organs). In the process of conversion, part of the mass is lost as respiration. The dry matter produced is partitioned among the various plant organs using partitioning factors defined as a function of the plants' phenological

cycle. The dry mass of the plant organs is obtained by integration of the growth rates over time. The plants winter either as a system composed by rooted plants and subterranean tubers or tubers alone. Environmental factors and plant characteristics vary with depth. Therefore, the model partitions the water column and the associated plant-related processes into 0.1-m depth layers. All calculations are performed on an m^2 basis.

The models use input files that specify standard physiological properties, initial plant and tuber biomass, and water temperature. These input files can be changed by the user to reflect conditions at the study site. The models run at a daily time step for periods of 1 to 5 years.

Development and phenological cycle

The phenology of the plant community, for which the development phase is used as a measure, is modeled as a sequence of processes that take place over a period of time, punctuated by more or less discrete events. Development phase (DVS) is a state variable in the models. The DVS is dimensionless and its value increases gradually within a growing season. The development rate (DVR) has the dimension d^{-1}. The multiple of rate and time period yields an increment in phase. The response of DVR to temperature in the model is in accordance with the degree-day hypothesis (Thornley and Johnson 1990). Calibration according to this hypothesis allows for use of the model for the same plant species at other sites differing in climate (temperature regime). The relationships between the development phase, the day-of-year, and 3 °C day-degree sum for a temperate climate are presented in Appendix A, Table 3 for wildcelery and in Table 4 for sago pondweed.

Wintering and sprouting of wintering organs, and growth of sprouts to water surface

Modeled plant growth is initiated at a specified developmental phase, and a fixed number of plants develop through conversion of carbohydrates from hibernating organs (tubers, plants, or both) into plant material. The developmental phase and plant density (number of plants per m^2) are species-specific characteristics (Appendix A, Tables 3 and 4). Plant density is presumed to be constant throughout the year. This presumption is based on estimates of density of adolescent plants in the field, that indicate narrow density ranges for both species (Titus and Stephens 1983, Doyle 2000, Best and Boyd 2003a, Van Wijk 1989). It is possible that late in the growing season, density increases somewhat through emergence of rosettes or shoots from stolons, but the role of these organs in biomass production and population survival is deemed negligible because of their low carbon gain (shaded by neighbor plants), and absence or low production of small-sized tubers. Small-sized tubers have low survival value for both species. The dormant period is considerably longer in wildcelery than in sago pondweed, providing a relatively longer period for new plant establishment for sago pondweed. Remobilization proceeds until the tubers are depleted. Once a specified plant height has been reached (1.2 m or the water surface in wildcelery; the water surface in sago pondweed), plant mass is distributed following a fixed

pattern with a species-characteristic shape. Given the initial tuber mass, sprouts can elongate only a certain distance on these reserves. If net photosynthesis after this elongation period is negative for 23 consecutive days in wildcelery or for 27 days in sago pondweed, the sprouts are presumed to die. Larger tubers have longer survival periods, while smaller tubers have shorter survival periods. The next tuber class can sprout subsequently, provided floral initiation has not yet been reached, and temperature is within the range of 5-25 °C in wildcelery and DVS>0.211 in sago pondweed. In the elongation phase, shoot biomass is distributed equally over the successive 0.1-m depth layers, with each layer growing after the preceding layer achieves a minimum shoot biomass. After reaching maximum shoot height, biomass is distributed according to the species-characteristic spatial distribution (pyramid-shaped in wildcelery, umbrella-shaped in sago pondweed). A relational diagram illustrating wintering and sprouting of tubers is presented in Figure 2.

Light, photosynthesis, and growth

The measured daily total irradiance (wavelengths of 300-3000 nm), and maximum and minimum temperatures of the site are used as input for the model in the form of a separate weather file. Only half of the irradiance reaching the water surface is presumed to be photosynthetically active radiation (PAR) and 6 percent of the remaining PAR is presumed to be reflected by the water surface.

In the models, daily irradiance in the water column is attenuated following the Lambert-Beer law. Although subsurface irradiance is attenuated by both color and particles within the water column, no distinction between these factors has been made, and one site-specific light extinction coefficient accounts for sub-surface attenuation. The vertical profiles of light within the vegetation layers also are characterized, and the light absorbed by each horizontal vegetation layer is derived using these profiles. The plant community-specific extinction coefficient, *K*, is presumed to be constant throughout the year and is 0.0235 m^2 g DW^{-1} for wildcelery and 0.095 m^2 g DW^{-1} for sago pondweed (Titus and Adams 1979a, Best and Boyd 2003a).

Instantaneous gross photosynthesis (*FGL* in g CO_2 m^{-2} h^{-1}) in the models depends on the standing crop per depth layer *i* (SC_i in g DW m^{-2} layer $^{-1}$); the photosynthesis light response of individual shoot apices at ambient temperature (*AMAX* in g CO_2 g DW^{-1} h^{-1}); the initial light use efficiency (*EE* in g CO_2 J^{-1} absorbed); the absorbed light energy (*IABSL* in J m^{-2} s^{-1}), and temperature (°C, relative function *AMTMPT*). The photosynthesis light response of leaves is described by the exponential function

$$FGL_i = SC_i \cdot AMAX \left[1 - \exp\left(\frac{-EE \cdot IABSL_i \cdot 3600}{AMAX \cdot SC_i}\right)\right] \quad (1)$$

For photosynthetic activity at light saturation and optimum temperature (*AMX*), the values of 0.0165 g CO_2 g DW^{-1} h^{-1} for wildcelery and 0.019 g CO_2 g DW^{-1} h^{-1} for sago pondweed were used (Titus and Adams 1979a; Van der Bijl et al. 1989). The photosynthetic activity at ambient temperature (*AMAX*) is

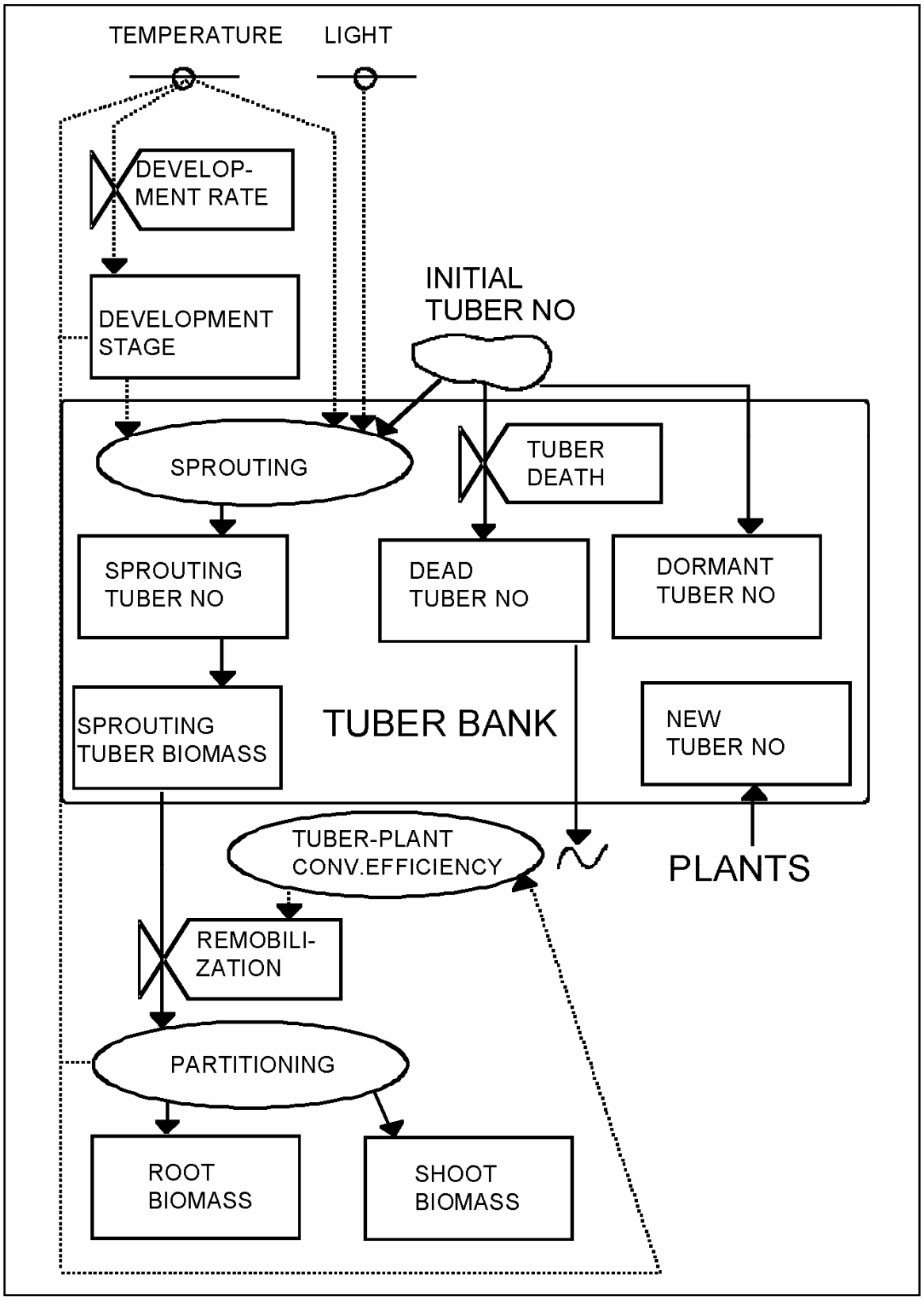

Figure 2. Relational diagram illustrating the wintering and sprouting of tubers

calculated proportionally from the photosynthetic activity at optimum temperature using a relative function fitted to data for wildcelery (Titus and Adams 1979a) and sago pondweed (Best and Boyd 2003a). For photosynthetic light use efficiency (*EE*) a value of 11.10^{-6} g CO_2 J^{-1}, typical for C_3 plants is used (Penning de Vries and Van Laar 1982a, b). Substituting the appropriate value for the absorbed PAR yields the assimilation rate for each specific shoot layer.

The instantaneous rate of gross assimilation over the height of the vegetation is calculated by relating the assimilation rate per layer to the community-specific biomass distribution and by subsequent integration of all 0.1-m-high vegetation layers. The daily rate of gross assimilation is then computed using a three-point Gaussian integration method (Goudriaan 1986; Spitters 1986).

Maintenance costs are calculated based on the chemical composition characteristic for plant organs, usually ranging from 0.010 to 0.016 g CH_2O g $AFDW^{-1}$ (Penning de Vries and Van Laar 1982a, b). Maintenance costs for the tubers are negligible. A temperature increase of 10 °C is assumed to increase maintenance respiration by a factor of about 2 (with a reference temperature of 30 °C; Penning de Vries and Van Laar 1982a, b).

Assimilates in excess of maintenance costs are converted into structural plant material. Growth efficiency and concomitant CO_2 evolution (= growth respiration) are accounted for using the assimilate requirement for growth. The assimilates required to produce one unit weight of plant organ are calculated from its chemical composition, and typical values are 1.46 g CH_2O g DW^{-1} for leaves, 1.51 for stems, and 1.44 for roots (Penning de Vries and Van Laar 1982; Griffin 1994).

As summarized in Equation 2 below, plant growth (*GTW* expressed as g DW m^{-2} d^{-1}) equals remobilized carbohydrates (*REMOB* in g DW m^{-2} d^{-1}, converted to g glucose m^{-2} d^{-1} by multiplication with CVT, a conversion factor of translocated dry matter into glucose) augmented with gross photosynthesis (*GPHOT*) and decreased by downward translocation (*TRANS*) and maintenance respiration (*MAINT*), all expressed as g glucose m^{-2} d^{-1}, divided by the assimilate requirement for plant biomass production (*ASRQ* expressed as g glucose g DW^{-1}).

$$GTW = \frac{\left[\left(REMOB \,.\, CVT\right) + GPHOT - TRANS - MAINT\right]}{ASRQ} \qquad (2)$$

The assimilate allocation pattern in plants (excluding tubers) is proportional to the biomass distribution pattern and depends on the physiological age. The typical patterns are followed when shoots have reached their maximum height and are 72 percent to leaves, 16 percent to stems, and 12 percent to roots in wildcelery (Haller 1974; Titus and Stephens 1983), and 73 percent of the total to leaves, 18 percent to stems, and 9 percent to roots in sago pondweed (Best and Boyd 2003a).

The vertical biomass distribution within the water column follows typical patterns, being pyramid-shaped in wildcelery with 78 percent of the shoot biomass in the lower 0.5 m of the water column (Titus and Adams 1979a), and

umbrella-shaped in sago pondweed with 78 percent of the shoot biomass in the upper 0.5 m of the water column (Best and Boyd 2003a). This entails the distribution of shoot biomass in the lower (wildcelery) or upper (sago pondweed) five 0.1-m vegetation layers according to a specific fitted function (*DMPC*) based on the respective species-characteristic shapes, followed by equal distribution of the remaining biomass over the remaining 0.1-m layers up to a total biomass share of 5 percent per layer and proportional distribution of the then-remaining biomass over all 0.1-m vegetation layers. A species-characteristic share of the total biomass is allocated to the roots, presumed to be situated in the upper 0.1 m of the sediment. The vertical biomass distribution pattern is recalculated and redistributed by the models when a rooting (=water) depth other than the nominal one is chosen. A relational diagram illustrating photosynthesis, respiration, biomass formation and senescence in the plants is presented in Figure 3.

Flowering, translocation, and senescence

Flowering affects metabolic activity of the modeled plants by initiating substantial downward translocation of assimilates to form tubers in both wildcelery and sago pondweed. Translocation and tuber formation have been formulated similarly for both species, but the parameter values are species-specific. In wildcelery, translocation occurs after flowering is initiated, at a day length <14.7 hours, and at a temperature between 5 and 25 °C (Titus and Stephens 1983, Donnermeyer and Smart 1985). Wildcelery tubers grow at a maximum rate of 24.7 percent of net production per day (Donnermeyer and Smart 1985). Translocation continues as long as plant biomass is greater than 0. In sago pondweed, translocation occurs after flowering is initiated, at a day length < 16 hours (Best and Boyd 2003a), and in a temperature between 5 and 25 °C (Spencer and Anderson 1987). Sago pondweed tubers grow at a maximum rate of 19 percent of net production per day (Wetzel and Neckles 1986), with remaining assimilates available for other processes.

Tuber production is based on the hypothesis that plants produce the largest possible tubers at their ambient light levels, because large tubers have the largest potential to survive future adverse low temperatures, low irradiance, and a short growth season. This hypothesis is supported by field data on sago pondweed (Van Dijk et al. 1992) and experimental data on wildcelery and sago pondweed (Doyle 2000). The variation in tuber size found in the field is attributed to the inability of the plants to complete the last tuber class with such a large tuber size. In the models, after reaching a given tuber size, all concurrently initiated tubers of that “class” are added to the tuber bank, and a new tuber class is initiated. A fixed, linear relationship was found in both species, indicating that the tuber number concurrently initiated increases with tuber size, with a smaller range for wildcelery than for sago pondweed (Figure 4).

Senescence is modeled by defining a death rate as a certain fraction of plant biomass per day when the conditions for growth deteriorate. The timing and values of relative death rates of plants have been derived from field observations on shoot biomass for wildcelery by Titus and Stephens (1983) and for sago pondweed by Best and Boyd (2003a). The timing was found by running the models repeatedly with different development rates, and base and reference

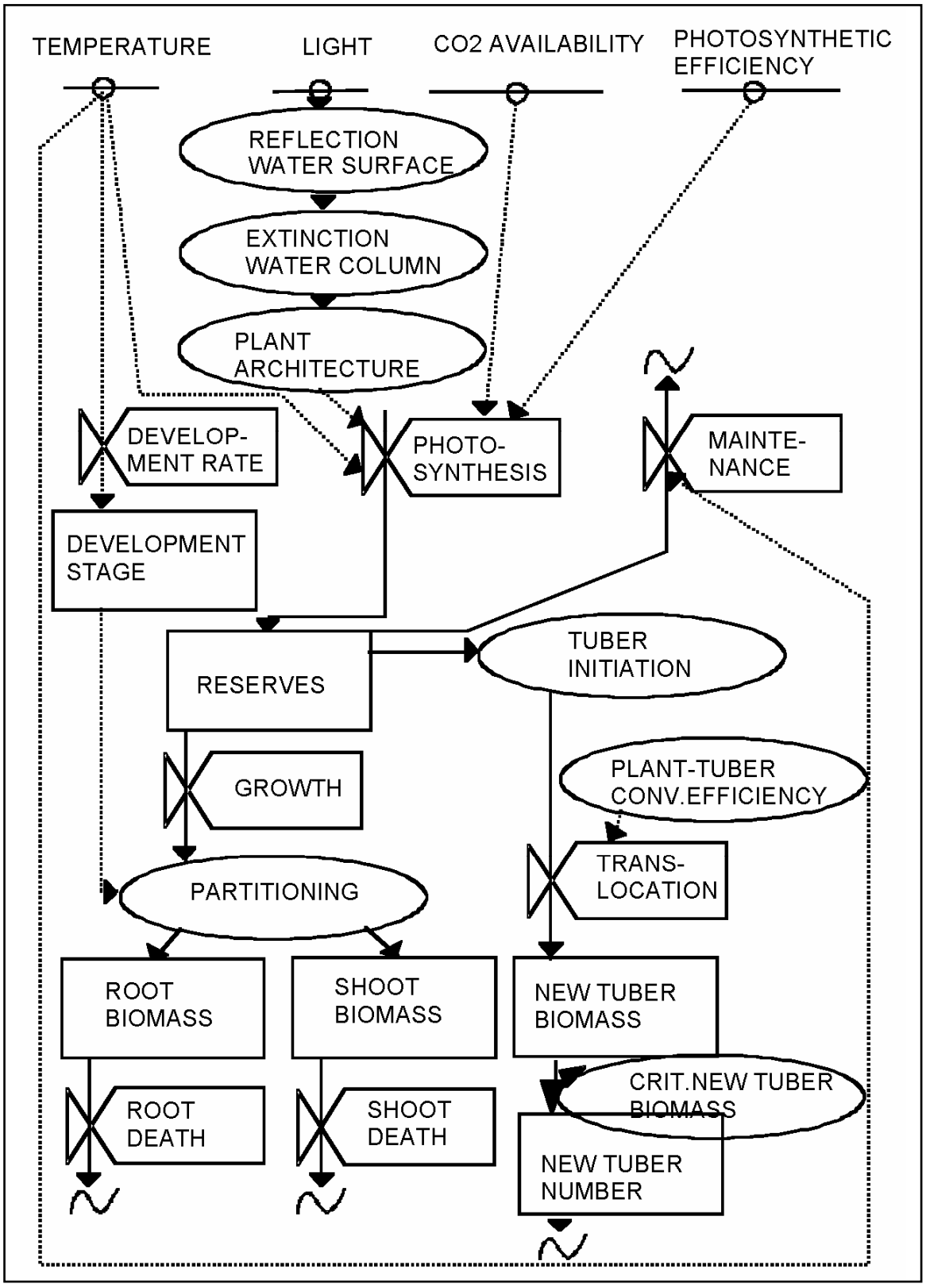

Figure 3. Relational diagram illustrating photosynthesis, respiration, biomass and tuber formation and senescence

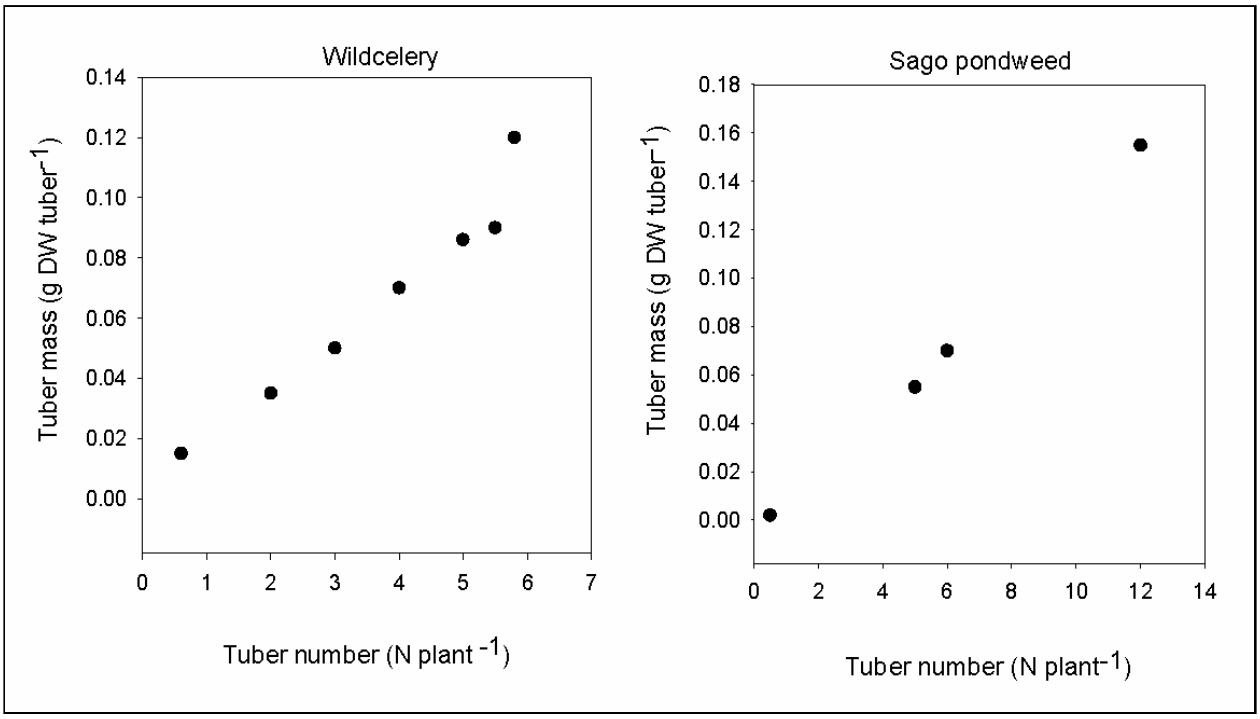

Figure 4. Relationship between tuber number concurrently initiated per plant and tuber mass

temperatures, until a realistic timing for decreasing shoot biomass occurred. Values for the relative death rates were found by applying the same differential equation that is commonly used for simple exponential growth to describe exponential decrease in biomass after flowering, with a negative specific decrease rate (Hunt 1982; Thornley and Johnson 1990). Following this approach, relative death rates of 0.021 g DW g DW^{-1} d^{-1} for wildcelery and of 0.047 g DW g DW^{-1} d^{-1} for sago pondweed were calculated. The timing and values of relative death rates for the tubers have been derived similarly from published data on tuber bank dynamics (Titus and Stephens 1983; Van Wijk 1989). Figure 3 illustrates translocation, tuber formation, and senescence in the models.

Initial model calibration and simulation results default runs

Initial calibration of both plant growth models was accomplished using data sets on plant biomass, and environmental and climatological parameters pertaining to sites in North America and The Netherlands, respectively. VALLA was calibrated on field data on wildcelery biomass and water transparency from Chenango Lake, New York (Titus and Stephens 1983), and climatological data from Binghamton (air temperatures) and Ithaca (irradiance), New York, 1978. POTAM was calibrated on field data on sago pondweed biomass and water transparency from the Western Canal near Zandvoort, The Netherlands (Best and Boyd 2003a), and climatological data from the nearby weather station at De Bilt (air temperatures and irradiance), The Netherlands, 1987. In general, simulated plant biomass compared well with average plant biomass measured.

For wildcelery, plant biomass reached its maximum at the same time, and peak biomass was somewhat higher in the simulated than in the measured plant community, notably 56.1 versus 50.1 g DW m^{-2} (Figure 5). The latter was attributed to the relatively large tuber size /concurrently initiated tuber number combination (0.09 g DW $tuber^{-1}$, 5.5 tubers $plant^{-1}$) used to initiate this nominal run. Measured tuber size was 0.055 g DW $tuber^{-1}$, and another model run starting with the measured tuber size generated a peak biomass of 48 g DW m^{-2}.

For sago pondweed, plant biomass reached its maximum 13 days later, and peak biomass was somewhat higher in the simulated than in the measured plant community (Figure 6). The slightly higher simulated biomass compared to the measured biomass was attributed to the use of air temperatures instead of the measured water temperatures in the model run, and/or the low frequency of field data collection. Air temperatures with a lag-period of seven days (default) were used because the temperature of the water surrounding the majority of the plant shoots in summer was closer to the air temperature than to the temperature of the canal water originating largely from upward seepage. The low frequency of field data collection yielded a maximum biomass value of 78.5 g DW m^{-2} at the end of July, while actual maximum plant biomass may have occurred at the end of August, as found for the sago pondweed population in the same canal but rooting at 2.5 m water depth (Best and Boyd 2003a).

Comparison Results of Original and Modified Models with Plant Biomass Values Measured in 1999, 2000, and 2001

Both models were tested first against field data collected in 1999 and 2000 at the UMR, and also against field data collected in 2001, after modification to include the effect of current velocity on biomass production, to identify strengths and weaknesses, and, if needed, to improve their predictive power by further modification and/or expansion.

Field data on plant biomass

Plant samples are collected annually by the UMESC according to a stratified random sampling design under the Long Term Resource Monitoring Program (LTRMP; Yin et al. 2000). In this program, plant biomass is harvested annually in mid summer at locations determined by a spatially stratified-random design within areas less than 3 m deep. Randomly selected sample sites are located by Universal Transverse Mercator (UTM) coordinates using a Global Positioning System (GPS) device. A field data set was available, collected in UMR Pool 8 in 1999 and 2000, comprised of biomass values of aquatic plants (g dry weight m^{-2}, various submersed and floating-leaved species). This field data set served as a source of information on common species-characteristic biomass values in UMR-Pool 8.

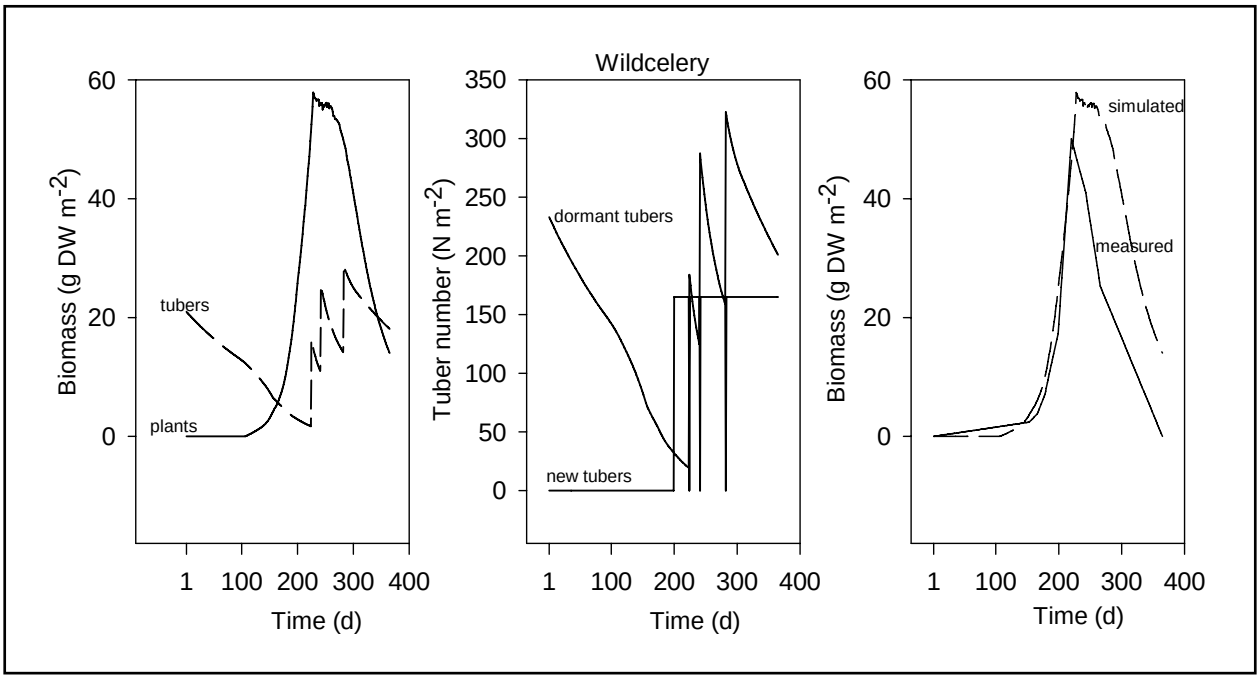

Figure 5. Simulated biomass of plants, dormant and new tuber numbers, and measured plant biomass of a wildcelery community in Chenango Lake, New York. Nominal run. Field data from Titus and Stephens (1983); climatological data 1987, Binghamton, New York (longitude 75^{o} 50' E, latitude 42^{o} 15'N); water depth 1.4 m; light extinction coefficient 0.43 m^{-1}

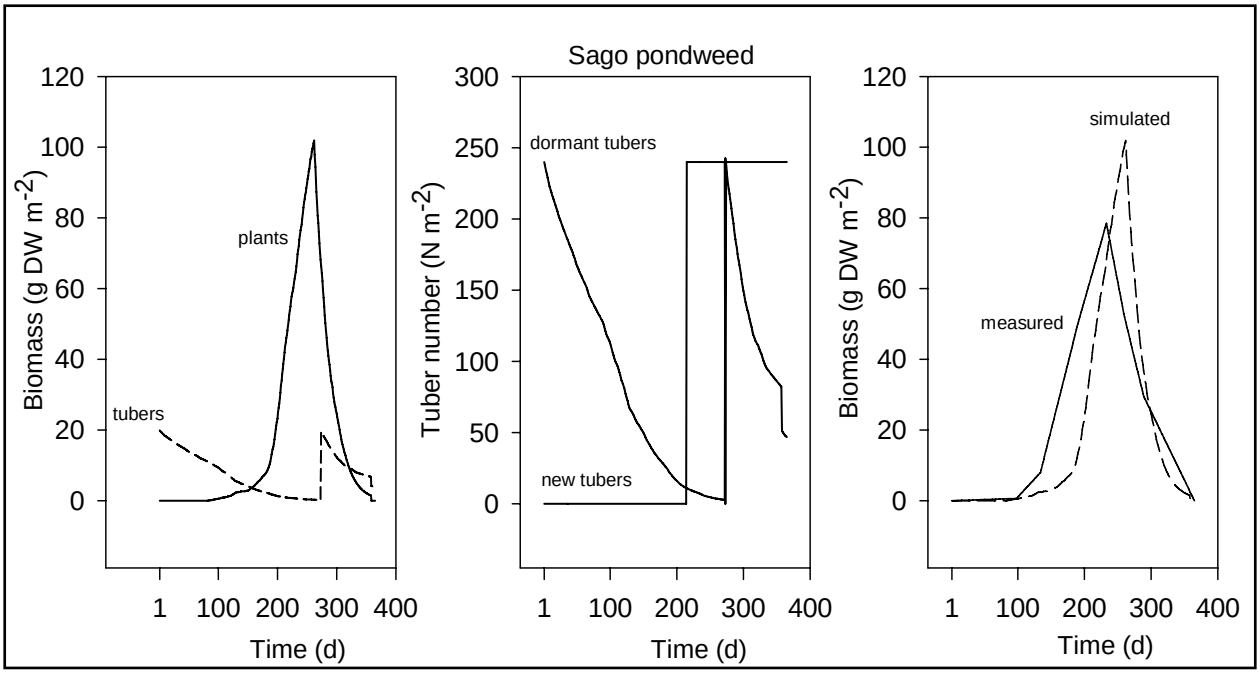

Figure 6. Simulated biomass of plants, dormant and new tuber numbers, and measured plant biomass of a sago pondweed community in the Western Canal near Zandvoort, The Netherlands. Nominal run. Field data from Best, Jacobs, and Van de Hagen (1987, unpubl.; In Best and Boyd 2003a); climatological data 1987, De Bilt, The Netherlands (longitude 05o 11' E, latitude 52o 06'N); water depth 1.3 m; light extinction coefficient 1.07 m-1

Of all 211-data collected in 1999-2000, only 13 percent (28 sites) was vegetated by wildcelery, 5 percent (11 sites) by sago pondweed, and 46 percent (98 sites) was barren, almost completely vegetated by emergent vegetation, temporary dry, terrestrial, or vegetated by terrestrial vegetation.

In 2001, plant biomass and environmental data were collected differently, i.e., at five selected water quality monitoring stations in UMR Pool 8 (stations Target Lake, Lawrence Lake, Lawrence Lake Marina, Turtle Island, and Above Dam 8-West side). At each station, up to five independent samples were collected, each composed of four quadrants. Of the biomass data collected in 2001, 16 values pertained to wildcelery and 23 values pertained to sago pondweed in Pool 8. All sites were located close to (maximum distance approx. 50 m) water quality monitoring stations.

Initial values model runs

The **original models Version 1.0** were run using default numbers as initial values for plant biomass and tuber bank characteristics since site data were missing. The default values are comprised in the data sets used for initial model calibration, originating for VALLA from Chenango Lake, New York (Titus and Stephens 1983) and for POTAM from the Zandvoort Canals, The Netherlands (at a latitude similar to that of Maine; Best and Boyd 2003a).

For **VALLA**, initial values were: plant biomass = 0, tuber bank density = 233 m^{-2}, tuber size 0.12 g DW $tuber^{-1}$ (reported by Donnermeyer and Smart (1985) for UMR-Pool 9) instead of the default value of 0.090 g DW $tuber^{-1}$.

For **POTAM**, initial values were: plant biomass = 0, tuber bank density = 240 m^{-2}, tuber size 0.155 g DW $tuber^{-1}$ (presuming that, like wildcelery, sago pondweed would be able to produce its maximum tuber size) instead of the default value of 0.083 g DW $tuber^{-1}$.

The **modified models Version 1.1** were also run using default numbers as initial values for plant biomass and tuber bank characteristics.

For **VALLA**, initial values were: plant biomass = 0, tuber bank density = 233 m^{-2}, tuber size 0.090 g DW $tuber^{-1}$.

For **POTAM**, initial values were: plant biomass = 0, tuber bank density = 240 m^{-2}, tuber size 0.083 g DW $tuber^{-1}$.

Environmental and climatological data

The site-specific, daily values for the required environmental factor input were generated as described below. An overview of the environmental data used as input for the simulations is presented in Table 1.

Table 1
Environmental Data Used as Input for the Simulations

Year	Environmental Data					
		Temperature				
	Irradiation	Air	Water	Water Depth	Light Extinction Coefficient	Current Velocity
1999	La Crosse, 1999	LC, 1999	-	Pool 8, 1999; interpolation between nearest gaging stations	Pool 8, 1999 (1 channel site)	Modeled hydrodynamics
2000	La Crosse, 2002	LC, 2000	-	Pool 8, 1999; interpolation between nearest gaging stations	Modeled from suspended sed. conc. Pool 8 (Copeland et al. 2001)	Modeled hydrodynamics
2001	La Crosse, 2002	-	Pool 8, 2001 (4 sites)	Pool 8, 2001 (4 sites)	Pool 8, 2001 (4 sites)	Pool 8, 2001 (4 sites)
2002	La Crosse, 2002	-	Pool 8, 2002 (3 sites) Pool 13, 2002 (1 site)	Pool 8, 2002 (3 sites) Pool 13, 2002 (1 site)	Pool 8, 2002 (3 sites) Pool 13, 2002 (1 site)	Pool 8, 2002 (3 sites) Pool 13, 2002 (1 site)

Water depth. For each site of harvest, water depth was calculated by linear interpolation in space between the values measured at the nearest USACE gauging stations in UMR Pool 8 in 1999. The water depth values calculated for the sites of harvest were corrected for differences in elevation between sites of harvest and gauging stations. Daily water depth values were derived by linear interpolation in time from these limited time series, composed by maximally 25 data pairs per site. The same approach was followed for data pertaining to subsequent years.

Light extinction coefficients. For data pertaining to 1999, the light extinction coefficients measured at one station just north of the channel in lower UMR Pool 8, near Stoddard, WI, were used (daily values period 10 June-10 September 1999; Sullivan 2000). Light extinction at this station was expected to be representative for lower Pool 8, i.e., for the areas with a fetch of 2-3 km, but not for the rest of this Pool. Water is expected to be more transparent at sites with a lower fetch, and far more turbid at sites with a higher fetch due to a higher wind-induced resuspension.

For data pertaining to 2000 and 2001, light extinction coefficients were calculated from modeled suspended solids concentrations. Suspended solids concentrations were converted into Secchi disk depths using Soballe's (Unpublished, 2001) regressions for UMR Pool 8, and Secchi disk depths were converted, in turn, into light extinction coefficients using the relationship of Giessen et al. (1990). This relationship, described by

$$\text{light extinction } (m^{-1}) = 1.65/\text{Secchi disk depth (m)}$$

was chosen, because it is valid for turbid, shallow water with a Secchi depth range of 0.5-2.0 m, similar to conditions found in the UMR – IWW system.

Current velocity. The following current velocity data were used. For 1999-2000, daily values resulting from hydrodynamic modeling (Copeland et al. 2000). From 2001 onwards, the current velocity values measured at the monitoring stations were used. Daily current velocity values were derived by linear

interpolation in time from the limited time series, composed by maximally 25 data pairs per site.

Weather data. Climatological data from La Crosse airport, Wisconsin (irradiance and air temperatures), were used in 1999 and 2000. From 2001 onwards, irradiance data from the La Crosse, WI airport and water temperatures measured at the water quality stations were used.

Comparison measured plant biomass data and data simulated by the original models

After eliminating the 1999-2000 field sites vegetated by other plant species, barren, or terrestrial, only seven validation data points remained. No correlation was found between plant biomass data generated by the original Version 1.0 VALLA and POTAM models and mean plant biomass measured at 211 sites in UMR Pool 8. Correlation between plant biomass simulated, and biomass measured on the remaining seven sites was still poor. In general, simulated values greatly exceeded measured values.

The far higher simulated than measured plant biomass values were largely attributed to the fact that the models did not account for the effect of current velocity, which may reduce biomass by a factor of 2 at a current velocity of 0.45 m s^{-1} (*Callitriche stagnalis*; Madsen and Sondergaard 1983) and eliminate biomass at velocities > 0.73-1.0 m s^{-1} (*Potamogeton pectinatus*; Chambers et al. 1991). From a map of current velocity in Pool 8 at a high discharge condition of 90,000 cubic feet per second (cfs); 5 percent exceedence condition (Sullivan 2000), it became apparent that current velocity in large part of lower Pool 8 exceeded 0.45 m s^{-1} and would, therefore, form an unsuitable habitat for sago pondweed, and even more for plant species less resistant to high current velocities. Other tentative reasons for the lack of correlation between simulated and measured biomass values were the scarcity of field data, i.e., data on both plant biomass, and pertinent environmental factors.

First model modification

For the second comparison, both models were expanded with equations describing the relationship between current velocity and plant biomass. Curves were constructed that relate maximum photosynthetic rate at light saturation to current velocity; for details see Chapter 3, *Expansion of the Source Codes of Both Models*. These equations were based on data of: (1) Best and Boyd 2003a.; current velocity $\leq$ 0.08 m s^{-1}; species *Ceratophyllum demersum, Elodea nuttallii, P. pectinatus;* and (2) Chambers et al. (1991; current velocity $\geq$ 0.10 m s^{-1}; species *P. pectinatus*). A similar relationship between current velocity, and photosynthetic rate and biomass formation was also assumed. At low current velocity (range 0 to 0.08 m s^{-1}), data on *E. nuttallii* (member of the same family as wildcelery) were used for wildcelery, and data on sago pondweed were used for sago pondweed. At higher current velocity (range 0.08 to 1.00 m s^{-1}), data on sago pondweed were used for both species, because no values for the effect of current velocity on wildcelery were published prior to the field study reported in

Chapter 7, *Field Study to Determine the Effects of Current Velocity on Plant Biomass of V. americana.* These relationships were incorporated into the Versions 1.1 of both models.

Comparison measured plant biomass data and data simulated by the modified models

Simulations for the field sites that were devoid of plants in 1999-2000 indicated that, based on the processes and factors included in the models, plant biomass should occur. This led us to believe that factors other than those included in the models might prevent plant persistence at those sites.

Additional factors considered were: (1) Moderate to severe wave action from a low degree of shelter and from navigation movements during the growth season; and (2) Unsuitable substrates for plant anchorage (too dense or to fluid; Roseboom et al. 1992). With only two validation data points left for wildcelery and one for sago pondweed, the likelihood to find a correlation between simulated and measured values became negligible.

Simulated and measured plant biomass of wildcelery in 2001 was in the same order of magnitude. However, comparison of the model results, with and without accounting for current velocity effects, suggested that current velocity may affect the biomass of wildcelery in a different way than that of sago pondweed.

Simulated biomass greatly exceeded measured biomass of sago pondweed. This was attributed to a higher than actual light interception by the plant tissues in the model plants compared to that in natural plants.

Factors leading to the overestimate of light interception in POTAM considered were as follows:

a. The typical plant biomass distribution over the vertical axis of the water column in turbid water may be different from that in clear water. The species-specific light interception coefficient depends on this biomass distribution. Most calibration data for POTAM have been collected in the clear water of the Western Canal, The Netherlands; however, validation data pertained also to other, more turbid waters. So far only lower coefficients have been published than the currently used default value of 0.095 m^2 g^{-1} DW (Best and Boyd 2003a);

b. Submersed plants can be covered by epiphytes that absorb part of the irradiation before reaching the submersed plant light-capturing tissues;

c. The sago pondweed population in the UMR may start to grow from a lower than default tuber bank density. The latter may be due to early loss of senescing plant shoots torn off by strong wave action caused by wind (also reported in shallow Dutch lakes by Van Wijk 1988) and/or navigation activities, preventing plants from reaching their full tuber potential at the end of the year. Another possibility is that the plants reach their full tuber potential, but that the tuber bank density is greatly decreased through grazing by waterfowl. Korschgen et al. (1988) estimated that

40percent of wildcelery tubers on UMR Pool 7 were consumed by waterfowl during fall 1980. UMR Pools 7 and 8 are also used extensively as foraging area (largely for tubers of wildcelery, sago pondweed, and arrowhead) by tundra swans. Tundra swan use has increased from 29,305 use days during the early 1980s (1981-1984) to 431,000 during 1997-2002, accounting for 52 percent of river-wide swan use in 2002 (Kenow et al. 2003). A use day is one birds' use of an area for one day.

Based on the results of the latter comparison, the following recommendations were made (Best et al. 2002).

a. Include pertinent calibration data on the effects of current velocity on plant biomass of wildcelery in VALLA.

b. Expand both models with equations describing the shading effects by epiphytes on the light availability for wildcelery and sago pondweed, and collect pertinent calibration data pertaining to the UMR.

c. Verify the self-shading coefficient of sago pondweed in the UMR.

d. Expand the field data set on plant biomass of wildcelery, sago pondweed and pertinent environmental factors, all to the same sites in the UMR.

3 Expansion of the Source Codes of Both Models

Inclusion of Effects of Current Velocity on Photosynthesis

The source codes of both models were expanded with equations relating photosynthesis to current velocity. This entailed insertion of (1) an on/off switch for the effect of current velocity on photosynthesis and (2) a species-characteristic curve relating photosynthesis to current velocity via a relative, dimensionless factor ($\leq$1) into the ASSIM subroutine, in which photosynthesis is calculated.

The model input files were expanded with the pertinent calibration data:

for **VALLA Version 2.0** data pertaining to the related *E. nuttallii* at low current velocity (Best and Boyd 2003a) and data pertaining to wildcelery at high current velocity (this study, Chapter 7, *Field Study to Determine the Effect of Current Velocity on Plant Biomass of V. americana*);

for **POTAM Version 2.0** data pertaining to sago pondweed (Best and Boyd 2003a; Chambers et al. 1991).

The source codes of both models were expanded with equations relating photosynthesis to current velocity. This entailed insertion of (1) an on/off switch for the effect of current velocity on photosynthesis and (2) a species-characteristic curve relating photosynthesis to current velocity via a relative, dimensionless factor ($\leq$1) into the ASSIM subroutine, in which photosynthesis is calculated.

The model input files were expanded with the pertinent calibration data:

for **VALLA Version 2.0** data pertaining to the related *E. nuttallii* at low current velocity (Best and Boyd 2003a) and data pertaining to wildcelery at high current velocity (this study, Chapter 7, Field *Study to Determine the Effect of Current Velocity on Plant Biomass of V. americana*);

for **POTAM Version 2.0** data pertaining to sago pondweed (Best and Boyd 2003a; Chambers et al. 1991).

The relationships between current velocity and relative photosynthesis are presented in Figure 7. In these functions the relative photosynthetic rate decreases linearly from 1.0 at a current velocity of 0.07 m s^{-1} to 0 at a current velocity of 0.82 m s^{-1} for wildcelery, and to 0 at a current velocity of 0.94 m s^{-1} for sago pondweed.

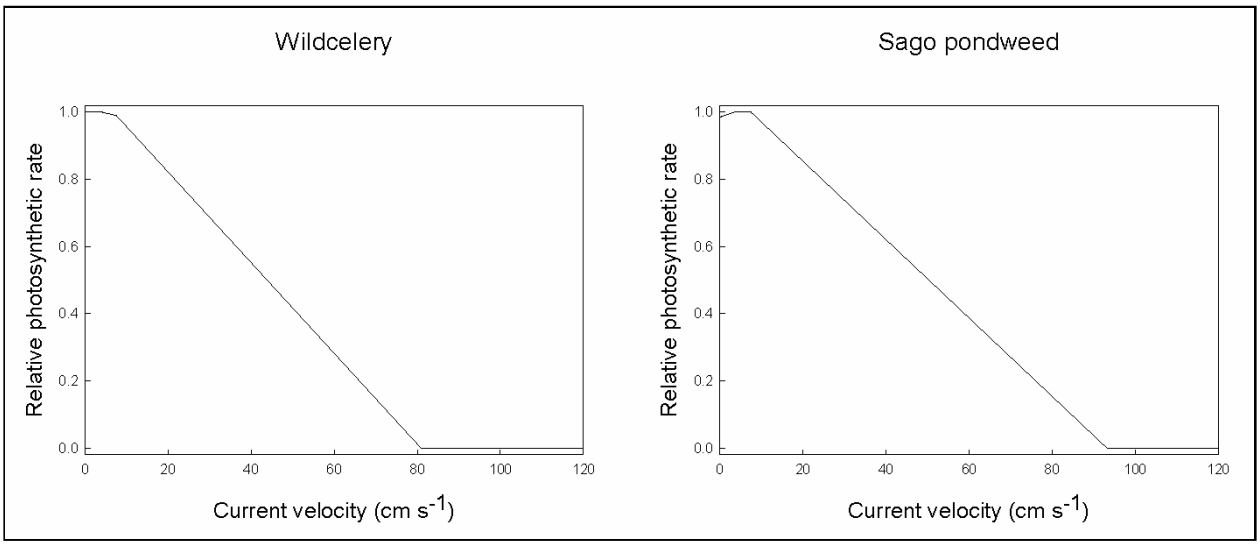

Figure 7. Relationship between current velocity and relative photosynthetic rate used for model calibration

The following lines were added to the ASSIM subroutines of both models:

* Calculation of current velocity in cm s^{-1} from monthly values provided in input file (April 2001)

```
IF (VELSWT.GT.1.E-1)  THEN
      VEL = LINT (WVEL,ILWVEL,DAY)
```
(3)

* Calculation of multiplication factor (fraction≤1) to AMAX, based on current velocity

* (VEL) calculated above

```
REDAM2 = LINT(REDAM1, ILRDM1,VEL)
ELSE
REDAM2 = 1
ENDIF
```

* Shoot photosynthesis at light saturation and daytime temperature effect on shoot photosynthesis

AMAX = AMAX * REDAM2

where

AMAX	is actual CO_2 assimilation rate at light saturation for individual shoots (g CO_2 g^{-1} DW $h^{-1)}$
DAY	is Julian day number
REDAM1	is reduction factor for AMAX to account for effects of current velocity, read from input file (-, cm s^{-1})
REDAM2	is reduction factor for AMAX to account for effects of current velocity, used in calculation source code (-, cm s^{-1})
VEL	is current velocity as function of day number, used in calculation source code (cm s^{-1}, d)
VELSWT	is on/off switch for effect current velocity on photosynthesis
WVEL	is current velocity as function of day number, read from input file (cm s^{-1}, d)

Inclusion of Shading Effects by Epiphytes on the Light Availability for Submersed Plants

The source codes of both models were modified to include equations reducing the light interception by plants with a relative factor accounting for light interception by epiphytes. This entailed insertion of (1) an on/off switch for the effect of epiphyte shading on light interception by the plant and (2) a species-characteristic curve relating light interception by epiphytes to development stage (DVS) of the plant via a relative, dimensionless factor ($\leq$1) into the ASSIM subroutine, in which photosynthesis is calculated.

The model input files were modified to include pertinent calibration data:

for **VALLA Version 2.0** data pertaining to wildcelery in UMR Pools 8 and 13;

for **POTAM Version 2.0** data pertaining to sago pondweed in UMR Pools 8 and 13 (this study Chapter 8, *Field Study to Determine the Shading Effects by Epiphytes on the Light Availability for V. americana and P. pectinatus*).

The relationships between DVS and relative light interception by epiphytes are presented in Figure 8. In these functions, light interception by epiphytes increases linearly from 0 at the beginning of the year to a maximum value (of 0.43 for wildcelery and of 1.0 for sago pondweed) at DVS=2, when plant senescence sets in, and decreases subsequently extremely slowly to 0 at the end of the year (DVS~2.3 in a temperate climate, DVS>2.3 in warmer climates). This curve describes the typical behavior of submersed plants in a temperate climate that hibernate as tubers—usually completely covered by silt and epiphytes—

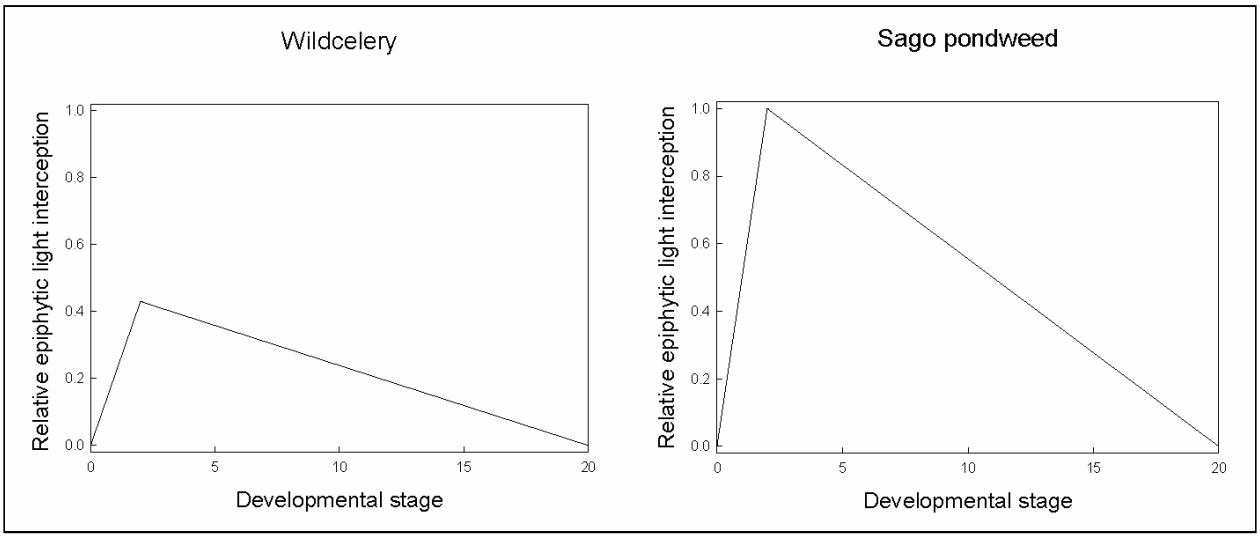

Figure 8. Relationship between developmental stage and relative epiphytic light interception used for model calibration

sprout and strongly elongate in early spring, losing their epiphytic cover, flower and successively senesce, becoming increasingly covered by epiphytes (Best and Visser 1987).

The following lines were added to the ASSIM subroutines of the source codes of both models.

* Addition of the epiphyte shading/reduction factor

```
IF (EPHSWT. GE.1.) THEN
        EPISHD = LINT(EPHY,ILEPHY,DVS)
ENDIF
```

(4)

```
IF (EPHSWT. LT. 1.) THEN
        EPISHD = 0.0
```

* Total irradiation on top of stratum I

$$IRZ_{i+1} = IRZ_i \times exp(-TL \times L - K \times SC_i)$$

$$IABS_i = \frac{(IRZ_i - IRZ_{i+1}) \times SC_i \times K}{(K \times SC_i + TL \times L)} \times (1.0 - EPISHD)$$

where

DVS	is development phase of the plant (-)
EPISHD	is epiphyte shading effect on light interception by the plant as function of DVS, used in calculation source code (-, -)
EPHSWT	is on/off switch effect epiphyte shading on photosynthesis
EPHY	is epiphyte shading effect on light interception by the plant as function of DVS, read from input file (-,-)
$IABS_i$	is total irradiance absorbed per depth layer containing plant material (J m^{-2} s^{-1})
IRZ_i	is total irradiance on top of depth layer I (J m^{-2} s^{-1})
K	is plant species-specific light extinction coefficient (m^2 g^{-1} DW)
L	is water type specific light extinction coefficient (m^{-1})
SC_i	is shoot dry matter in depth layer I (g DW m^{-2} $layer^{-1}$)
TL	is thickness per depth layer (m)

The variable listing and available output parameters of the Version 2 of the plant growth models are presented in Appendix B; the input files are presented in Appendix C. Examples illustrating calculations needed for runs with changed default values are described in Appendix D.

4 Simulations Using the Refined Models

Approach

Both expanded and recalibrated models, Versions 2.0, were tested against field data collected in 2001 and 2002 in the UMR Pools 8 and 13.

Field data on plant biomass used for validation

The validation field data comprised mean biomass values of wildcelery and sago pondweed (g dry weight m^{-2}), collected in UMR Pools 8 and 13 in 2001 and 2002. Each mean biomass value was calculated as the average of up to four harvested quadrants for each site where one of the studied plant species predominated. Non-vegetated quadrants were not included in this average, based on the observation that they were not supportive of submersed plant growth. For each plant species up to five sites were harvested as close as possible to each monitoring station.

In 2001, shoot biomass and environmental data were collected at five water quality monitoring stations situated on or close to the channel borders in UMR Pool 8 (stations Target Lake, Lawrence Lake, Lawrence Lake Marina, Turtle Island, and Above Dam 8-West side; Figure 9, Table 2). Sixteen mean shoot biomass values were collected on wildcelery and 23 mean shoot biomass values on sago pondweed (Tables 3 and 4). For sago pondweed >5 sites were sampled in Target Lake and Lawrence Lake Marina to make up for the <5 sites found in Lawrence Lake and Above Dam 8 (Table 4). All sites were located as close as possible to the water quality monitoring stations.

In 2002, shoot biomass and environmental data were collected at five water quality monitoring stations in UMR Pools 8 and 13 (stations Target Lake, Lawrence Lake, Lawrence Lake Marina, Turtle Island, Above Dam 8-West side, and Channel station in Pool 13; Figure 9, Table 2). Sixteen mean shoot biomass values were collected on wildcelery and six values on sago pondweed (Tables 3 and 4). All sites were located as close as possible to the water quality monitoring stations.

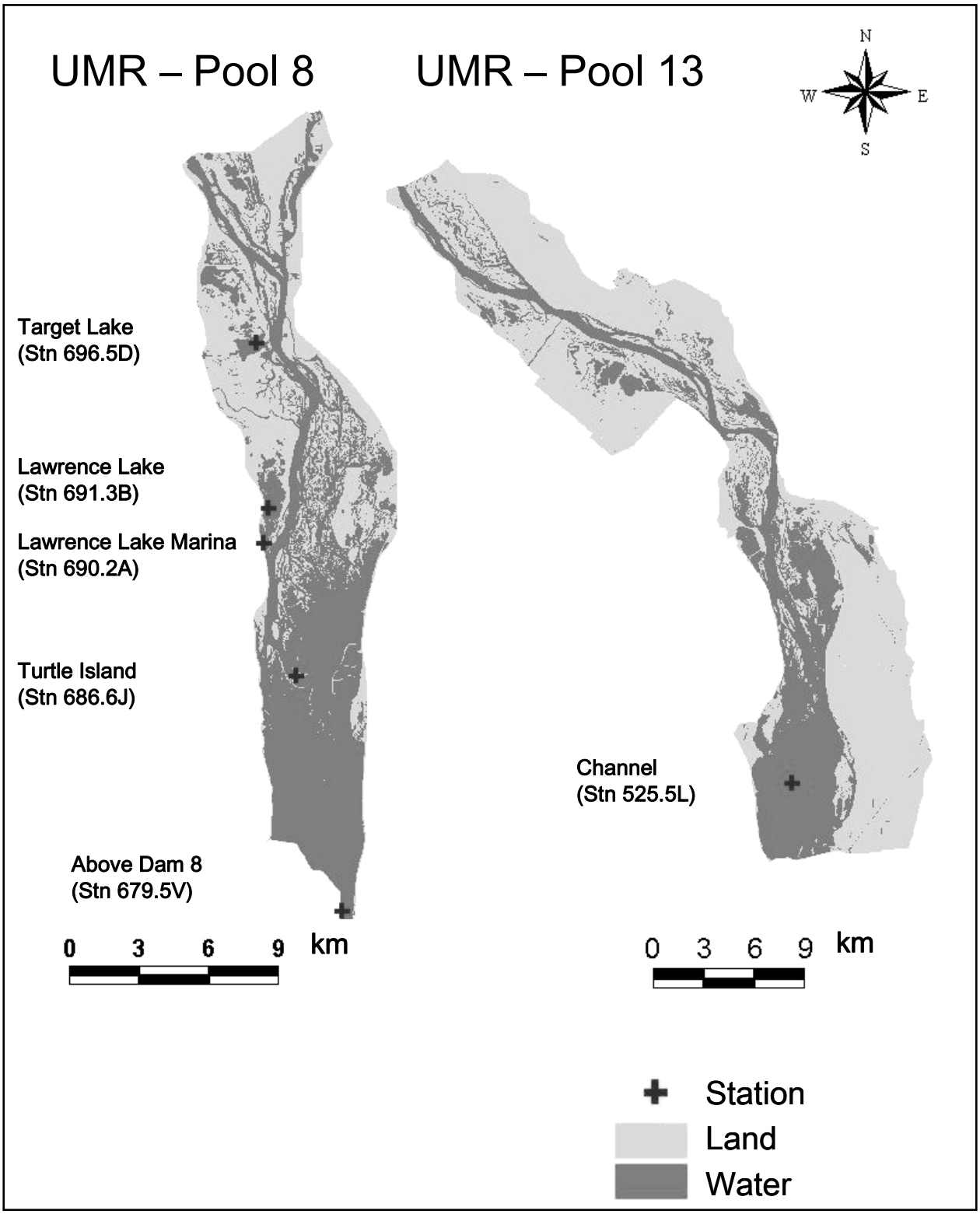

Figure 9. Situation of water quality monitoring stations where plant samples and data on environmental factors were collected in Upper Mississippi River Pools 8 and 13, in 2001 and 2002

Table 2
Sampling Stations Where Plant Biomass was Collected. Sampling was conducted in 2001 on 30-31 July 2002 in Pool 8, and in 2002 on 30-31July in Pool 8 and 17-18 July in Pool 13

Environmental Station Code	UTM-Coordinates EW	UTM-Coordinates NS	SAV present	Characteristics
Pool 13				
M525.5L	735830	4646920	+	Channel
Pool 8				
M696.5D	638947	4850291	+	Target Lake
M691.3B	639442	4843204	+	Lawrence Lake
M690.2A	639243	4841764	+	Lawrence Lake Marina
M686.6J	640620	4836021	+	Turtle Island
M679.5V	642609	4825913	+	Above Dam 8, west side

Note: UTM = Universal Transverse Mercator; EW = east-west; NS = north-south; SAV = submersed aquatic macrophyte.

Initial values model runs

The *refined models Version 2.0* were run varying the initial values for plant biomass and tuber bank characteristics.

> for **VALLA**, default initial values were used unless stated otherwise: plant biomass=0, tuber bank density=233 m^{-2}, tuber size 0.090 g DW $tuber^{-1}$.
>
> for **POTAM**, default initial values were used, concomitant with far lower tuber bank densities unless stated otherwise: plant biomass=0, tuber bank density=10 m^{-2}, tuber size 0.083 g DW $tuber^{-1}$. Default tuber bank density is 240 tubers m^{-2}.

Environmental and climatological data

The site-specific, daily values for the required environmental factor input were generated as described below. An overview of the environmental data used as input for the simulations is presented in Table 1.

Water depth. For each site of harvest, water depth was calculated by linear interpolation in space between the values measured at the nearest USACE gauging stations in UMR Pools 8 and 13, respectively, in 2001 and 2002. The water depth values calculated for the sites of harvest were corrected for differences in elevation between sites of harvest and gauging stations. Daily water depth values were derived by linear interpolation in time from these limited time series, composed by maximally 25 data pairs per site.

Table 3
Simulated Shoot Biomass and End-of-Year Tuber Numbers of *V. americana*, Corrected for Current Velocity and Epiphyte Shading Effects. Measured shoot biomass presented for comparison (range indicated)

Station/ Sample ID	Harvest day	Measured Shoot Biomass (g DW m^{-2})		Simulated Biomass *V. americana*					
				Initial Tuber Number = 10 m^{-2}			Initial Tuber Number = 233 m^{-2}		
		Mean	Range	Shoot at Day of Harvest (g DW m^{-2})	Max. Shoot (g DW m^{-2})	EOY-Tuber Number (N m^{-2})	Shoot at Day of Harvest (g DW m^{-2})	Max. Shoot (g DW m^{-2})	EOY-Tuber Number (N m^{-2})
Year 2001									
Target Lake									
EB1I	214	9.82	3.60-16.10	3.46	11.64	27.02	9.79	32.08	95.35
Lawrence Lake Marina									
EB4A	212	9.88	9.88	7.00	29.57	73.24	20.53	76.94	143.10
EB4B	212	6.96	6.96	7.61	33.72	110.34	22.33	87.62	257.12
EB4F[1]	212	0.08	0.08	7.95	37.04	97.81	23.43	99.19	211.36
EB4G[1]	212	49.94	0.10-100.00	7.95	37.04	97.81	23.43	99.19	211.36
EB4H[1]	212	0.16	0.16	0	0.45	0	0	1.35	0
Turtle Island									
EB5A	213	44.68	6.70-94.70	4.41	17.92	52.22	11.91	44.83	69.48
EB5B	213	109.40	22.9-179.00	4.41	17.92	52.22	11.91	44.83	69.48
EB5C	213	83.12	37.40-144.40	4.41	17.88	52.22	11.91	44.83	69.48
EB5D	213	94.60	2.30-250.10	4.19	16.23	61.38	11.33	40.81	74.26
EB5E	213	80.99	5.90-200.70	4.19	16.23	61.38	11.33	40.81	74.26
Above Dam 8									
EB3A[2]	213	3.34	1.40-6.20	5.59	21.85	49.11	15.78	55.85	67.02
EB3B	213	141.6	124.40-154.40	5.22	18.71	21.19	14.74	47.95	77.82
EB3C	213	167.3	96.00-263.20	5.22	18.71	21.19	14.88	49.47	73.08
EB3D[2]	213	36.08	1.60-106.30	5.59	21.85	49.11	15.91	57.47	65.75
EB3E[2]	213	36.42	13.10-59.70	5.59	21.85	49.11	15.91	56.94	65.75
Year 2002									
Lawrence Lake Marina									
EB4A	212	42.68	42.68	3.25	6.15	0.12	9.53	17.27	2.81
EB4B	212	2.16	2.16	4.19	11.69	27.45	12.16	31.33	101.67
Turtle Island									
EB5A	213	131.44	76.72-240.50	3.67	19.87	71.01	10.81	53.96	242.59
EB5B	213	143.76	83.72-190.68	2.71	11.81	64.81	8.02	32.86	62.07
EB5C	213	76.40	21.16-174.40	2.71	11.81	64.81	8.02	32.86	62.07
EB5D	213	52.32	3.60-126.96	2.52	10.09	21.62	7.48	28.28	69.75
EB5E	213	129.59	14.24-207.96	2.51	9.71	21.62	7.44	27.72	70.96
Above Dam 8									
EB3A	213	116.19	82.04-145.20	6.06	20.59	59.49	17.89	55.76	70.27
EB3B2	213	69.50	18.56-96.12	6.11	20.75	58.83	18.04	56.17	70.27
EB3C2	213	40.88	40.88	6.97	26.78	44.42	20.48	70.09	161.41
EB3D2	213	60.60	30.96-80.76	8.77	34.48	69.96	25.66	86.98	130.58
EB3E2	213	23.22	2.36-41.08	7.21	26.49	45.19	21.20	69.80	161.41
Channel Pool 13									
EB1A	198	58.42	0.64-110.64	1.21	3.82	0.02	3.61	10.92	0.37
EB1B	198	36.88	6.64-67.12	1.21	3.82	0.02	3.61	10.92	0.37
EB1C	199	43.04	16.72-66.68	1.19	3.22	0.02	3.46	9.24	0.37
EB1D	199	51.80	45.36-58.24	1.28	3.92	0.02	3.68	11.18	0.37

Note: EOY- end of year
[1] Sites with anchorage depth<0.1 m.
[2] Strong competition by other submersed plants.

Table 4
Simulated Shoot Biomass and End-of-Year Tuber Numbers of *P. pectinatus*, Corrected for Current Velocity and Epiphyte Shading Effects. Measured shoot biomass presented for comparison (range indicated)

Station/ Sample ID	Harvest Day	Measured Shoot Biomass (g DW m^{-2})		Simulated Biomass *V. pectinatus*					
				Initial Tuber Number = 10 m^{-2}			Initial Tuber Number = 240 m^{-2}		
		Mean	Range	Shoot at Day of Harvest (g DW m^{-2})	Max. Shoot (g DW m^{-2})	EOY-Tuber Number (N m^{-2})	Shoot at Day of Harvest (g DW m^{-2})	Max. Shoot (g DW m^{-2})	EOY-Tuber Number (N m^{-2})
Year 2001									
Target Lake									
EB1A	214	6.70	3.40-10.00	19.26	46.25	15.40	40.95	68.37	0.35
EB1B	214	11.32	11.32	20.18	49.08	14.31	41.98	70.77	0.35
EB1C	214	2.54	0.90-4.20	20.33	49.21	14.31	42.25	71.01	0.35
EB1D	214	4.56	0.70-8.40	20.64	49.48	14.31	42.78	71.40	0.35
EB1E	214	12.52	12.52	20.83	49.76	14.31	43.00	71.63	0.35
EB1F	214	10.70	2.50-18.90	21.71	50.99	14.31	44.37	72.95	0.35
EB1G	214	1.20	1.20	22.29	52.73	13.80	45.34	74.78	0.35
EB1H	214	2.53	0.30-6.80	23.01	55.00	12.84	46.38	76.91	0.35
EB1I	214	5.75	0.70-14.30	23.88	74.60	12.84	46.21	76.76	0.35
EB1A	214	6.70	3.40-10.00	19.26	46.25	15.40	40.95	68.37	0.35
Lawrence Lake									
EB2A	212	5.36	1.00-9.70	23.66	28.33	0	47.02	71.37	0
EB2B	212	16.64	16.64	29.72	58.82	0	55.82	81.85	0.20
EB2C	212	7.03	3.40-11.60	29.71	58.56	0	55.75	81.60	0.20
EB2D	212	7.05	0.10-9.70	30.29	60.38	0	57.37	83.80	0.20
EB2E	214	16.30	7.60-52.00	32.60	64.81	0	65.20	88.77	0.20
Lawrence Lake Marina									
EB4A[2]	212	4.44	4.44	34.00	73.58	12.84	64.32	100.46	0.35
EB4C[2]	212	2.68	0.24-5.10	41.49	132.01	36.08	104.32	223.11	38.83
EB4D	212	18.12	18.12	41.49	132.01	36.08	104.02	223.11	38.83
EB4E[1]	212	10.03	2.64-21.36	0.23	0.38	0.01	0.69	1.14	0.35
EB4F[2]	212	3.68	3.68	41.49	132.01	36.08	104.02	223.11	38.83
EB4H[12]	212	13.12	13.12	0.23	0.38	0.01	0.69	1.14	0.35
EB4I	212	10.40	10.40	34.00	73.58	12.84	64.32	100.46	0.35
EB4J[2]	212	6.64	6.64	34.00	73.58	12.84	64.32	100.46	0.35
Above Dam 8									
EB3C[2]	213	2.97	0.10-5.90	20.73	51.47	11.63	0	3.24	0
Year 2002									
Lawrence Lake Marina									
EB4A[2]	212	5.44	5.44	36.55	53.97	8.75	63.06	78.01	0.39
EB4C[2]	212	13.37	13.37	37.62	55.93	8.75	66.20	80.63	0.39
EB4D[2]	212	12.32	12.32	37.57	55.89	8.75	66.16	80.60	0.39
Turtle Island									
EB4A[2]	212	7.50	1.76-13.24	25.01	73.06	26.52	51.05	110.62	24.81
EB4B[2]	212	6.24	6.24	24.69	74.15	26.12	52.15	110.62	24.81
Channel Pool 13									
EB1A	198	0.03	0.03	7.28	37.05	0	19.23	58.46	0

Note: EOY- end of year.
[1] Sites with anchorage depth<0.1 m.
[2] Strong competition by other submersed plants.

Light extinction coefficients. Light extinction coefficients were calculated from the Secchi disk depth values measured at the monitoring stations according to Giessen et al. (1990).

Current velocity. From 2001 on, the current velocity values measured at the monitoring stations were used. Daily current velocity values were derived by linear interpolation in time from the limited time series, composed by maximally 25 data pairs per site.

Weather data. From 2001 onwards irradiance data from La Crosse airport, Wisconsin, and water temperatures measured at the water quality stations were used.

Incomplete environmental variable data sets

Incomplete data sets were amended by insertion of data previously collected at the same station, or by insertion of data measured at nearby stations with similar characteristics (Appendix E). In several cases, large part of the environmental data set had to be amended in this manner.

Runs of Both Refined Plant Models

Two sets of model runs were performed for all sites at which field data on shoot biomass had been collected. Field data on tubers were not available. The first set was started from a tuber bank density that generated shoot biomass results in the same order of magnitude as the measured range: for wildcelery a tuber bank density of 233 m^{-2} (default) and for sago pondweed a tuber bank density of 10 m^{-2} (strongly decreased compared to default, representative for a population affected by strong wave action and/or grazing; see this study Chapter 2, *Aquatic Plant Growth Models: Initial Performance and Improvements Suggested*). The second set was started from another tuber bank density that may occur in the UMR; for wildcelery a tuber bank density of 10 m^{-2} (representative for a population affected by strong wave action and/or grazing) and for sago pondweed a tuber bank density of 240 m^{-2} (default). From the results of each run, three values were selected, notably: (1) shoot biomass at day of harvest, (2) peak shoot biomass, and (3) end-of-year tuber number, all per m^2.

The results of these model runs are summarized in the Tables 3 and 4.

The performance of both models is evaluated by discussing results of runs pertaining to (1) the site for which the modeled shoot biomass at the day of harvest and/or the modeled peak shoot biomass is within the measured range and (2) another site for which the modeled shoot biomass deviates considerably from the measured range. Furthermore, results of one to two model runs are evaluated in which initial input values or parameter values have been changed. Finally, in Chapter 5, *Comparison Values Simulated Using Refined Models and Modeled Values,* the general trends in all model results are discussed, and reasons for large discrepancies between measured and modeled shoot biomass data are explored.

Model Runs *V. americana*

Results of a default model run performed for *Turtle Island, site EB5B, in 2001* indicated that simulated shoot biomass at the day of harvest, without and with corrections for epiphyte shading effects, was within the range of the measured shoot biomass, but with corrections for current velocity and both epiphyte shading and current velocity it was below the measured range (Figure 10). All simulated peak shoot biomass values were within the range of the measured values. Peak shoot biomass, without corrections for the effects of current velocity and epiphyte shading, was similar to mean shoot biomass measured at the day of harvest, but was about 30 days delayed in time. Peak biomass generated by runs corrected for current velocity effects was 50 percent lower, corrected for epiphyte shading 10 percent lower, and corrected for both effects 64 percent lower than peak biomass without corrections (Figure 10).

Simulated end-of-year tuber number was always substantial, ranging from 80 to around 350 tubers m^{-2}. This indicates that the wildcelery population would persist because the end-of-year tuber number was $\geq$ 1, and the tuber size was large enough to enable sprouts to become self-supporting in their carbon gain at shallow sites (0.5 m depth at relatively turbid water common in the UMR; Best and Boyd 2003a). This Turtle Island site is characterized by very shallow water (depth of 0.2 m at the day of harvest), current velocities tolerable for submersed plants (ranging from 0.03 to 0.37 m s^{-1}), and high turbidity in the plant growth period (light extinction coefficients ranging from 3.00 to 4.23 m^{-1}; Table 5).

Results of a default run performed for *Above Dam 8, site EB3B, in 2001* showed that simulated shoot biomass was generally below the measured range (Figure 11). It appeared that at this site, shoot biomass was influenced by current velocity to the same extent as at the Turtle island site, but that the epiphyte shading effect on shoot biomass was less. Simulated end-of-year tuber number at this site was also substantial, ranging from 80 to 150 tubers m^{-2}, indicating a high potential for wildcelery persistence. This Above Dam 8 site is characterized by a highly variable water depth (range 0.20 to 2.40 m), variable current velocity (0 to 1.14 m s^{-1}), and high turbidity (light extinction coefficients ranging from 1.18 to 4.13 m^{-1}; Table 5).

Results of a second run performed for the same *Turtle Island site EB5B in 2001* (Figure 10) but starting from a high tuber size of 0.20 g DW, as measured in Pool 9 by Donnermeyer (1982), indicated that in this instance a higher peak shoot biomass, but lower end-of-year tuber number, would be produced than in a wildcelery population starting from default plant characteristics (Figure 12). Simulated shoot biomass at the day of harvest and peak biomass, whether or not corrected for current velocity, epiphyte shading, or both, were within the measured range. The vegetation would persist.

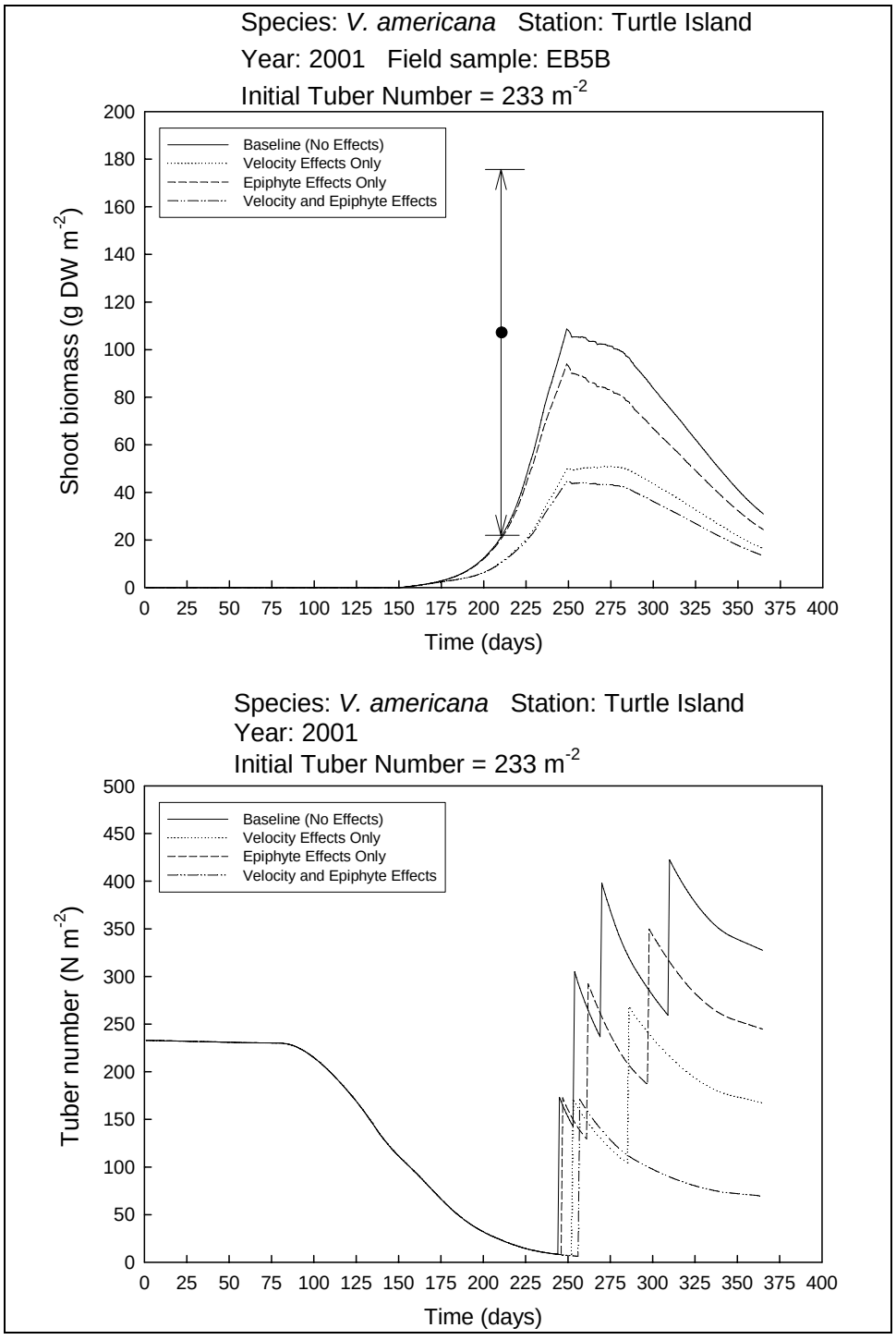

Figure 10. Simulated biomass of plants and tubers of a wildcelery community in Upper Mississippi River Pool 8 at Turtle Island, in 2001, starting from default tuber bank density. Simulations were conducted for situations with and without accounting for the effects of current velocity and epiphyte shading. Measured shoot biomass values are indicated by the mean (solid circle) and range (<->)

Table 5
Data on Environmental Variables at Water Quality Monitoring Stations of the Upper Mississippi River Pool 8 Collected in 2001 (Continued)

Day No.	Water Temp °C	Water Depth m	Current Velocity m s^{-1}	Secchi Disk Depth m	Light Extinction Coefficient Water Column, m^{-1}
Target Lake					
11	0.2	0.20	0	0.65	2.54
23	0	0.20	0	0.44	3.75
37	0	0.13	0	0.61	2.70
53	0.1	0.15	0.02	0.57	2.89
67	0.3	0.08	0	0.52	3.17
79	1.6	0.07	0	0.33	5.00
95	4.8	0.65	0.02	0.86	1.92
108	6.4	0.20	0.07	0.36	4.58
123	13.1	0.20	0.1	0.69	2.39
136	21.1	1.33	0.02	0.98	1.68
151	17.8	1.65	0	0.68	2.43
164	24.2	0.79	0	0.54	3.06
178	26.8	1.24	0	2.14	0.77
192	28.2	0.55	0	0.30	5.50
206	27.1	0.30	0.01	0.49	3.37
221	29.3	0.36	0	0.63	2.62
235	23.6	0.34	0	0.68	2.43
247	24.3	0.20	0	0.50	3.30
261	15.6	0.31	0	0.61	2.70
Lawrence Lake					
11	1.1	0.20	0	0.83	1.99
22	1.6	0.20	0	0.83	1.99
37	1.6	0.20		0.64	2.58
53	1.0	0.20	0	0.84	1.96
67	2.6	0.20	0	0.75	2.20
79	3.1	0.20	0	0.66	2.50
95	3.0	0.20	0	0.83	1.99
108	6.6	0.20	0.37	0.35	4.71
123	13.3	0.20	0.36	0.72	2.29
136	23.6	0.90	0	0.82	2.01
151	20.1	0.70	0	0.64	2.58
164	24.3	0.60	0	0.47	3.51
178	28.2	0.20	0.02	0.42	3.93
192	27.4	0.20	0	0.49	3.37
208	26.6	0.31	0	0.42	3.93
221	30.7	0.20	0.03	0.58	2.84
235	26.4	0.32	0	0.64	2.58
247	24.2	0.30	0	0.60	2.75
261	17.3	0.39	0	0.74	2.23
277	15.4	1.76	0	1.40	1.18
289	9.5	1.83	0	1.64	1.01
309	9.1	1.47	0	0.90	1.83
317	8.4	1.62	0.02	0.88	1.88
333	5.3	1.66	0	1.36	1.21
349	2.3	1.65	0.04	1.36	1.21

(Continued)

Table 5 (Concluded)

Day No.	Water temp °C	Water depth m	Current velocity m s^{-1}	Secchi disk depth m	Light extinction coefficient water column, m^{-1}
Lawrence Lake Marina					
151	19	0.20	0	0.58	2.84
151	16.6	2.96	0	0.58	2.84
164	23.9	0.20	0.06	0.51	3.24
164	20.8	2.64	0.06	0.51	3.24
178	28.1	0.20	0	0.45	3.67
178	24.2	3.16	0	0.45	3.67
192	27.0	0.20	0.03	0.38	4.34
192	24.2	2.40	0.03	0.38	4.34
208	26.0	0.20	0	0.39	4.23
221	30.7	0.20	0.08	0.43	3.84
221	28.3	2.05	0.08	0.43	3.84
235	25.7	0.20	0.04	0.58	2.84
235	22.3	2.10	0.04	0.58	2.84
Turtle Island					
151	17.5	0.20	0.36	0.55	3.00
164	23.4	0.20	0.11	0.39	4.23
178	25.8	0.20	0.37	0.44	3.75
192	27.6	0.20	0.29	0.55	3.00
205	28.2	0.20	0.06	0.4	4.13
221	30.5	0.20	0.25	0.48	3.44
235	24.9	0.20	0.03	0.55	3.00
Above Dam 8					
11	0.2	0.20	0.10	1.30	1.27
24	0.2	0.54	0.04	1.07	1.54
37	0.2	0.20	0.05	1.04	1.59
53	0.2	0.63	0.06	1.25	1.32
67	0.1	0.75	0.06	1.29	1.28
79	0.1	0.48	0.05	1.40	1.18
95	5.8	0.20	0.23	0.49	3.37
122	13.3	0.20	1.14	0.62	2.66
136	20.4	0.20	0.49	0.70	2.36
151	17.3	0.20	0.27	0.56	2.95
165	22.2	0.20	0.22	0.51	3.24
178	25.9	0.20	0.23	0.42	3.93
192	26.4	0.20	0.11	0.53	3.11
204	25.9	0.20	0	0.42	3.93
221	29.2	0.20	0.21	0.50	3.30
235	25.2	0.20	0.05	0.40	4.13
247	24.0	0.34	0.02	0.71	2.32
261	17.9	0.62	0.06	0.68	2.43
277	15.9	1.12	0.05	0.68	2.43
289	10.5	2.40	0.05	0.59	2.80
309	9.1	0.92	0	0.84	1.96
317	8.3	1.38	0.06	0.98	1.68
333	5.8	1.88	0.25	1.31	1.26
349	2.6	1.20	0.10	0.72	2.29

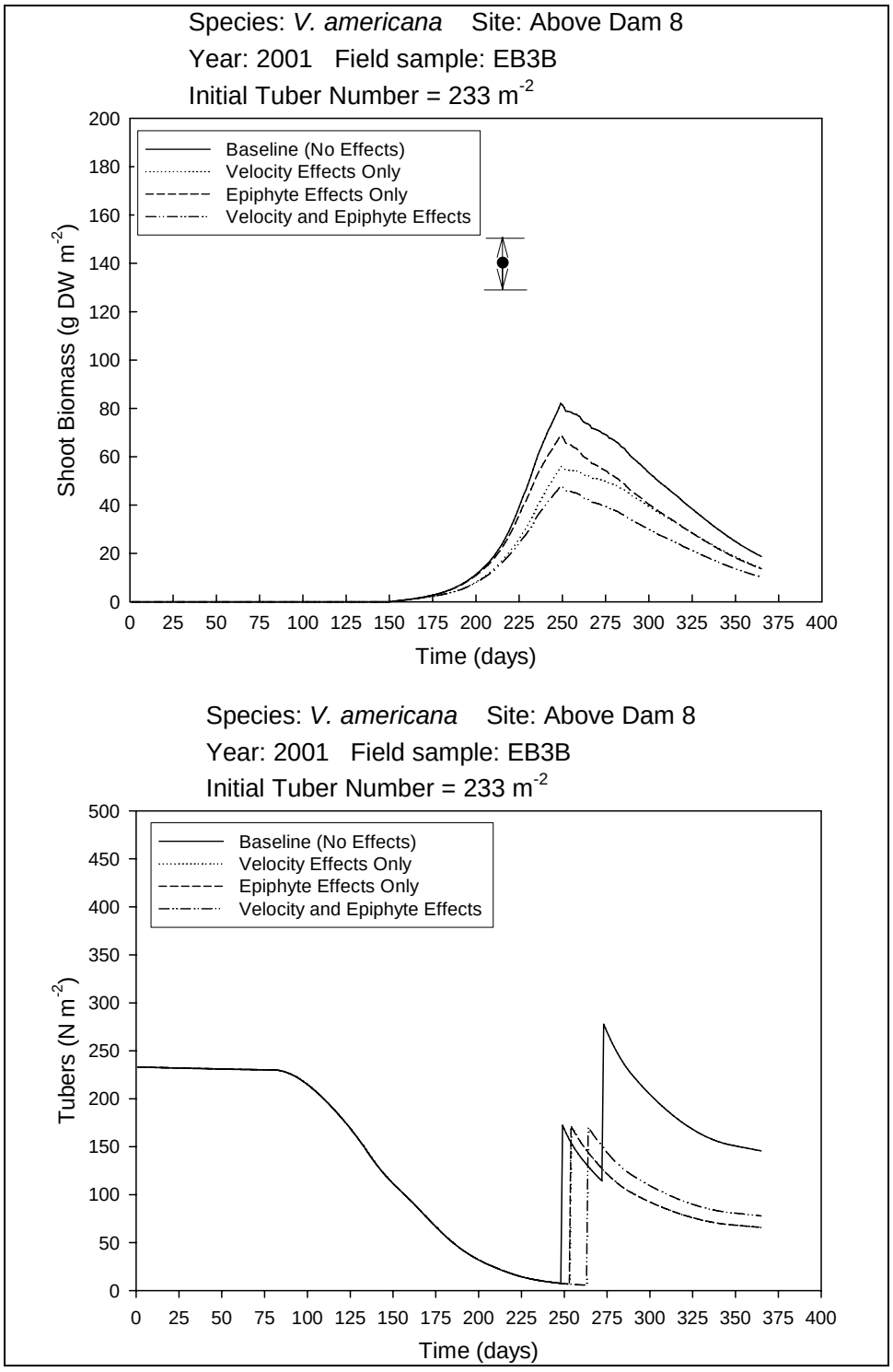

Figure 11. Simulated biomass of plants and tubers of a wildcelery community in Upper Mississippi River Pool 8 at the Lawrence Lake Marina, in 2001, starting from default tuber bank density. Simulations were conducted for situations with and without accounting for the effects of current velocity and epiphyte shading. Measured shoot biomass values are indicated by the mean (solid circle) and range (<->)

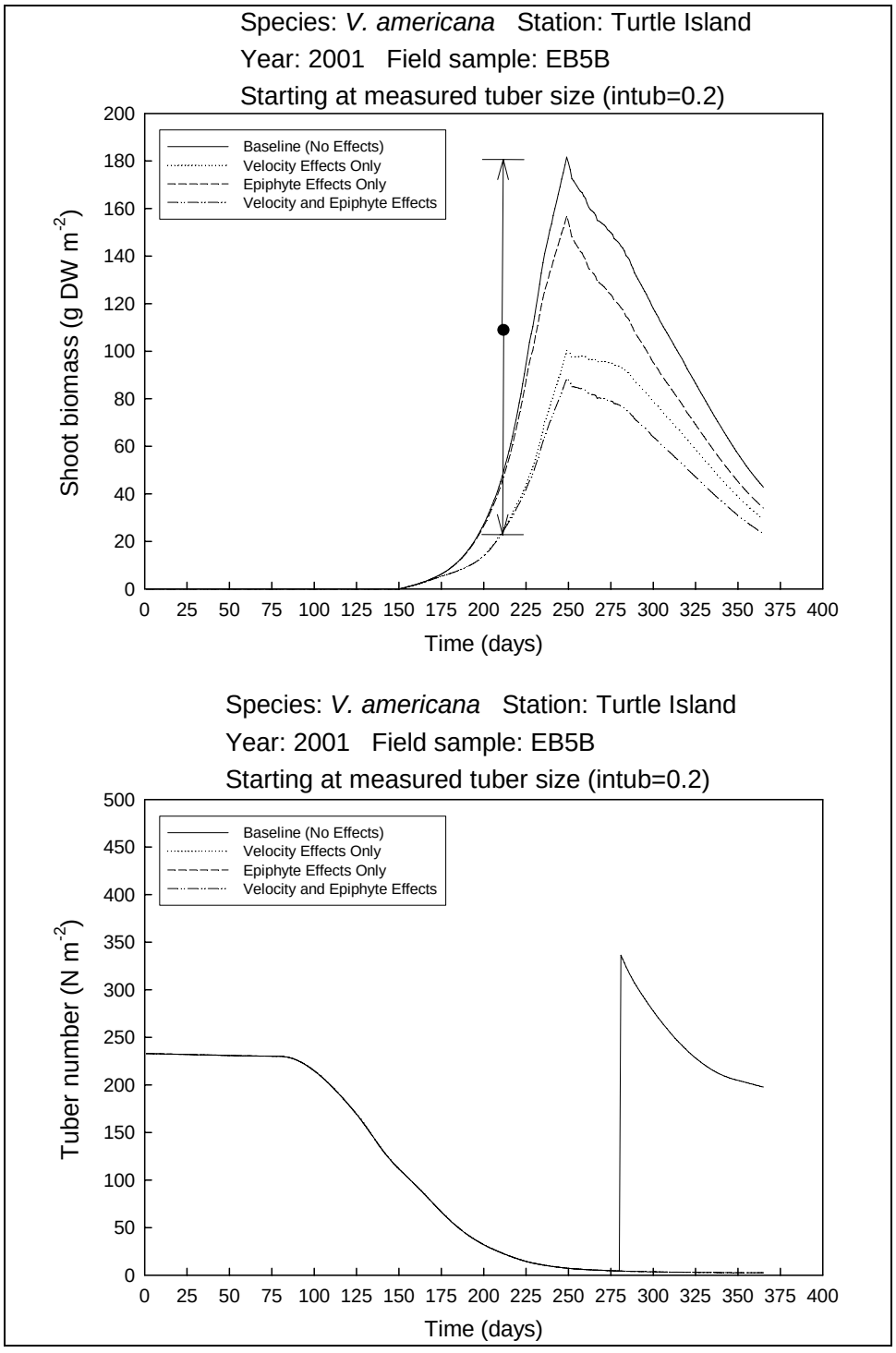

Figure 12. Simulated biomass of plants and tubers of a wildcelery community in Upper Mississippi River Pool 8 at Turtle Island, in 2001, starting from default tuber bank density and high measured tuber size. Simulations were conducted for situations with and without accounting for the effects of current velocity and epiphyte shading. Measured shoot biomass values are indicated by the mean (solid circle) and range (<->)

Model Runs *P. pectinatus*

When started from a low tuber bank density of 10 tubers m^{-2}, a good match between simulated shoot biomass at the day of harvest—corrected for the effects of current velocity and/or epiphyte shading; corrected for the effects of both factors; and measured shoot biomass—was found for one *Lawrence Lake site, EB2E, in 2001* (Figure 13). Simulated peak biomass exceeded shoot biomass measured at the day of harvest. Decreasing effects of current velocity on shoot biomass were minimal, and effects of epiphyte shading were large, i.e., in the order of 40 percent. End-of-year tuber number was 0 when corrected for epiphyte shading effects, but could amount to 64 tubers m^{-2} without correction for epiphyte shading (Figure 13, Table 4). Thus, epiphyte shading would prevent the persistence of the sago pondweed population by the inhibition of tuber production at this site. This site is characterized by a highly fluctuating water level (0.20 to 1.83 m), low current velocities (ranging from 0 to 0.37 m s^{-1}), and high turbidity in the plant growth period (light extinction coefficients ranging from 1.01 to 4.71 m^{-1}; Tables 5 and 6).

Simulated shoot biomass at the day of harvest exceeded measured shoot biomass at one *Target Lake site, EB1A, in 2001* (Figure 14). The decreasing effect of current velocity was minimal, but of epiphyte shading large, i.e., on the order of 55 percent. End-of-year tuber number, approximately 55 tubers m^{-2}, was substantial whether or not corrected for the effect of current velocity, but decreased sharply to around 15 tubers m^{-2} when corrected for the effect of epiphyte shading. In all simulations for the sites at Target Lake, the sago pondweed population would persist (Figure 14, Table 4). This Target Lake site is characterized by a fluctuating water level (0.20 to 1.65 m), low current velocities (ranging from 0 to 0.10 m s^{-1}), and variable turbidity in the plant growth period (light extinction coefficients ranging from 0.77 to 5.50 m^{-1}; Tables 5 and 6).

Results of a second run performed for the same site, started from a low tuber bank density of 10 tubers m^{-2} and using the recently measured UMR-characteristic, high, self-shading coefficient of 1.79 m^2 g^{-1}DW (Chapter 9, *Field Study to Determine the Self-shading Coefficient of P. pectinatus in the Upper Mississippi River*) indicated that this population would be able to form shoot biomass at the day of harvest with or without corrections for the effects of current velocity and epiphyte shading in the range of the measured values. However, only the end-of-year tuber numbers simulated for an unaffected population and a current velocity-affected population were sufficient to maintain a viable population, while populations affected by epiphyte shading alone and affected by current velocity and epiphyte shading combined would become extinct (Figure 15). A high self-shading coefficient provides a large potential light-capturing surface area for a canopy-forming submersed plant. This capacity would enable a high carbon gain, and, thus, biomass production, which is (almost) completely inhibited by epiphyte shading when plant senescence sets in (see Chapter 3, *Expansion of the Source Codes of Both Models*).

Results of default runs always overestimated measured shoot biomass of sago pondweed (Figure 16).

Table 6
Data on Environmental Variables at Water Quality Monitoring Stations of the Upper Mississippi River Pools 8 and 13 Collected in 2002

Day No.	Water Temp °C	Water Depth, m	Current Velocity, m s^{-1}	Secchi Disk Depth, m	Light Extinction Coefficient Water Column, m^{-1}
Lawrence Lake Marina					
163	22.3	2.71	0.04	0.68	2.43
177	24.9	2.77	0.08	0.35	4.71
190	27.6	2.60	0.06	1.08	1.53
210	26.6	2.39	0.04	0.65	2.54
218	26.0	2.32	0.05	0.41	4.02
231	23.2	2.32	0.08	0.68	2.43
Turtle Island					
163	22.6	1.18	0.33	0.53	3.11
177	25.3	0.99	0.39	0.42	3.93
190	28.9	1.48	0.40	0.58	2.84
210	26.8	0.80	0.27	0.75	2.20
218	26.6	0.52	0.06	0.52	3.17
231	24.1	0.58	0.07	0.58	2.84
Above Dam 8					
14	-0.1	1.92	0.10	1.92	0.86
24	0.1	1.92	0.12	1.85	0.89
36	0.1	1.84	0.13	1.84	0.90
52	1.8	1.19	0.15	0.48	3.44
77	2.3	1.74	0.24	0.67	2.46
95	2.6	2.60	0.30	0.61	2.70
108	13.8	3.10	0.85	0.47	3.51
123	11.7	0.80	0.33	0.80	2.06
136	15.3	1.80	0.26	0.52	3.17
149	20.1	0.85	0.10	0.63	2.62
163	23.1	0.92	0.12	0.30	5.50
177	24.4	0.96	0.14	0.28	5.89
190	30.1	0.40	0.03	0.40	4.13
204	25.8	0.86	0.20	0.46	3.59
219	25.0	0.80	0.17	0.53	3.11
231	22.5	0.55	0.07	0.55	3.00
Channel Border Pool 13					
8	0	1.09	0.12	1.09	1.51
23	-0.1	1.16	0.10	1.16	1.42
35	0.1	1.05	0.10	1.05	1.57
53	3.2	1.08	0.12	0.60	2.75
66	0.1	1.04	0.10	0.70	2.36
77	3.0	1.04	0.14	0.50	3.30
94	5.0	1.20	0.16	0.42	3.93
107	16.5	1.10	0.16	0.34	4.85
120	10.7	1.50	0.32	0.48	3.44
134	13.6	1.04	0.21	0.28	5.89
148	18.5	0.97	0.19	0.42	3.93
163	23.6	1.10	0.17	0.28	5.89
176	27.1	0.95	0.05	0.45	3.67
190	28.2	1.10	0.05	0.33	5.00
204	27.1	1.16	0.11	0.53	3.11
218	26.3	1.00	0.11	0.48	3.44
232	23.6	1.08	0.03	0.46	3.59

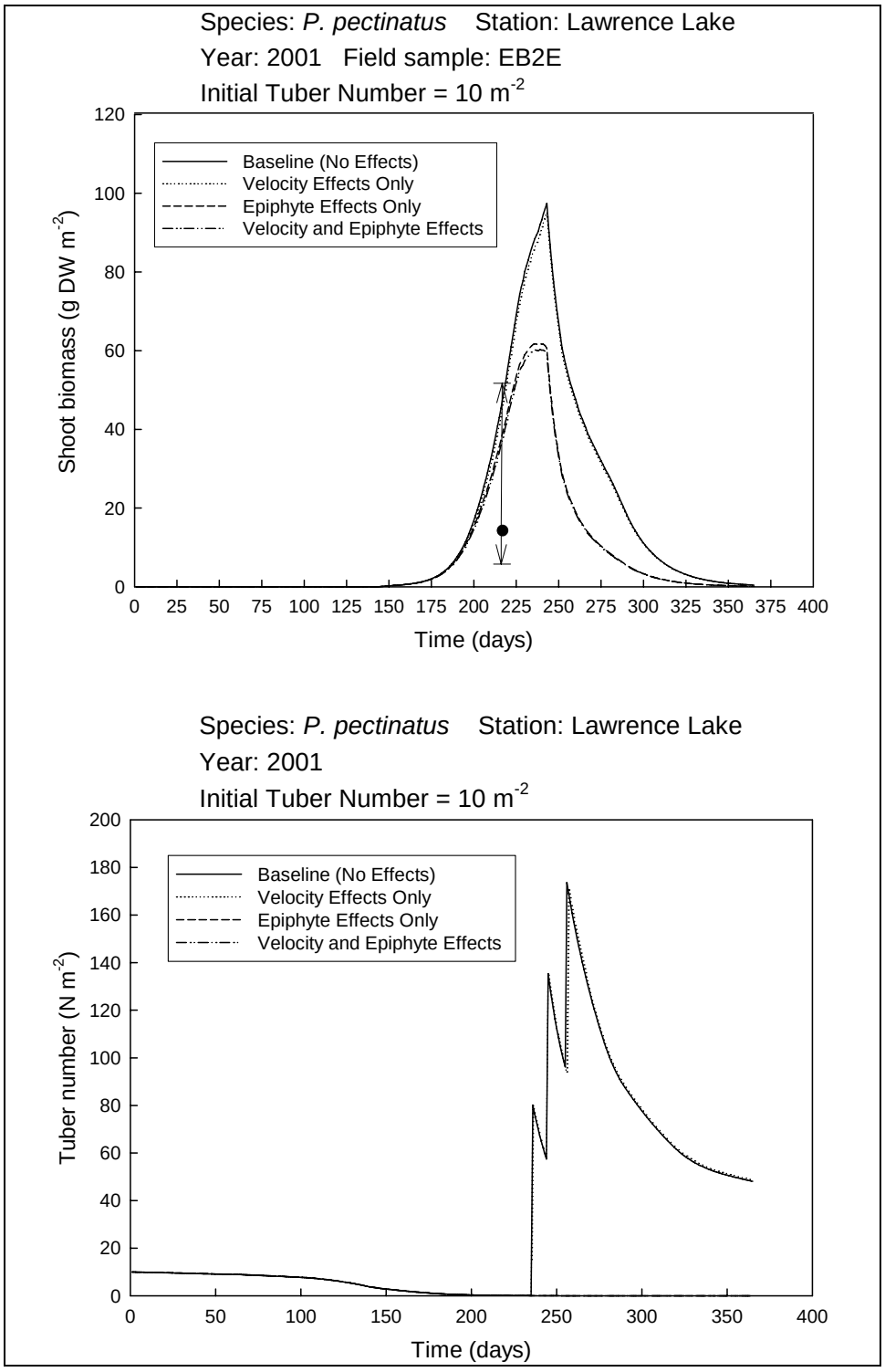

Figure 13. Simulated biomass of plants and tubers of a sago pondweed community in Upper Mississippi River Pool 8 at Lawrence Lake, in 2001, starting from a low tuber bank density. Simulations were conducted for situations with and without accounting for the effects of current velocity and epiphyte shading. Measured shoot biomass values are indicated by the mean (solid circle) and range (<->)

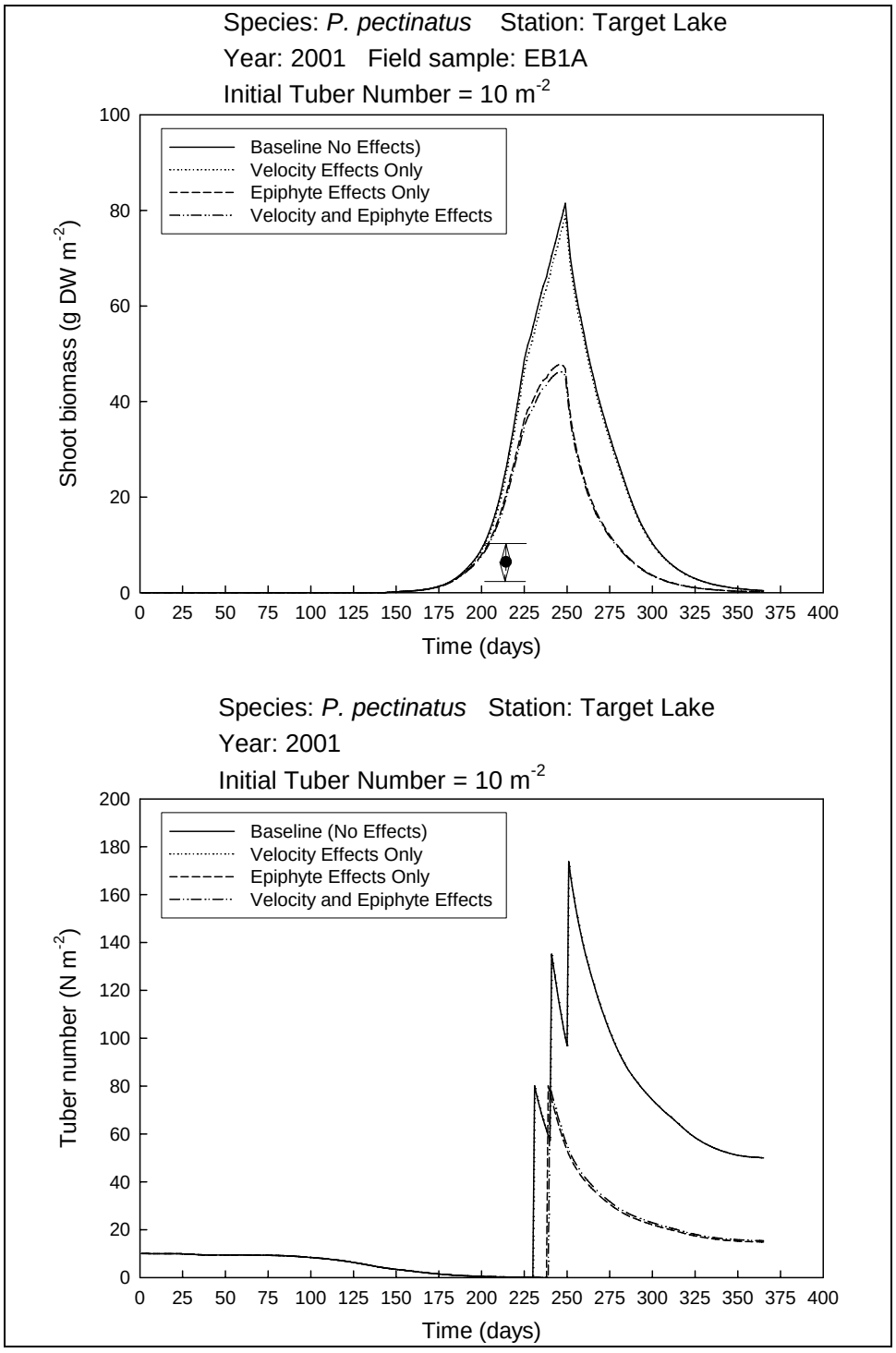

Figure 14. Simulated biomass of plants and tubers of a sago pondweed community in Upper Mississippi River Pool 8 at Target Lake, in 2001, starting from a low tuber bank density. Simulations were conducted for situations with and without accounting for the effects of current velocity and epiphyte shading. Measured shoot biomass values are indicated by the mean (solid circle) and range (<->)

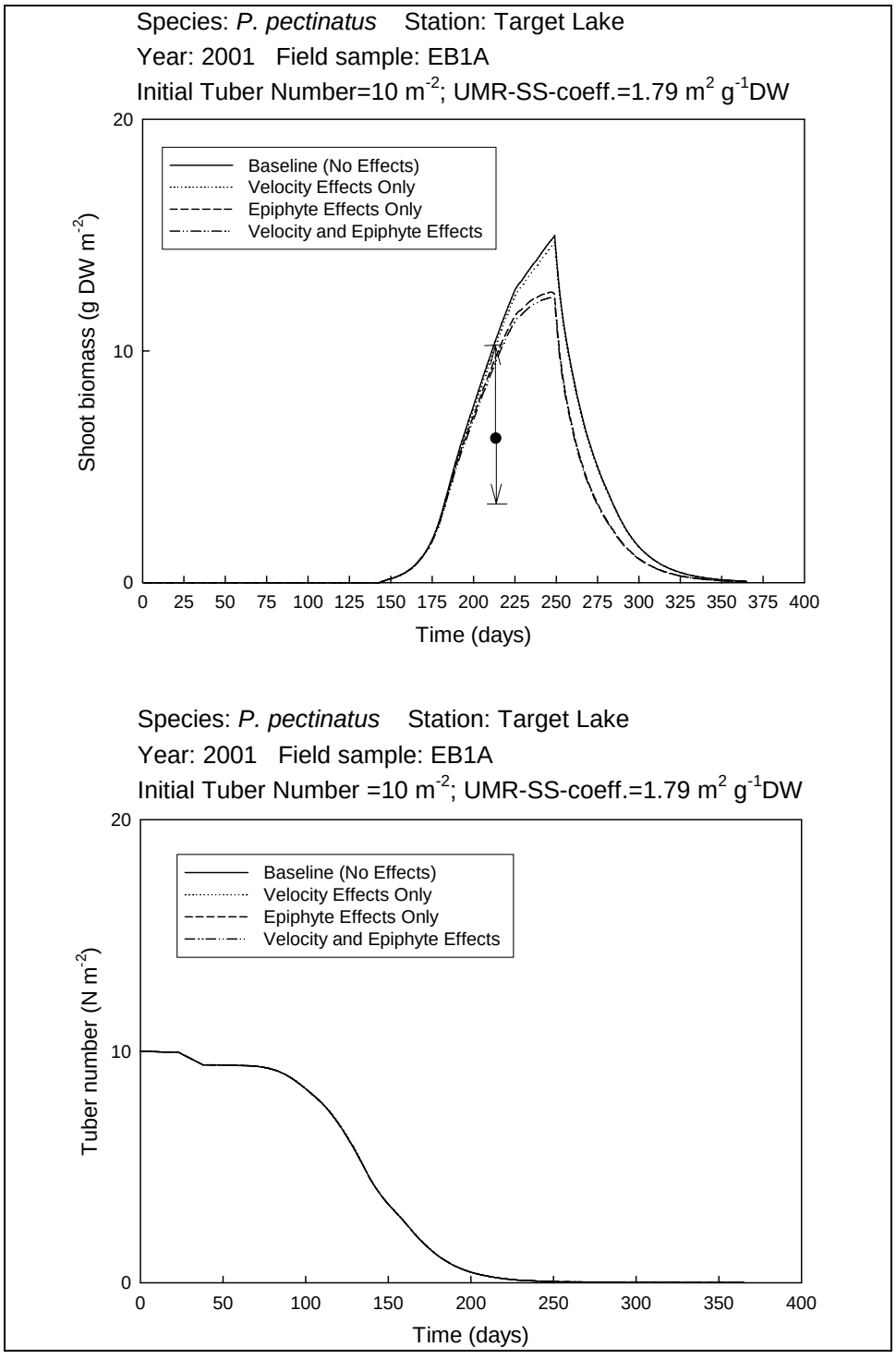

Figure 15. Simulated biomass of plants and tubers of a sago pondweed community in Upper Mississippi River Pool 8 at Lawrence Lake, in 2001, starting from a low tuber bank density and using the UMR-specific self-shading coefficient. Simulations were conducted for situations with and without accounting for the effects of current velocity and epiphyte shading. Measured shoot biomass values are indicated by the mean (solid circle) and range (<->)

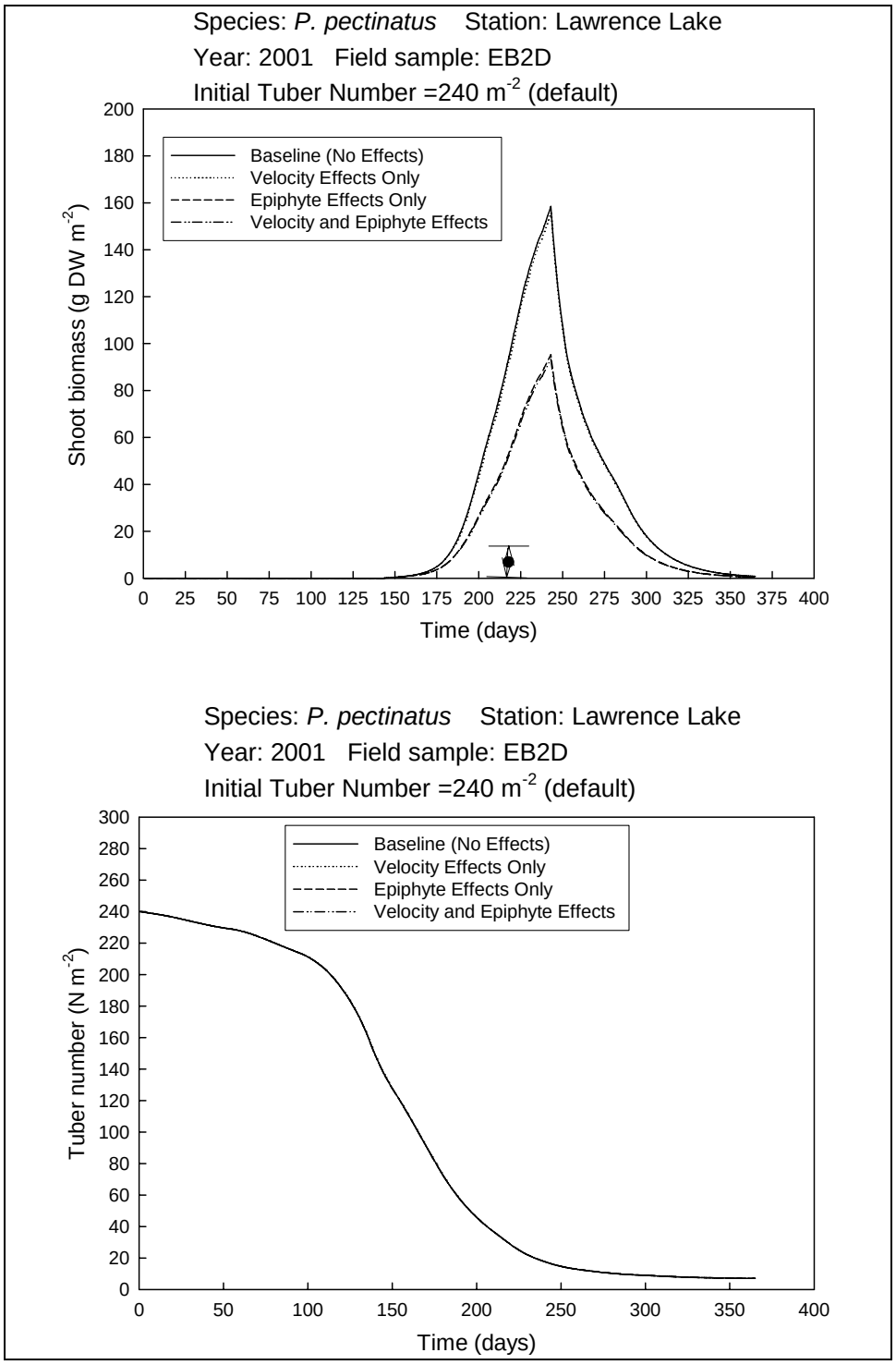

Figure 16. Simulated biomass of plants and tubers of a sago pondweed community in Upper Mississippi River Pool 8 at Lawrence Lake, in 2001, starting from default tuber bank density. Simulations were conducted for situations with and without accounting for the effects of current velocity and epiphyte shading. Measured shoot biomass values are indicated by the mean (solid circle) and range (<->)

5 Comparison Values Simulated Using Refined Models and Measured Values

Comparison of Simulated and Measured Shoot Biomass *V. americana*

For wildcelery, **simulated shoot biomass at the day of harvest** started from the default tuber bank density was generally lower than mean measured shoot biomass at each site (Figure 17a). In 14 out of 32 cases, simulated biomass was within the range of, or close to, the values measured at each individual site of each station (Table 3). However, the simulated biomass usually fell within the full range of shoot biomass measured at all sites of each station (Table 3).

Measured shoot biomass varied considerably among all sites at individual stations. Part of this variation was probably due to temporary desiccation, where anchorage depth was <0.1 m, and to competition for space and/or light by other aquatic plants (Table 3). In contrast, **simulated** shoot biomass was similar at all sites per individual station since initial plant characteristic values were equal and all environmental factors except anchorage depth were the same (Table 3). The shoot biomass simulated for a wildcelery vegetation at a rooting depth<0.1 m is believed not to be realistic, since the modeled spatial distribution of biomass over the water column requires a water depth of $\geq$0.2 m (Best and Boyd 2001a).

Simulated shoot biomass varied among stations, and this was due to differences in rooting depth, water transparency, water temperature, and current velocity. The latter combination of environmental factors allowed the lowest peak shoot biomass production at the Channel station in Pool 13 (1 m rooting depth, turbid water) and the highest at the Lawrence Lake Marina station in Pool 8 (water level fluctuating between 0.2 and 3.16 m, water less turbid than in Pool 13). Assuming that the presence of at least one, default-sized tuber at the end of the year would allow the wildcelery population to persist, the simulation indicates that a suitable environment exists for wildcelery at all stations in Pool 8 but not in Pool 13.

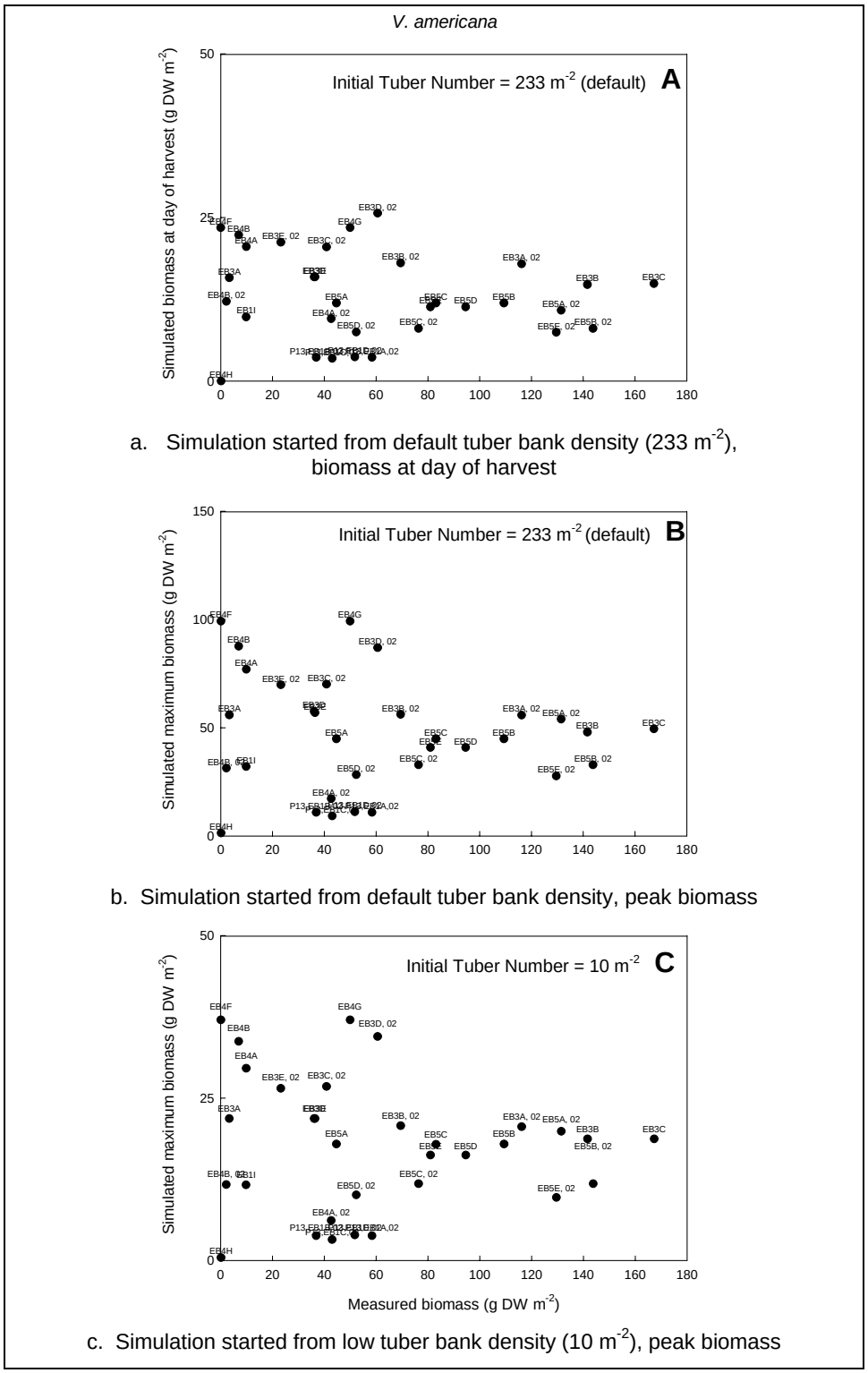

a. Simulation started from default tuber bank density (233 m^{-2}), biomass at day of harvest

b. Simulation started from default tuber bank density, peak biomass

c. Simulation started from low tuber bank density (10 m^{-2}), peak biomass

Figure 17. Plots of simulated versus measured shoot biomass of wildcelery

Simulated peak biomass, started from default tuber bank density, was also generally lower than mean measured shoot biomass (Figure 17b), and in 16 out of 32 cases simulated biomass was within, or close to, the range of values measured at each individual site at each station (Table 3).

When started from a low tuber bank density of 10 tubers m^{-2}, **simulated peak biomass** was far lower than mean measured shoot biomass (Figure 17c). In 12 out of 32 cases, simulated biomass was within, or close to, the range of, values measured at each individual site at each station (Table 3).

Comparison of Simulated and Measured Shoot Biomass *P. pectinatus*

For sago pondweed, **simulated shoot biomass at the day of harvest**, started from a low tuber bank density of 10 tubers m^{-2}, was higher than mean measured shoot biomass (Figure 18a). In only 2 out of 29 cases, simulated biomass was within the range of, or close to (in case only one measured value existed) the values measured at each individual site of each station (Table 4). Simulated biomass fell within the full range of shoot biomass measured at all sites of the Target Lake and Lawrence Lake stations in 2001, but exceeded the full range at all other stations.

Measured shoot biomass varied considerably between all sites per individual station. Part of this variation was probably due to temporary desiccation, where rooting depth was <0.1 m, and to competition for space and/or light by other aquatic plants (Table 4). In contrast, **simulated** shoot biomass was similar at all sites per individual station, since initial plant characteristics were equal and all environmental factors except rooting depth were the same (Table 4). The shoot biomass simulated for a sago pondweed vegetation at a rooting depth<0.1 m is believed not to be realistic, since the modeled spatial distribution of biomass over the water column requires a water depth of $\geq$0.2 m (Best and Boyd 2003a).

Simulated shoot biomass varied among stations. As was the case for wild-celery, the combination of rooting depth, water transparency, water temperature and current velocity produced the lowest peak shoot biomass production at the Channel station in Pool 13 and the highest at the Lawrence Lake Marina station in Pool 8. Assuming that the presence of at least one, default-sized tuber at the end of the year would enable the persistence of a sago pondweed population, the pertinent environmental factors allowed persistence of sago pondweed at all stations except Lawrence Lake in Pool 8 but not in Pool 13.

Simulated peak biomass, started from a low tuber bank density, was also higher than mean measured shoot biomass (Figure 18b), and in only 1 out of 29 cases was the simulated biomass within the range of the measured values (Table 4).

When started from the default tuber bank density, **simulated peak biomass** was far higher than mean measured shoot biomass (Figure 18c).

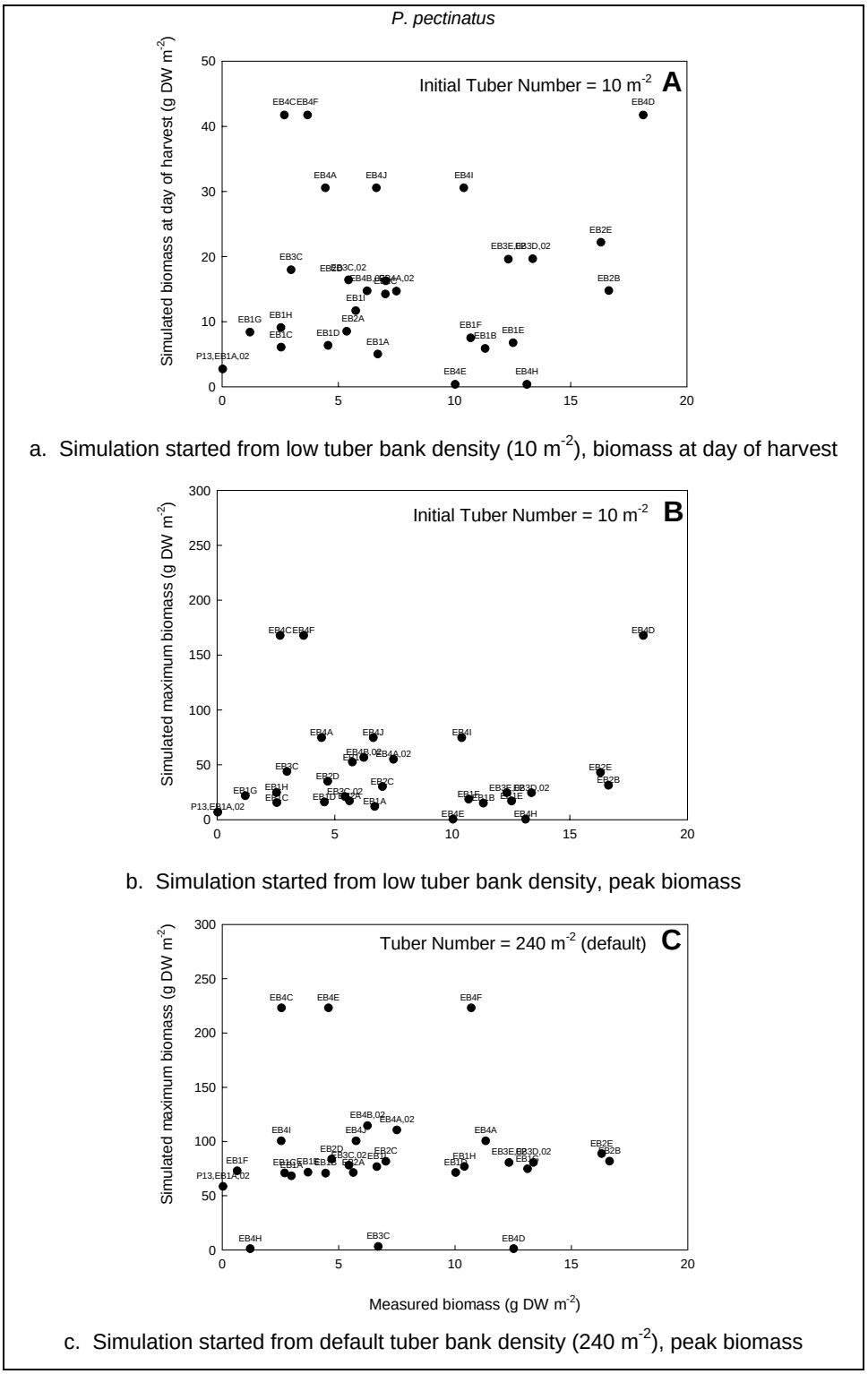

a. Simulation started from low tuber bank density (10 m^{-2}), biomass at day of harvest

b. Simulation started from low tuber bank density, peak biomass

c. Simulation started from default tuber bank density (240 m^{-2}), peak biomass

Figure 18. Plots of simulated versus measured shoot biomass of sago pondweed

6 Discussion Refined Model Performance

Sensitivity Analysis

Process variable analysis

A sensitivity analysis of a simulation model is required to assess the parameters likely to strongly affect model behavior. The current analysis was based on the effect of a change in a parameter when all other parameters are kept the same. Each parameter was once increased by 20 percent and once decreased by 20 percent. The relative sensitivity (RS) of a parameter was then defined as the relative change in the variable on which the effect was tested divided by the relative change in the parameter (Ng and Loomis 1984). The effects of 10 parameters on 2 variables, representing plant biomass aspects, were tested. A model variable is considered sensitive to a change in the value of a parameter at RS>0.5 and <-0.5. The current sensitivity analysis was performed over a one-year period.

$$RS = \frac{(yield_i - yield_r)/yield_r}{(param_i - param_r)/param_r}$$

where

$yield_i$ = value at parameter value *i*

$yield_r$ = value at reference parameter value

$param_i$ and $param_r$ as *above*

VALLA. As reference level for American wildcelery, the nominal parameter values were chosen as presented in Appendix A, Table 1, under Chenango Lake, New York conditions at 1.4 m water depth. In a one-year simulation starting with a tuber size of 0.09 g DW and a tuber bank density of 233 m^{-2}, the value of the parameter under study was changed. The results were compared with those of a nominal run.

Maximum plant biomass proved most sensitive to changes in potential CO_2 assimilation at light saturation for shoots, but far less sensitive to changes in light use efficiency (Table 7). Maximum biomass was also strongly affected by changes in plant density, but less than by photosynthetic activity at light saturation. It was more strongly influenced by pre-anthesis than by post-anthesis development rate. It was strongly influenced by individual tuber weight

Table 7
Relative Sensitivity of Two VALLA Model Variables to Deviations in Parameter Values from Their Nominal Values as Presented in Appendix A -Table 1 (Results were obtained in a 1-year simulation under Chenango Lake, New York, 1978 conditions, starting from 233 tubers m^{-2})

Parameter Name	Parameter Value	Relative Sensitivity	
		Maximum Live Plant Biomass	End-of-Year Tuber Number
Potential CO_2 assimilation rate at light saturation for shoot tips	0.0165		
	0.0200	5.00	4.46
	0.0149	3.02	2.04
Light use efficiency	0.000011		
	0.000013	0.50	-0.73
	0.000008	0.56	1.44
Relative death rate leaves, stems and roots	0.021		
	0.025	2.25	0.71
	0.017	-3.03	0.22
Individual tuber weight	0.090		
	0.108	3.25	-1.79
	0.072	-0.92	-0.03
Relative conversion rate of tubers into plant material	0.0576		
	0.069	2.65	-0.43
	0.046	-1.37	2.33
Relative tuber growth rate	0.247		
	0.296	1.76	-0.77
	0.198	-2.62	2.19
Plant density	30		
	36	3.39	-0.01
	24	-0.82	2.71
Pre-anthesis development rate	0.015		
	0.018	0.56	-2.5
	0.012	-6.04	-1.39
Post-anthesis development rate	0.040		
	0.048	0.98	-2.47
	0.032	-2.19	0.24

and relative death rate of shoots and roots. Effects of changes in relative conversion rate of tubers into plant material and of relative tuber growth rate were in the same order of magnitude, and lower than those of changes in the other parameters.

In general, the same parameter changes that influenced maximum plant biomass were important determinants of end-of-year tuber numbers, with potential CO_2 assimilation at light saturation, development rates, and plant density exhibiting the largest effects. This illustrates the utmost importance of the tubers for local survival and biomass production of wildcelery.

Earlier or later flowering biotypes are suited to different environments. The effect of flowering date can be tested with the model by varying the development rate of the vegetation. Slower rates represent later and faster rates earlier biotypes. Development rate slower or faster than the nominal rate leads to lower biomass. Faster development leads to a shorter growing season and less vegetative dry matter, incomplete light interception, and lower carbohydrate availability for organ formation. At the same time, however, the rate of organ formation increases but the duration of each organ formation shortens. Intuitive prediction

of biotype behavior under such highly variable climatic conditions is therefore hazardous. The model shows some promise in being able to reproduce some of these complex responses of the vegetation and may be useful in evaluating long-term implications of differences in development rate.

Although as far as we know no publications exist on what the temperature requirements of aquatic plants are to traverse development from anthesis to senesced state, differences in post-anthesis development rates for several wheat and rice cultivars are known to be small and have little effect on yield (Van Keulen 1976).

Maximum plant biomass proved to be sensitive to changes in all development rates except an increase in pre-anthesis development rate, while end-of-year tuber number was sensitive to changes in all development rates except a decrease in post-anthesis development rate. Intuitive prediction of aquatic plant biotype behavior under variable climatic conditions is hazardous. The VALLA and POTAM models show promise in being able to reproduce some of the complex vegetation responses ,and may be useful in evaluating long-term implications of differences in development rate.

POTAM. As reference level, the nominal parameter values were chosen as presented in Appendix A, Table 2, under Western Canal, The Netherlands, conditions at 1.3 m water depth. In a one-year simulation starting with a tuber size of 0.083 g DW and a tuber bank density of 240 m^{-2}, the value of the parameter under study was changed. The results were compared with those of a nominal run.

Maximum plant biomass proved most sensitive to changes in potential CO_2 assimilation at light saturation for shoots, but not to changes in light use efficiency (Table 8), the latter in contrast to VALLA. It was also strongly affected by changes in pre-anthesis development rate. Maximum plant biomass proved to be insensitive to changes in the other parameters tested.

End-of-year tuber number was sensitive to seven out of the nine parameters tested. Sensitivity was greatest to changes in pre-anthesis development rate, followed by changes in relative tuber growth rate, potential assimilation rate, light use efficiency, post-anthesis development rate, plant density, and relative death rate of the plants. End-of-year tuber number was insensitive to changes in individual tuber weight and relative conversion rate of tubers into plant material. This illustrates the utmost importance of the tubers for local survival and biomass production of sago pondweed.

A faster pre-anthesis development rate than the nominal one leads to a lower peak plant biomass and end-of-year tuber number, but a slower pre-anthesis development rate to a lower peak plant biomass and higher end-of-year tuber number. The decreased peak biomass and increased tuber number in the latter case may be due to the relatively longer period in summer in which tubers can be initiated at the cost of plant biomass formation. Faster pre-anthesis development leads to a shorter growing season and less vegetative dry matter, incomplete light interception, and lower carbohydrate availability for organ formation. At the same time, however, the rate of organ formation increases, but the period in

Table 8
Relative Sensitivity of Two POTAM Model Variables to Deviations in Parameter Values from Their Nominal Values as Presented in Appendix A -Table 2 (Results were obtained in a 1-year simulation under Western Canal, The Netherlands, 1987 conditions, starting from 240 tubers m^{-2})

Parameter Name	Parameter Value	Relative Sensitivity	
		Maximum Live Plant Biomass	End-of-Year Tuber Number
Potential CO_2 assimilation rate at light saturation for shoot tips	0.019		
	0.0228	1.720	-1.577
	0.0152	1.941	5
Light use efficiency	0.000011		
	0.000013	0.245	-0.832
	0.000008	0.324	-3.095
Relative death rate leaves, stems and roots	0.047		
	0.0564	0	0
	0.0376	0	-2.931
Individual tuber weight	0.083		
	0.0996	0.246	0
	0.0664	0.341	0.192
Relative conversion rate of tubers into plant material	0.0576		
	0.069	0.092	0
	0.046	0.136	0
Relative tuber growth rate	0.19		
	0.228	-0.103	-2.153
	0.152	-0.102	5
Plant density	30		
	36	0.276	1.204
	24	0.346	1.140
Pre-anthesis development rate	0.015		
	0.018	-1.360	-3.363
	0.012	-0.913	4.914
Post-anthesis development rate	0.040		
	0.048	-0.392	-0.426
	0.032	-0.451	-3.123

which each organ is formed shortens. Changes in post-anthesis development rates did not affect peak plant biomass to a large extent, but a slower rate did decrease the end-of-year tuber number. The latter decrease may be due to the relatively shorter period in which tubers can be initiated determined by the plants' development stage concomitant with the occurrence of suitable environmental conditions for tuber initiation.

Environmental factor analysis

The impacts of various changes in environmental factors were assessed using the relative sensitivity of the affected variables as "measure." For this purpose, parameter changes were based on value ranges taken from literature, which sometimes differed more than 20 percent from the nominal parameter value given in Appendix A, Table 1.

Climate

Climate greatly affects plant species distribution, phenological cycle, and biomass production. Both models can be used to calculate climate change effects on the chronological timing of the phenological events and on biomass production. The models cannot be used to assess climate change effects on (1) plant species distribution and (2) the phenological cycle itself since the phenological cycle has been used for calibration.

VALLA. Running the model under more southern climatological conditions, i.e. changing the latitude from 42^{o} N to 27^{o} N demonstrated that end-of-year tuber number is more sensitive to this climate change than maximum plant biomass (Table 9).

Table 9
Environmental Factor Analysis, Expressed as Relative Sensitivity of Two VALLA Model Variables to Deviations in Parameter Values from Their Nominal Values as Presented in Appendix A -Table 1 (Results were obtained in a 1-year simulation under Chenango Lake, New York, 1978 conditions, starting from 233 tubers m^{-2})

Parameter Name	Parameter Value	Relative Sensitivity	
		Maximum Live Plant Biomass	End-of-Year Tuber Number
Climate			
Chenango Lake (1978)	Latitude 42^{o} N	-	-
Ft. Lauderdale ponds (1975-84)	Latitude 27^{o} N	-0.49	-0.87
Light reflection coefficient by water surface	0.06		
	1.00 (+1567%)	-0.06	-0.06
	0.00* (-100%)	-0.43	-0.05
Light extinction coefficient water column	0.43		
	0.52 (+20%)	2.09	0.04
	0.34 (-20%)	-2.79	0.66
Water depth	1.4		
	1.7 (+20%)	1.47	-2.16
	1.1 (-20%)	-2.43	0.48

Note: To enable calculation of the RS, a very low value of 0.000001 was used.

POTAM. Running the model under more southern climatological conditions, i.e. changing the latitude from 52^{o} N to 38^{o} N demonstrated that both maximum plant biomass and end-of-year tuber number are sensitive to this climate change (Table 10).

Light reflection coefficient by water surface

The irradiance reflected by the water surface usually averages about 6 percent over a day. The values of this parameter tested were 0 and 1. Reflection may theoretically have the value 0 when no reflection occurs at a 90^{o} incoming angle of the radiation on a completely calm water surface (wind and wave action are minimal). The highest value of 1 may occur at a close to 180^{o} incoming angle of the radiation and at very rough water surfaces.

Table 10
Relative Sensitivity of Two POTAM Model Variables to Deviations in Parameter Values from Their Nominal Values as Presented in Appendix A - Table 2 (Results were obtained in a 1-year simulation under Western Canal, The Netherlands, 1987 conditions, starting from 240 tubers m^{-2})

Parameter Name	Parameter Value	Relative Sensitivity	
		Maximum Live Plant Biomass	End-of-Year Tuber Number
Climate			
Zandvoort, NL (1987)	Latitude 52° N	-	-
Davis, CA (1990)	Latitude 38° N	-1.540	1.425
Light reflection coefficient by water surface	0.06	0	-
	1.00 (+1567%)	-0.063	-0.063
	0.00* (-100%)	-0.016	0.085
Light extinction coefficient water column	1.07		
	1.284 (+20%)	-0.122	0.181
	0.856 (-20%)	-0.084	0.426
Water depth	1.3		
	1.56 (+20%)	-0.019	0
	1.04 (-20%)	0.034	0

Note: To enable calculation of the RS, a very low value of 0.000001 was used.

VALLA. Increasing the light reflection coefficient to 1 annihilated plant biomass within the year. That low RS values were nevertheless found (Table 9) is an artifact of the calculation method employed. Decreasing the light reflection coefficient increased maximum biomass and end-of-year tubers to a relatively small extent, probably because the majority of the plant material is located in the lower half of the water column (Table 9).

POTAM. Increasing the light reflection coefficient to 1 brought plant biomass back to zero within the year. That low RS values were nevertheless found (Table 10) is an artifact of the calculation method employed. Decreasing the light reflection coefficient barely affected maximum biomass and end-of-year tubers, probably because the majority of the plant material is located at the water surface (Table 10).

Light extinction coefficient of water column

VALLA. A light extinction coefficient of on average 0.43 m^{-1} is used for nominal runs of the model (Chenango Lake, New York). Changing the light extinction coefficient of the water column demonstrated large effects on maximum plant and smaller ones on end-of-year tuber numbers. A nominal value of 2 m^{-1} has been found typical for eutrophic fen lakes where submersed vegetation can just persist (Best et al. 1985).

POTAM. A light extinction coefficient of on average 1.07 m^{-1} is used for nominal runs of the model (Western Canal, The Netherlands). Changing the light extinction coefficient of the water column demonstrated small effects on maximum plant and larger effects on the end-of-year tuber numbers.

Water depth

VALLA. This model has been calibrated for a water depth of 1.4 m, the rooting depth of an extensively studied wildcelery community in Chenango Lake, New York. The model has the capability to respond to fluctuations in water level between years and within year, by (re)distributing plant biomass over the desired water depth (number of water layers). This technique for biomass distribution over the vertical axis of the community works well and gives realistic outcomes over a depth range of 0.5 to 6 m. Running VALLA at an increased or decreased water depth showed considerable effects on maximum plant biomass and end-of-year tuber number (Table 9). The RS of peak plant biomass and of end-of-year tuber number to changes in water depth was in the same order of magnitude as to changes in light extinction coefficient.

POTAM. This model has been calibrated for a water depth of 1.3 m, the rooting depth of an extensively studied sago pondweed community in the Western Canal, The Netherlands. Running POTAM at an increased or decreased water depth showed negligible effects on maximum plant biomass and end-of-year tuber number, probably because the majority of the plant material is located at the water surface. Larger effects are expected in plants with most of their biomass located near the sediment, such as American wildcelery.

The Models are Sensitive

The sensitivity and environmental factor analyses give indications of the sensitivity of maximum plant biomass and end-of-year tuber number for variations in plant parameters and environmental factors over a one-year period.

The models are sensitive to changes in light climate experienced by the submersed plants because they are based on carbon gain through the plant. The models account for variations in light climate for submersed plants due to changes in climate, water transparency, water depth, self-shading, and epiphyte shading, but not for those caused by floating-leaved plants and floating debris. The models are also sensitive to changes in temperature (water or air, depending on which of the two is used as model input), through the coupling of plant development to 3 °C-degree day sum, and through the temperature coefficients used in respiration and senescence processes. The models are also sensitive to changes in current velocity (not included in the sensitivity analysis), but they do not account for effects of developing plant beds on current velocity within the plant bed. The latter effects may also significantly affect plant biomass production.

It is to be expected that the small changes that occurred over the relatively short one-year period will increase with time and that extrapolations in time will yield information on the likelihood for plant populations to ultimately persist or become extinct. In particular, increased water turbidity, because of increased phytoplankton or epiphyte growth stimulated by eutrophication, increased erosion/resuspension, and seasonal herbivory have been mentioned as decisive for the persistence of submersed plant populations.

Discussion of Performance of Refined Models and Discrepancies Between Model Results and Validation Data

Two simulation models for the biomass dynamics of the submersed American wildcelery and sago pondweed have been refined. The original models allowed calculations of the effects of several environmental factors that affect biomass dynamics, including site-characteristic changes in climate, water temperature, water transparency, water level, pH and oxygen on carbon assimilation at light saturation, wintering strategies, and removal of shoot or tuber biomass (by mechanical harvesting, grazing, or wave action). The refinement expanded the model capabilities with calculations of the effects of current velocity on plant biomass and the effects of epiphyte shading on the light availability for the plant. Additional calibration data needed for the model expansions were collected in small-scale field studies described in Chapters 7, 8, and 9. A validation field data set on plant biomass of American wildcelery and sago pondweed, and on pertinent environmental factors pertaining to the same sites, was collected. The models enable the simulation of plant and tuber behavior over periods varying from one to three years, and they may be used to explore the habitat sustainability for the persistence of populations of wildcelery and sago pondweed in established plant beds. Grazing can be introduced in the simulations by decreasing the initial tuber bank density and/or removing shoot biomass at various, user-defined water depths during the growth season.

The refined aquatic plant growth simulation models generated shoot biomass data that were often in the same range as the measured data. Explanations for simulated values outside the range of the measured values may be among the following:

a. Simulated plant development was slightly delayed compared to local plant development in the UMR for wildcelery, but matched for sago pondweed.

b. Field data on shoot biomass were highly variable. This may be due to (1) highly variable environmental conditions at the five sites located close to each monitoring station, (2) highly variable substrate conditions (which are not taken into consideration in the model), (3) difficulty in harvesting exactly 0.25 m^2 shoot biomass of a submersed vegetation, and (4) harvesting of mixed vegetation, with submersed species other than wildcelery or sago pondweed sometimes predominating, or at least competing for resources.

c. The environmental data were collected at monitoring stations usually located outside plant beds. Within plant beds the current velocity is greatly decreased and water transparency far higher than in the open water, leading to far lower simulated biomass values than measured. Results of special simulations conducted for wildcelery at Turtle Island and Above Dam 8 in 2001, using a low light extinction coefficient of 1.1 m^{-1} typical for the clear-water phase in Pool 8 in winter (Sullivan 2000), indicated that simulated shoot biomass increased markedly under the latter conditions and matched the measured range (Figure 19).

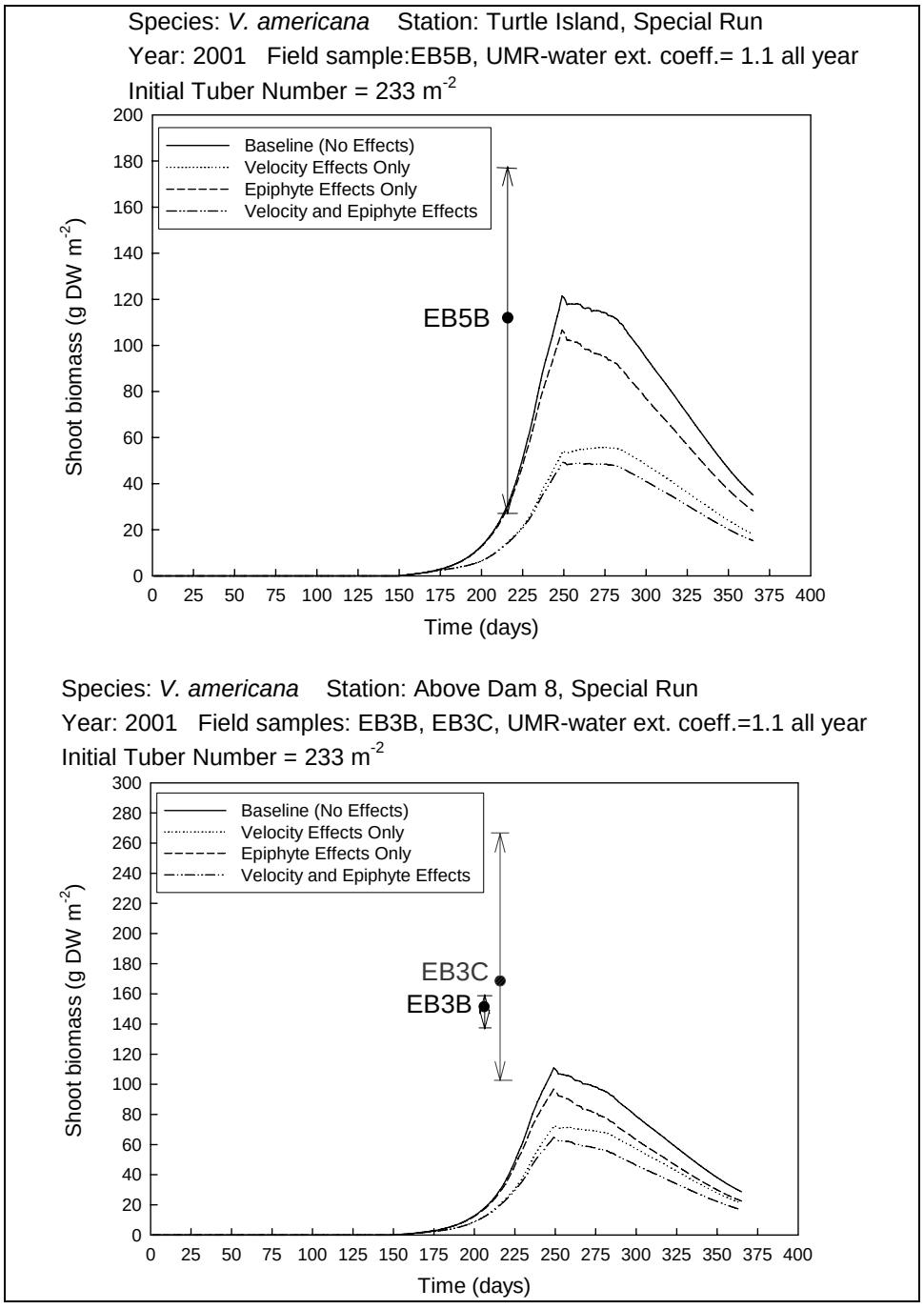

Figure 19. Special simulations conducted to explore reasons for discrepancies between simulated and measured values for wildcelery (Case - *Turtle Island:* Simulated shoot biomass increased by 20 percent in runs with a low light extinction coefficient as found in well-developed plant beds. All simulated peak biomass values, either or not accounting for current velocity and epiphyte shading effects, fell within the measured range. Case - *Above Dam 8:* Simulated values increased by 20 percent, and peak biomass fell within the range of one of the five sites sampled at Dam 8 (EB3C)).

d. The measured shoot biomass data of wildcelery were often higher than simulated. This may point to overestimating the measured biomass caused by the harvesting method used.

e. The actual initial tuber bank density and tuber size in the UMR were largely unknown. A simulation for sago pondweed starting from default values strongly overestimated measured shoot biomass. However, populations may start from far lower tuber bank densities, particularly in cases where the population is grazed by waterfowl, and/or tuber production is prevented by breakage of senescing shoots by water movements. This is illustrated by the results of a special simulation conducted for sago pondweed at Lawrence Lake Marina in 2001, starting from 1 tuber m^{-2}, and otherwise default values. Under these conditions simulated shoot biomass was within the measured range (Figure 20).

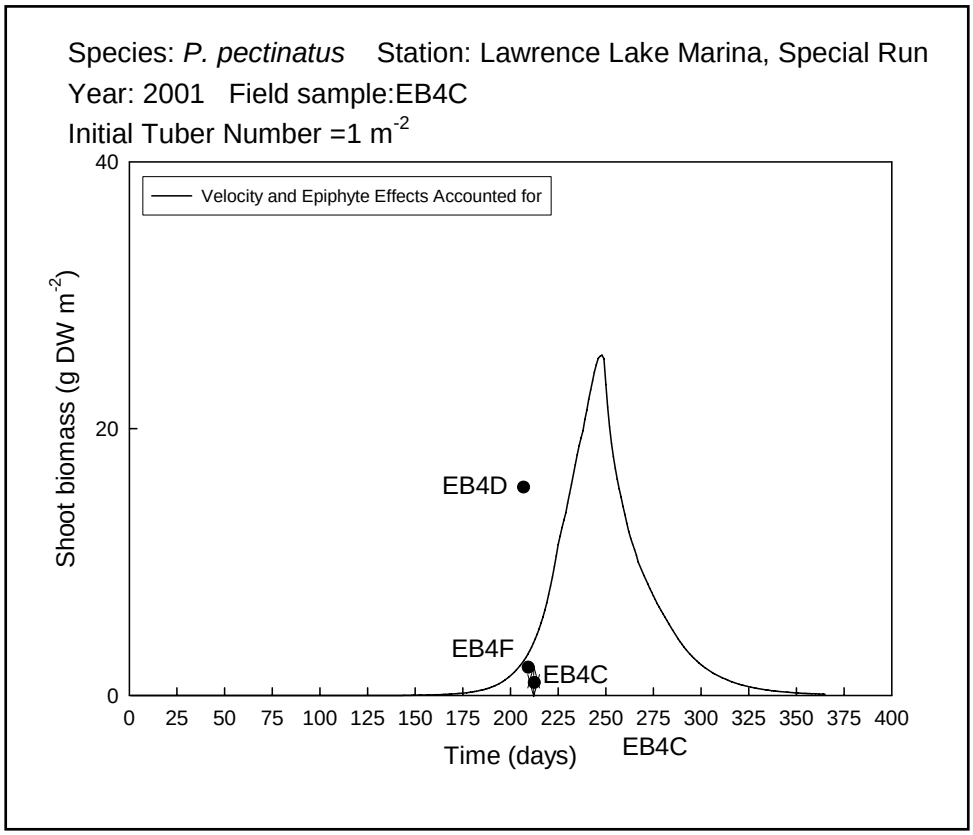

Figure 20. Special simulations conducted to explore reasons for discrepancies between simulated and measured values for sago pondweed (Case - *Lawrence Lake Marina:* Simulated shoot biomass greatly decreased in runs started from a very low tuber bank density that may occur under heavy grazing pressure. Simulated shoot biomass at the day of harvest was close to the mean measured values at sites EB4C and EB4F, peak biomass was higher than measured biomass at site EB4D-but a local temperature regime slightly different from the measured temperatures at the monitoring station could easily shift the simulated biomass curve in the direction of the measured biomass value.)

Importance of Initial Values

The simulated biomass resulting from runs started from default tuber density/ tuber size was in the same range as the measured biomass for wildcelery, but consistently overpredicted measured plant biomass of sago pondweed. The latter observation led us to believe that in UMR Pool 8 the sago pondweed vegetation may start from a far lower tuber density (in the order of 10 m^{-2}) than default (240 m^{-2}), possibly because of the high grazing pressure by waterfowl. Interpretation of simulated plant biomass data by comparison with measured values was greatly impeded by (a) the large variability in measured shoot biomass data, (b) the lack of measured plant growth curves, tuber bank density, and tuber size, and (c) the relative scarcity of measured environmental data requiring large-scale interpolation and derivation of values pertaining to other sites within the same water body.

Conclusions and Recommendations

Conclusions

We conclude that the refined models can be used to explore effects of changes in existing river management practices that affect the physical environment for submersed aquatic plants, and to implement operational scenarios aimed at conserving and establishing submersed aquatic vegetation. Grazing can be introduced in the simulations by decreasing the initial tuber bank density and/or removing shoot biomass at various water depths during the growth season.

Based on our simulations using the refined models, we believe that at the field sites in UMR Pool 8:

a. Wildcelery populations may grow from the default values for tuber bank density, tuber size/concurrently initiated tuber number, and self-shading coefficient, with effects of current velocity and epiphyte shading approximated by the equations currently inserted into the VALLA Version 2.0 source code.

b. Sago pondweed populations may grow from the low tuber bank density of around 10 tubers m^{-2} or less, the default tuber size/concurrently initiated tuber number, and a self-shading coefficient that may vary with the water level fluctuations between the default value of 0.095 $m^2\ g^{-1}$ DW at a high water level and 1.79 $m^2\ g^{-1}$ DW at a low water level, with effects of current velocity and epiphyte shading approximated by the equations currently inserted into the **POTAM Version 2.0** source code.

Recommendations

These models can be helpful in evaluating alternative management scenarios aimed at conserving and establishing submersed aquatic vegetation. If these models are applied to other locations, we strongly recommend that sufficient field data be collected on environmental conditions (such as climate, typical

water transparency, depth, and current velocity) and plant parameters (such as tuber bank density and tuber size) to accurately initiate the model runs.

7 Field Study to Determine the Effect of Current Velocity on Plant Biomass of *V. americana*

Introduction

A short-term field study was conducted to quantify the effect of current velocity on the biomass production of American wildcelery in the Red Cedar River, Barron County, Wisconsin, a relatively slow-flowing, clear river close to the UMRS in the United States. The study encompassed one-season determinations of current velocity and plant biomass production of natural and planted wildcelery plants at sites covering a current velocity range over which considerable effects on macrophyte biomass are to be expected (Biggs 1996). The experiments were conducted from June through August, 2002. The experimental approach was modified after Chambers et al. (1991).

Methods

Site description

The Red Cedar River is a tributary of the Chippewa River in west-central Wisconsin and originates at Red Cedar Lake in Barron County. The river flows southward through a watershed predominated by agriculture in the Barron and Dunn counties. The field site selected for the study is located in Cameron, East of Barron, Wisconsin (Figure 21; UTM coordinates: 596387 E, 5026985 N). Selection of the site was based on the presence of a relatively uniform submersed plant cover with wildcelery predominating and being representative of general stream conditions (Borman and Schreiber 1992). At this field site, four plant beds were selected for monitoring and experimental activities, based on the criterion that the current velocities at these beds ranged from 0.19 to 0.78 m s^{-1} at the beginning of the study, a range within which significant effects on plant biomass could be expected (Chambers et al. 1991). The plant beds were characterized as: near the border of the river (B), fast-flowing (F), mid-streams (M), and in shallow water (S) (Figure 22). The study was started on 12 June, and three additional field visits were made on 24 June, 22 July, and 5 August, 2002.

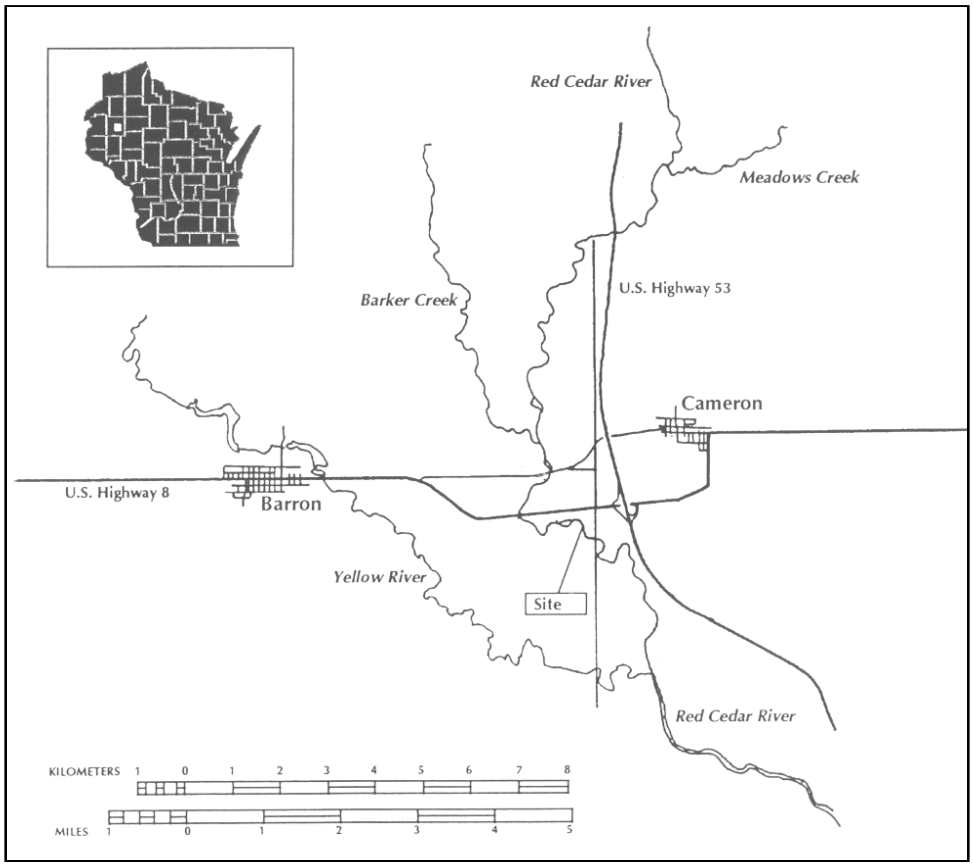

Figure 21. Location of the Red Cedar River in Wisconsin

Plant biomass production

Natural Wildcelery Plants. At each field visit and site, except the first visit, five plant biomass samples were harvested within a 0.2 m × 0.2 m quadrat at each of four sample plant beds. Biomass samples consisted of shoots and belowground organs rooting up to a depth of 0.3 m into the river bed. The plant samples were stored in plastic bags, transported in a cooler on ice, and fresh and dry (24 h at 105 °C) weights were determined in the laboratory.

Planted Wildcelery Plants. During the first field visit, wildcelery sprouts (arising from winter buds) were planted in buckets, filled with local river sediment (six sprouts per bucket; five buckets per site), and buckets were inserted into the river bottom adjacent to the four natural plant beds at depths ranging from 0.30 to 0.68 m. The plant material was purchased from Wildlife Nurseries, Oshkosh, WI. The dimensions of the buckets were 4.8 L (1-gallon) and 0.0266 m^2 surface area. The sediment surface in the buckets was covered by a layer of cobblestones to prevent uprooting of the seedlings. All plant biomass was harvested at the end of the eight-week period and transported to the laboratory. These plant samples were processed in the same manner as the natural plants.

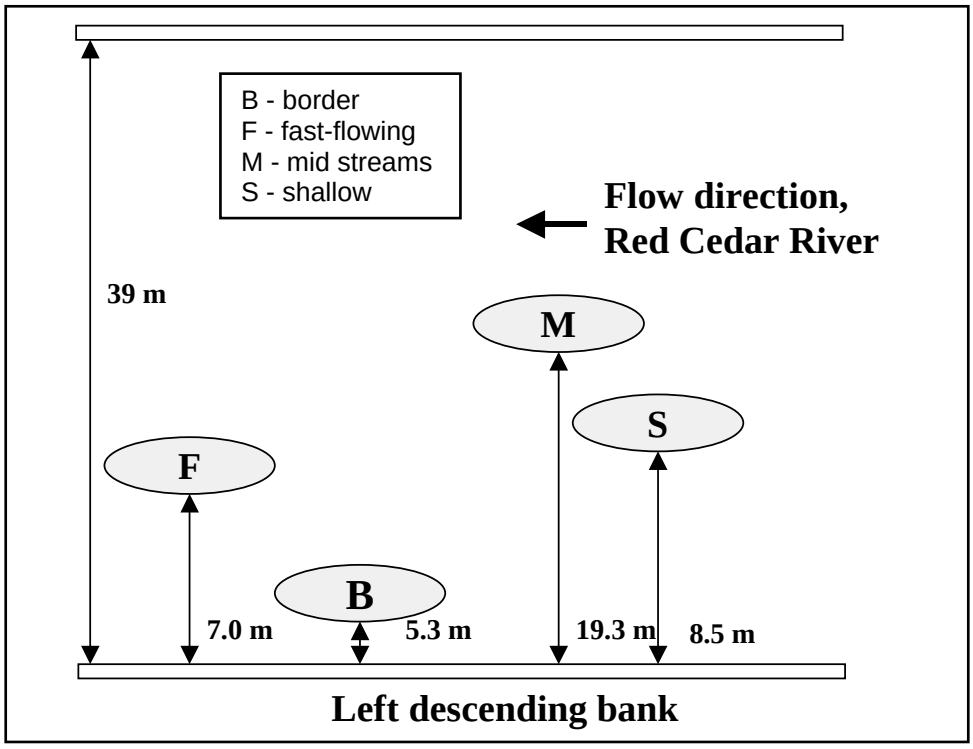

Figure 22. Location of the wildcelery beds at the field site in the Red Cedar River at Cameron, Wisconsin

Determinations of current velocity and underwater light climate in the field

During each field visit, depth (m) of the water column was determined at each site, and five series of readings on current velocity and water transparency, respectively, were taken. Current velocity (m s^{-1}) was measured within each plant bed with a FLO-MATE flow meter (Marsh-McBirney, Inc., Model 2000, Frederick, MD) at every 0.10 m, beginning from the river sediment to the water surface. Each reading represented a value integrated over a 6-s period. Water transparency was determined by measuring the light within the water column (μmol s^{-1} m^{-2}) using an underwater quantum sensor (LI-COR, Inc, LI-192SA, Lincoln, NE) just above and just below the water surface, and every 0.10 m between the water surface and river bottom.

Results and Discussion

Plant biomass at the end of the eight-week growth period was variable, but usually in the same order of magnitude in both the natural and planted vegetation (211-332 g DW m^{-2}; Table 11). Natural plant biomass was higher at bed F than at all other sites. The extremely high value of 1808 g DW m^{-2} reported for natural vegetation on 5 August (day 217) at bed F is believed to be an artifact, possibly caused by harvesting a larger area than the quadrat surface area, since the highest published biomass for wildcelery is 496 g DW m^{-2} (Haller 1974). This high value was omitted from the calculations.

Table 11
Density and Biomass of *V. americana* Plant Beds at the Field Site in the Red Cedar River at Cameron, Wisconsin, in 2002. Initial planted biomass was 51.9 ± 14.8 g DW m^{-2}

Plant Bed [1]/ day #	Distance From Left Shore (m)	Current Velocity[2] (m s^{-1})	Water Transparency (% irradiance at river bottom)	Plant Biomass (g DW m^{-2})			
				Natural		Planted	
				Shoots	Plants	Shoots	Plants
B, day 163	5.3	0.19 ± 0.02					
B, day 175		0.46 ± 0.02	51.9 ± 6.1	39.4 ± 16.8	68.3 ± 27.9		
B, day 203		0.35 ± 0.02	9.4 ± 3.2	231.8 ± 120.5	293.4 ± 152.8		
B, day 217		0.39 ± 0.02	35.3 ± 10.1	169.7 ± 133.2	220.3 ± 171.7	184.4 ± 71.5	266.8 ± 102.4
F, day 163	7.0	0.47 ± 0.01					
F, day 175		0.59 ± 0.01	31.9 ± 4.4	81.8 ± 17.1	113.0 ± 23.9		
F, day 203		0.14 ± 0.01	33.4 ± 15.5	264.3 ± 114.5	342.7 ± 133.9		
F, day 217		0.17 ± 0.01	20.0 ± 6.7	136.2 ± 50.4 [3]	754.3 ± 153. 0 [3]	214.7 ± 69.2	298.5 ±92.4
S, day 163	8.5	0.50 ± 0.01					
S, day 175		0.87 ± 0.04	29.7 ± 11.8	50.6 ± 15.5	84.2 ± 30.1		
S, day 203		0.27 ± 0.02	51.4 ± 21.5	186.9 ± 116.8	253.0 ± 152.9		
S, day 217		0.25 ± 0.0	16.9 ± 10.3	172.2 ± 117.8	221.2 ± 149.5	259.0 ± 177.2	332.6 ± 224.9
M, day 163	19.3	0.78 ± 0.03					
M, day 175		0.95 ± 0.0	26.7 ± 5.8	25.5 ± 10.6	39.8 ± 16.2		
M, day 203		0.51 ± 0.01	41.0 ± 4.4	193.7 ± 102.9	255.8 ± 126.9		
M, day 217		0.41 ± 0.03	29.5 ± 2.9	213.7 ± 166.7	272.4 ± 207.2	133.2 ± 46.9	211.3 ± 71.7

[1] B – border; F – fast-flowing; M – mid streams; S – shallow.
[2] Means all current velocities measured at 0.1 m intervals over the vertical axis of the water column.
[3] Unrealistically high value omitted.

The selection of the plant beds at the beginning of the study was based on the criterion that the current velocities at these sites ranged from 0.19 to 0.78 m s^{-1}. Current velocity at the beginning of the study increased in the relative order of B< S< F< M up to day 175 (Figure 22). It decreased subsequently relatively more in the F and S beds, resulting in a relative order of F<S<B<M, possibly because of the higher vegetation density in the F and S beds than in the B and M beds (Table 11). Mean current velocity ranged from 0.19 to 0.95 m s^{-1} (Table 11; 0.78 m s^{-1}, when the bottom 0.1 m water layer was omitted from the calculations). The latter values were excluded since the largest fraction of plant biomass exposed to current velocity is usually situated relatively close to the water surface, where current velocity is higher, than close to the bottom.

The on-site current velocity measurements were cross-calibrated with the continuously collected data on water level elevation and discharge at two gauging stations located close to the field site, i.e., a downstream station in the Red Cedar River at Menomonie and a tributary station in the Hay River at

Wheeler, both in Wisconsin. Based on the presumption that the instantaneous current velocity readings (averaged over the height of the water column) would be strongly related to the discharge data at nearby gauging stations, the measured current velocities were related to 15 min. and median daily discharge data of the Red Cedar River and of the Hay River over the plant growth season using linear regression. The measured current velocity data were less closely related to discharge data of the Red Cedar River (R^2 range 7 to 39 percent) than of the Hay River (R^2 range 38 to 65 percent; Table 12), despite the fact that discharge in both rivers was strongly correlated (R^2 = 80 percent). These regressions explained a relatively low part of the variation in the on-site measured current velocity data and, therefore, it was expected that further exploration would not produce better results than found when relating plant biomass to the on-site velocity measurements. However, from this comparison it was concluded that the on-site current velocity measurements had been made at dates representative for the full range of current velocities during the growth season because they coincided with the full range in water level elevations observed at the nearby Hay River, which showed the best fit with the measured data (Figure 23, upper chart).

Table 12
Relationships Between Mean Current Velocity Measured at the Field Site in the Red Cedar River at Cameron and Daily Discharge Data Measured at the Nearby Gaging Stations in the Red Cedar River at Menomonie and in the Tributary Hay River at Wheeler, WI (Y is measured current velocity in m s^{-1}, and X is discharge in ft^3 s^{-1})

Plant Bed [1]	Linear Regression Equation	P-Value	R^2-Value
Related to Red Cedar River, Menomonie			
B	$Y = 9 \times 10^{-5} X + 0.141$	0.54	0.39
F	$Y = 0.0001 X + 0.0963$	0.84	0.17
S	$Y = 0.0002 X + 0.0762$	0.44	0.24
M	$Y = 8 \times 10^{-5} X + 0.4741$	0.90	0.07
Related to Hay River, Wheeler			
B	$Y = 0.0004 X + 0.1385$	0.52	0.44
F	$Y = 0.0008 X – 0.0507$	0.89	0.46
S	$Y = 0.0012 X – 0.1479$	0.58	0.64
M	$Y = 0.0008 X + 0.2517$	0.71	0.38

[1] B – border; F – fast-flowing; M – mid streams; S – shallow.

The median current velocity was calculated for each site over the period in which the natural and planted plants were observed. The median current velocity decreased in the order F<B<S<M, with significant differences between velocities at all sites, and variability increasing with median current velocity (Figure 23, lower chart).

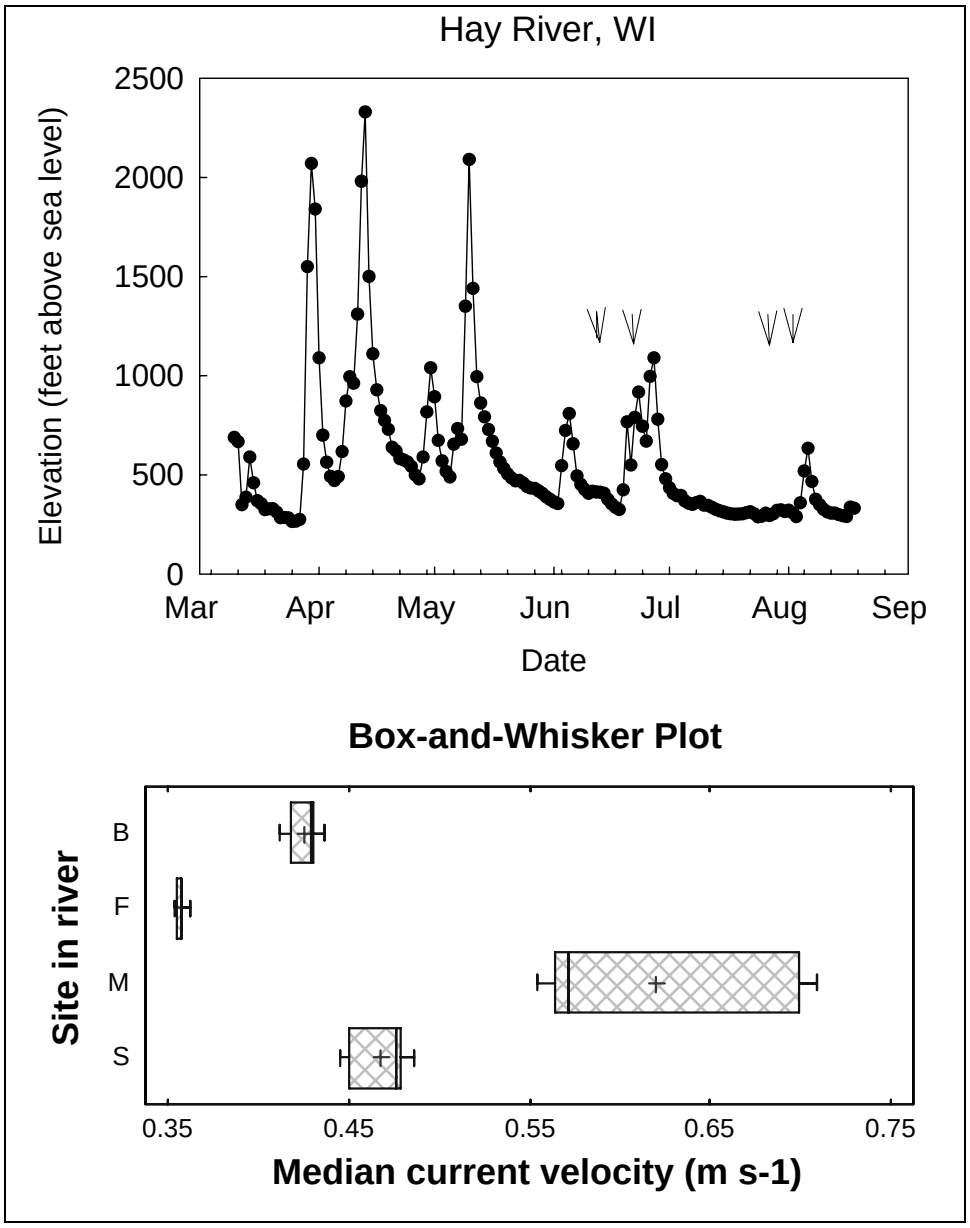

Figure 23. (Upper) Water level elevation of the Hay River at the gauging station at Wheeler, Wisconsin, in 2002. Dates when current velocity was measured in the field marked by arrows. (Lower) Median current velocity over the period in which the natural and planted wildcelery plants were observed in the Red Cedar River

Natural plant biomass increased with time ($p = 0.015$) and decreased with increasing median current velocity ($p = 0.047$), as demonstrated by multiple linear regression. However, both time and median current velocity together explained only 28 percent of the variability in the data set.

Final plant biomass, harvested on 5 August 2002, was related negatively to the median measured current velocity values over the height of the water column, excluding the values measured just above the bottom. Plant biomass (natural and

planted) was statistically significant related to median current velocity ($p = 0.03$). This linear relationship was described by the following equation:

$$Y = 660.29\text{-}742.40\ X$$

where

Y = plant biomass in g DW m^{-2}, and

X = median current velocity in m s^{-1} (Figure 24).

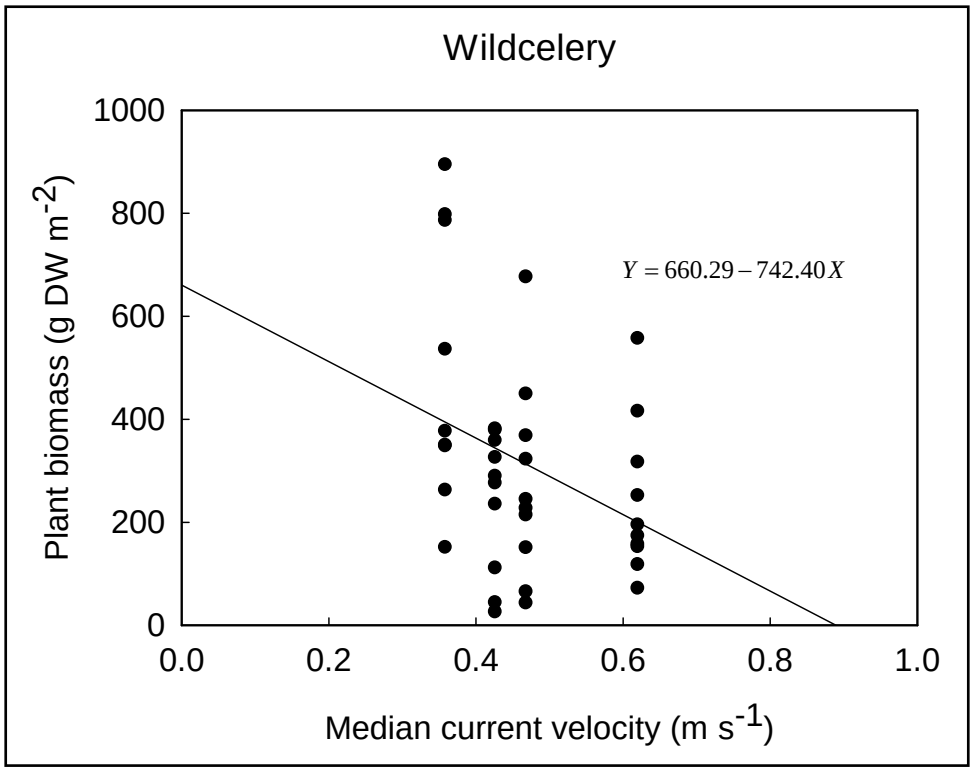

Figure 24. Relationship between median current velocity and final plant biomass of natural and planted wildcelery plants in the Red Cedar River, Wisconsin, in 2002

This equation would pertain to the median current velocity range of 0.35 to 0.70 m s^{-1}, since a regression is valid for the range of data included in the regression, leaving considerable uncertainty on the relationship between median current velocity and plant biomass outside this range. The R^2 of the linear regression fitted to the data was low, i.e., 11 percent, indicating that a relatively small portion of the data set was explained. By substituting 0 for Y, a value of 0.89 m s^{1} was found to be the "critical" current velocity at which wildcelery is prevented from producing biomass.

Analysis of variance indicated that the effect of median current velocity on final plant biomass was significantly different ($p = 0.020$) in natural and planted plants. Subsequent regression analysis of the data pertaining to natural plants alone indicated a significant relationship between final plant biomass and median

current velocity at a 90 percent confidence level ($p = 0.050$) of $Y = 1231.64 – 1736.49\ X$, with a higher R^2 of the linear regression of 19 percent. By substituting 0 for Y, a value of 0.71 m s^{-1} was found to be the "critical" median current velocity at which wildcelery is prevented from producing biomass.

Both "critical" current velocity values, calculated using the regression equations described above, are lower than the "critical value" of 0.94 m s^{-1} found for sago pondweed (Chambers et al. 1991). The value of 0.82 m s^{-1}, i.e., close to the average of the "critical values" found for all natural and planted plants, and that pertaining to natural plants alone, was considered as protective, and this value was further used to calibrate the VALLA model.

8 Field Study to Determine the Shading Effects by Epiphytes on the Light Availability for *V. americana* and *P. pectinatus* in the Upper Mississippi River

Introduction

For submersed plants the light availability within the water column is affected by (a) irradiance at the water surface, (b) water color imparted by dissolved materials, (c) shading by seston (phytoplankton, detritus, and sediment), (d) shading by epiphyton (algae, detritus, and sediment lying on top/attached to submersed plant), and (e) self-shading by plant biomass (Van Duin et al. 2001). A small-scale study was carried out to quantify the epiphyte biomass associated with submersed plant biomass and the tentative epiphytic light attenuating effect, focusing on wildcelery and sago pondweed from the UMR Pools 8 and 13. The study was conducted in July-August 2002. The experimental approach was modified after Sand-Jensen and Sondergaard (1981) and Gons (1982).

Methods

Sample collection in the field

Plant-epiphyte community samples were collected from three stations in Pool 8 (30 and 31 July 2002) and one station in Pool 13 (17 and 18 July 2002). At each station, up to five independent samples were collected, each composed by four quadrants. The total number of independent samples was $5 \times 4 = 20$ (total number of quadrants $5 \times 4 \times 4 = 80$ maximally).

From these field samples, 25 wildcelery and 9 sago pondweed subsamples were selected for inclusion into the epiphyte shading determination. Each subsample was collected by harvesting a few plants from the area included in the plant biomass sampling activities in 2002 (see Chapter 4, *Simulations Using the Refined Models*). Collection was done by gently pulling individual plants from the sediment, avoiding removal of the epiphytes from the plant surface as much as possible. The plants were slowly raised to the water surface and transferred to labeled plastic bags. Three 1-L surface water samples were collected concomitantly and transferred to Nalgene bottles. The plant-epiphyte and water samples were transported in a cooler to the laboratory for further processing. The size of the plant-epiphyte samples had to be kept as small as possible to keep sample processing manageable, but not too small as to make the light interception measurements meaningless.

Separation of plant-epiphyte complex into components

The plant-epiphyte complexes were separated into their components in the laboratory by vigorously shaking them in beakers containing 1 L of tap water using a vibromixer (20 min. per sample at 600 rpm, Lightnin TS2010). This treatment usually removes at least 75 percent of the epiphytes from the plant-epiphyte complexes in alkaline waters (Gons 1982). The plant material was removed from the beakers and further processed. The epiphyte suspensions were transferred into 1-L Nalgene bottles and stored in a refrigerator at 5 °C for further use.

Quantification of plant and epiphyte biomass

The plant material was blotted with paper towels and dried at 105 °C for 24 hours to constant mass. The dry plant samples were weighed to the nearest 0.01 g. The plant surface areas were derived from the plant weights using the total plant surface:dry weight relationships of 0.0715 $m^2\ g^{-1}$ DW for wildcelery and of 0.0149 $m^2\ g^{-1}$ DW for sago pondweed determined also in this study (following Sher-Kaul et al. 1995). The epiphytes in the 1-L epiphyte suspension were vacuum-filtered on a 0.40 μm glass fiber filter (pre-weighed). The suspension contained a large amount of particles, and only 50 mL of each sample could be filtered (in triplicate). The filters were dried at 105 °C to constant weight. After drying, samples were weighed to the nearest 0.001 g. Dry weight of the epiphytes was calculated as the difference between filter + epiphytes and filter alone. The epiphyte weight contained in the 1-L suspension was calculated from the weights of the subsamples. The organic matter content of the dried epiphytes on the filters was determined by loss on ignition at 440 °C, and re-weighing.

Light measurements

Each 1-L epiphyte suspension was poured into a 0.25 × 0.38 m (0.095 m^2) Pyrex glass settling chamber, and spread homogeneously over the surface area of the bottom. The light transmission through the chambers was measured after the settling of the particles was completed (usually 8-12 hours after pouring) using a

terrestrial quantum sensor (LI-COR, Inc, LI-1905A, Lincoln, NE). Eight measurements were taken for each sample. The light transmissions through settling chambers filled with 1-L river water and 1-L tap water, respectively, were also measured. The difference in light transmission through 1-L epiphyte suspension and 1-L river water in the same settling chamber was used as the measure for the epiphyte shading on a 0.095 m^2 surface area (in percent). The epiphyte shading was normalized to the plant surface area from which the epiphytes had been removed, using the plant surface:dry weight relationships. The latter normalization sometimes yields >100 percent light absorption values for epiphytes in cases where the plant surface area from which the epiphytes were removed is smaller than the surface area of the glass settling chamber. The latter is considered an artifact since light can be absorbed for only 100 percent, indicating a thick epiphyte-silt coating of the plants.

Results and Discussion

Light absorption by epiphytes was far lower on wildcelery (43 percent) than on sago pondweed (271 percent; Table 13). The organic matter content of the epiphytes on wildcelery was 23.71 ± 2.87 percent and on sago pondweed 37.62 ± 4.68 percent, indicating that over 50 percent was composed by inorganic material, possibly silt and carbonates.

The calculation of light absorption by epiphytes in the current study was based on the presumption that epiphytes were distributed more or less homogeneously over the plant shoots, including upper and lower sides of the leaves, and stems. Visual inspection of the plants indicated that the upper leaf surfaces were covered by an almost structureless silt layer, whereas the lower leaf surfaces showed the presence of stalked diatoms. However, the method used to separate the plant-epiphyte complex into its components did not allow for distinction between epiphytes on upper and lower leaf surfaces, and on stems. Thus, the shading effects reported in this paper are considered as estimates. The epiphytic light absorption on sago pondweed of >100 percent may indicate that virtually no light reached the plants' photosynthetic tissues at the time of harvest. Obviously, however, light did reach the photosynthetic tissues prior to harvesting since plant biomass was present. The latter may be attributed to movements of epiphytic components, such as stalked diatoms, with the waves and currents allowing the occasional penetration of light flashes (Meulemans 1989).

The epiphytic light attenuation on wildcelery is in the same order of magnitude as reported in several other aquatic plant communities (Sommer 1977; Sand-Jensen and Sondergaard 1981; Meulemans 1989), but the epiphytic light attenuation on sago pondweed is higher.

Epiphyton usually accumulates during the growth season from near zero on emerging plant leaves to a species-characteristic maximum as growth slows down in midsummer, probably contributing to earlier senescence by light interception. Parts of the epiphyton complex may become dislodged by increased currents, wave action, and loss of senescing plant parts. Therefore, for further calibration of the aquatic plant growth models, epiphytic shading was set to

Table 13
Biomass Components of the Submersed Plant-Epiphyte Communities Harvested from the Pools 8 and 13 of the Upper Mississippi River in 2002. After separation of the epiphytes from the plant-epiphyte complex, the absorption of light by epiphytes was calculated by subtracting the light absorption by river water from the absorption by epiphytes suspended in river water. Epiphytic light absorption in the 0.095-m^2 settling chamber was normalized to epiphytic light absorption on the plant surface area from which the epiphytes had been separated, using the plant surface area:dry weight ratios.

UMR Pool and Site Code	Biomass (g DW)		Light absorption (% incoming irradiance)			
	Submersed Plant	Epiphytes	River Water in Settling Chamber	Epiphytes + RW in Settling Chamber	Epiphytes in Settling Chamber	Epiphytes on Submersed Plant Surface
V. americana						
Pool 8-LLM SSEB3A	0.58 ± 0.00	0.23 ± 0.00	12.90 ± 0.00	32.83 ± 0.00	19.93	45.66 ± 0.00
Pool 8-TI SSEB4A	0.87 ± 0.01	0.45 ± 0.22	9.48 ± 7.45	42.72 ± 16.72	33.24	50.88 ± 18.33
Pool 8-TI SSEB4B	0.99 ± 0.36	0.56 ± 0.37	8.24 ± 6.57	45.49 ± 16.52	37.25	52.27 ± 13.60
Pool 8-TI SSEB4C	1.28 ± 0.43	0.58 ± 0.07	8.24 ± 6.57	50.22 ± 4.78	41.98	46.83 ± 14.57
Pool 8-TI SSEB4D	1.00 ± 0.15	0.32 ± 0.20	10.10 ± 4.85	39.02 ± 10.02	28.92	37.12 ± 13.90
Pool 13 SSEB1A	1.55 ± 0.44	1.43 ± 1.06	12.82 ± 8.59	61.99 ± 20.85	49.17	42.85 ± 19.08
Pool 13 SSEB1B	0.91± 0.00	0.47± 0.00	8.50 ± 0.00	32.90 ± 0.00	24.40	35.63 ± 0.00
Pool 13 SSEB1C	0.67 ± 0.10	0.53 ± 0.18	13.62 ± 7.72	29.14 ± 7.73	15.52	31.75 ± 11.24
Pool 13 SSEB1D	1.59 ± 0.06	2.18 ± 0.94	15.50 ± 9.90	78.52 ± 8.48	63.02	52.85 ± 0.93
Pool 13 SSEB1E	1.01± 0.00	0.58 ± 0.00	12.56 ± 0.00	38.89 ± 0.00	26.33	34.63 ± 0.00
Grand mean and SD	1.04 ± 0.34	0.73 ± 0.60	11.20 ± 2.60	45.17 ± 15.14	33.98 ± 14.39	43.05 ± 7.83
P. pectinatus						
Pool 8-LLM SSEB3C	0.68± 0.18	0.54 ± 0.44	6.00 ± 0.00	41.69 ± 25.04	35.69	314.35 ± 149.76
Pool 8-LLM SSEB3D	0.57 ± 0.16	0.56 ± 0.27	12.90 ± 0.00	52.98 ± 6.47	40.08	482.77 ± 211.98
Pool 8-LLM SSEB3D	0.91± 0.00	0.43 ± 0.00	18.03 ± 0.00	53.10 ± 0.00	35.07	245.70 ± 0.00
Pool 8-TI SSEB4A	1.25 ± 0.70	0.53 ± 0.40	8.98 ± 7.84	38.98 ± 21.21	29.99	160.39 ± 65.26
Pool 8-TI SSEB4B	1.56 ± 0.00	0.43 ± 0.00	4.51± 0.00	42.61 ± 0.00	38.11	155.74 ± 0.00
Grand mean and SD	0.99 + 0.30	0.50 + 0.06	10.09 ± 5.20	45.87 ± 7.42	35.79 ± 3.80	271.79 ± 136.68

increase from zero at the beginning of the year to the species-characteristic maximum at plant maturity, subsequently decreasing extremely slowly. The maximum epiphytic shading for wildcelery was set at 43 percent in VALLA, and for sago pondweed at 100 percent in POTAM.

9 Field Study to Determine the Self-Shading Coefficient of *P. pectinatus* in the Upper Mississippi River

Introduction

The self-shading coefficient is an important determinant of the amount of light intercepted by the plant, and, therefore, also of the amount of biomass produced. Published values for the species-specific light extinction coefficient of sago pondweed vary from 0.0183 to 0.095 $m^2 g^{-1}$ DW. Values of 0.0183 and 0.020 m^2 g DW^{-1} have been found by Sher-Kaul et al. (1995) and Westlake (1964; used in a simulation model for growth of sago pondweed other than POTAM, developed by Hootsmans 1991). The default value in POTAM is 0.095 $m^2 g^{-1}$ DW, and has been measured in 1987 (Best and Boyd 2003a).

A new determination of the self-shading coefficient of sago pondweed was made in 2002 to verify whether coefficients in sago pondweed communities in the shallow, turbid areas of the UMR differed from those in the deeper, clear Western Canal, The Netherlands.

Methods

Light measurements in the field

Light readings were taken just above the water surface, just below the water surface, and further at 0.10 m intervals down the water column just outside and within a sago pondweed plant bed in UMR-Pool 8 on 18 July 2002.

Sample collection in the field

The height of the vegetation within the water column was recorded, and five 0.25 m^2 vegetation quadrants were harvested. Samples were transported to the laboratory.

Plant biomass quantification

The vegetation was cut into 0.10 m sections from just above the sediment to the top of the vegetation, coded appropriately, and dried at 105 °C for 24 hours to constant mass. Dry weights were determined to the nearest 0.01 g. In instances where vegetation height exceeded water column height and plant biomass floated on the water surface, possibly because of water level decreases after spring-early summer flooding, the floating plant biomass was assigned to the upper 0.10 m vegetation section.

Calculations

The light intensity at a given depth (h [m]) from the upper surface of the plant community (z[m]), designated by I_{z+h} may be approximated by the following Lambert-Beer's law

$$I_{z+h} = I_z \exp(-\varepsilon_c h) = I_0 \exp(-\varepsilon_s z - \varepsilon_c h)$$

where

I_z = light intensity on a horizontal plane at the upper surface of the plant community (μmol m^{-2} s^{-1})

I_0 = light intensity passing through the water surface, approximated by the light intensity at 0.01 m depth under the water surface (μmol m^{-2} s^{-1})

ε_s = light extinction coefficient in the water outside the plant community (m^{-1})

ε_c = light extinction coefficient within the plant community (m^{-1})

The light extinction coefficient inside the plant community or ε_c represents the depth-dependent rate of light attenuation due to the absorption of light by both water and plant shoots. The light extinction coefficient due to the interception by shoots alone (ε_p in m^2 g^{-1} DW) was determined using the following equation:

$$\varepsilon_p = (\varepsilon_c h - \varepsilon_s h)/ w(h)$$

where

w = plant dry weight in g DW m^{-2}

Results and Discussion

The shoot-specific light extinction coefficient for sago pondweed was calculated for the upper 0.1 m water layer and for the water layer just above the sedi-

ment. In both cases similar values were found varying from 1.73 to 1.85 m^2 g^{-1} DW (Table 14). These values are far higher than reported by other investigators.

Table 14
Calculation of Species-Characteristic Light Extinction Coefficient for *P. pectinatus* growing in the Upper Mississippi River. I_0, light intensity just under the water surface; I_z, light intensity at depth z; and ε light extinction coefficient

Replicate	I_0, (µmol m^{-2} s^{-1}) Water Column	I_z, (µmol m^{-2} s^{-1}) Water Column	I_z, (µmol m^{-2} s^{-1}) Within Plant Community	ε water, (m^{-1}) Water Column	ε community (m^{-1}) Water & Plant Community	Plant Biomass (g DW m^{-2})	ε plant (m^{-1}) Plant
Upper 0.1-m Water Layer							
1	1478	1101	70.3	2.94	30.45	5.74	2.99
2	1372	941	389.6	3.77	12.59	2.06	1.08
3	1555	1255	323.2	2.14	15.71	2.30	1.48
4	1632	1193	194.1	3.14	21.30	1.86	1.96
5	1507	1102	378.1	3.13	13.83	1.26	1.13
Mean							**1.73**
0.1-m Water Layer Above the Sediment							
1	1478	333.5	42	4.38	10.47	6.16	3.32
2	1372	470.0	142	3.15	6.68	2.38	1.81
3	1555	468.2	230	3.51	5.62	2.62	1.45
4	1632	464.5	200	3.69	6.17	2.12	1.50
5	1507	413.7	201	3.80	5.92	1.50	1.15
Mean							**1.85**

The high self-shading of sago pondweed in mid-summer in the UMR may be explained as follows. In spring strong elongation of the sprouting seedlings occurs when shoots stretch to reach the water surface at high river water levels, with self-shading by shoot mass in the typical order of 0.018-0.095 m^2 g^{-1} DW. In subsequent periods with lower water levels, the already elongated plant shoots may form a dense mat on top of the water surface, with self-shading as high as 1.73-1.85 m^2 g^{-1} DW extinguishing not only the irradiance to which the plant mass is exposed, but also providing a large catch-all for particles within the water column. Fluctuating water levels are common in UMR pools, and it is therefore feasible that high self-shading period alternate with lower self-shading periods for which the earlier found "default" self-shading coefficient of 0.095 m^2 g^{-1} DW is representative. Consequently, the default self-shading coefficient was generally used for sago pondweed growth simulations, with results of a special run using the currently found high self-shading coefficient of 1.79 m^2 g^{-1} DW illustrating the strong biomass-decreasing effect.

10 The .Net Model: A User-friendly Version of VALLA and POTAM

Purpose of the .Net Model

New versions of the aquatic plant growth models were recently developed in Microsoft's .Net framework—using Visual Basic as the programming language—to meet the following objectives:

a. The model should be more user-friendly than the earlier FORTRAN executables of VALLA and POTAM, i.e., not requiring computer language programming skills.

b. The user should have direct access to all input data while conducting a simulation. He/she should be able to directly view and change the input data for a specific simulation without having to edit one specific input file.

c. The user should be able to conduct multiple runs of the model by changing the model input parameters, by importing different input files, and routing the output to different output files.

d. The user should be able to conduct simulations for both *V. americana* and *P. pectinatus* using the same user interface. In addition, the user should be able to make simulations for both species at one site without having to reload the climate files or quitting the run-time user-interface.

e. The model outputs should be routed automatically to Microsoft Excel files in addition to the standard output, Res.Dat-file, in such a way that most users can directly access the outputs.

f. The user should be able to plot standard graphs automatically within the shell, edit the graphs for presentations, and save them into standard Microsoft Office software packages (e.g., Word, Excel, PowerPoint) by simple cut-and-paste operations.

g. The user should be able to conduct multiple simulations with various options (e.g., with and without epiphyte shading and current velocity) for one plant species and plot the multiple results into one graph.

h. The variable names and equations of the .Net Model should comply with those in the original FORTRAN codes. Original model descriptions and user manuals would, therefore, be directly applicable to the .Net Model.

Incorporating the listed features into this version of the models is expected to considerably reduce the time required for data input preparation and analysis of the simulation results.

.Net Model Verification

The performance of the .Net Model was verified by comparing its outputs with outputs of the original FORTRAN versions of VALLA and POTAM for selected cases. For *V. americana,* the default model runs for *Turtle Island, site EB5B, 2001* (Figure 25) and *Above Dam 8, site EB3B, 2001* (Figure 26) were simulated. For *P. pectinatus*, the model runs for *Lawrence Lake, site EB2E, 2001* (Figure 27) and *Target Lake, site EB1A, 2001* (Figure 28) were simulated. All input variables and weather data were identical to the corresponding runs made with the original FORTAN codes. Results from .Net Model simulations are presented in Figures 23 through 26. In all four cases, the .Net Model generated results which were identical to those produced by the original FORTRAN codes.

Conclusions and Recommendations

The development of the .Net Model is complete and meets all requirements listed above under *Purpose of the .Net Model.* Performance of the .Net Model has been verified. However, since the .Net Model has been used only by the developer, S. K. Nair (Cadmus, Inc.), the graphical user interface (GUI) features could be further improved based on comments from other users.

Acknowledgments

Mr. K. Schreiber, Wisconsin Department of Natural Resources, is gratefully acknowledged for his assistance in selecting a suitable field site for the study on the effect of current velocity on plant biomass of wildcelery, and for his help during the initiation of this study. Mr. M. Steuck, Iowa Department of Natural Resources, and a field station team leader for the USGS Long Term Resource Monitoring Program, provided logistical assistance for the field work in UMR Pool 13. J. E. Lyon and R. K. Hines, UMESC, assisted with collection of plant biomass samples from UMR Pool 8. The Long Term Resource Monitoring Program (LTRMP) is acknowledged for making environmental data available for this study.

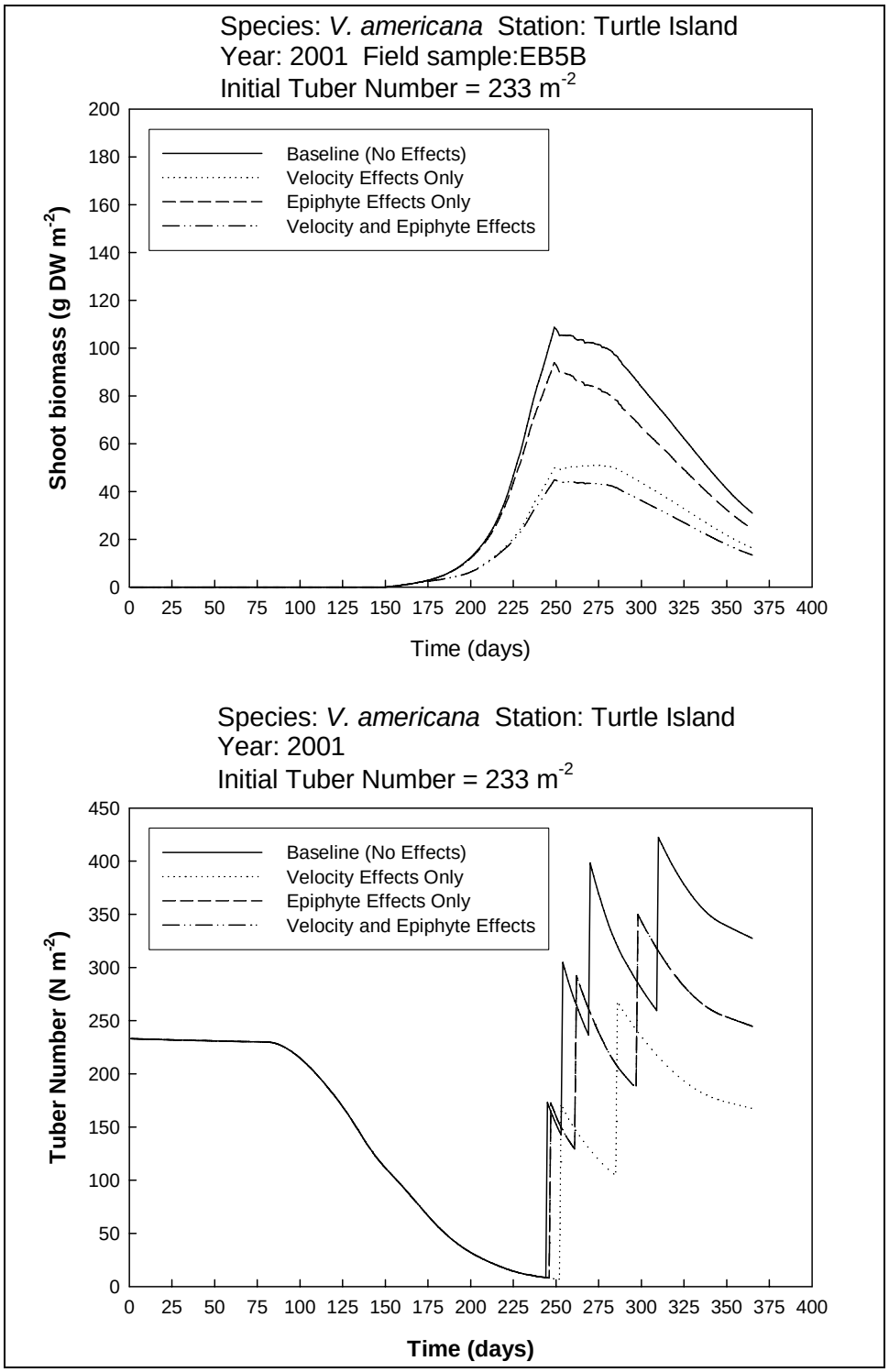

Figure 25. Visual Basic model-simulated biomass of plants and tubers of a wild-celery community in Upper Mississippi River Pool 8 at Turtle Island, in 2001, starting from default tuber bank density. Simulations were conducted for situations with and without accounting for the effects of current velocity and epiphyte shading. Results are identical to those in Figure 10

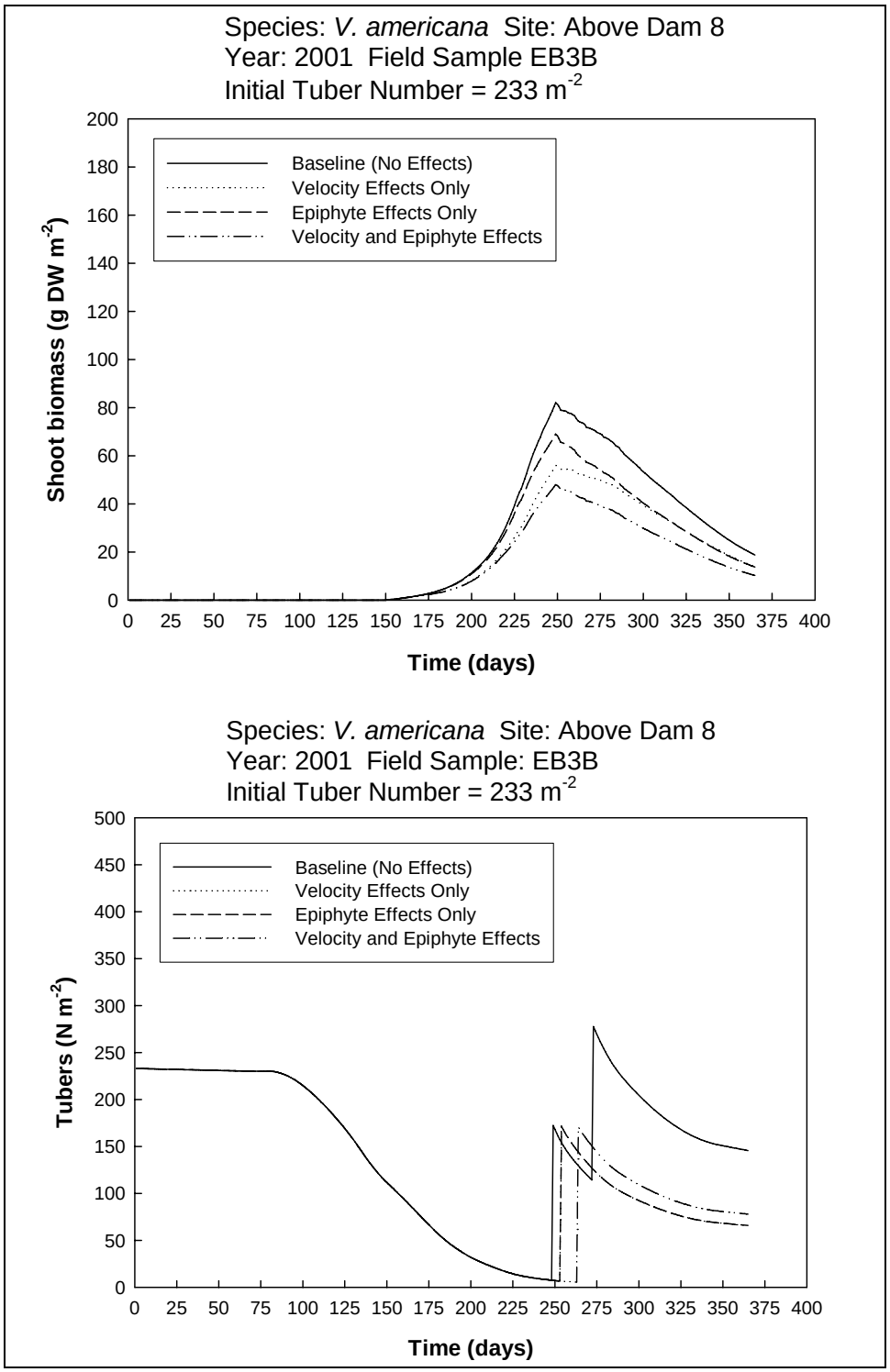

Figure 26. Visual Basic model-simulated biomass of plants and tubers of a wild-celery community in Upper Mississippi River Pool 8 at Lawrence Lake Marina, in 2001, starting from default tuber bank density. Simulations were conducted for situations with and without accounting for the effects of current velocity and epiphyte shading. Results are identical to those in Figure 11

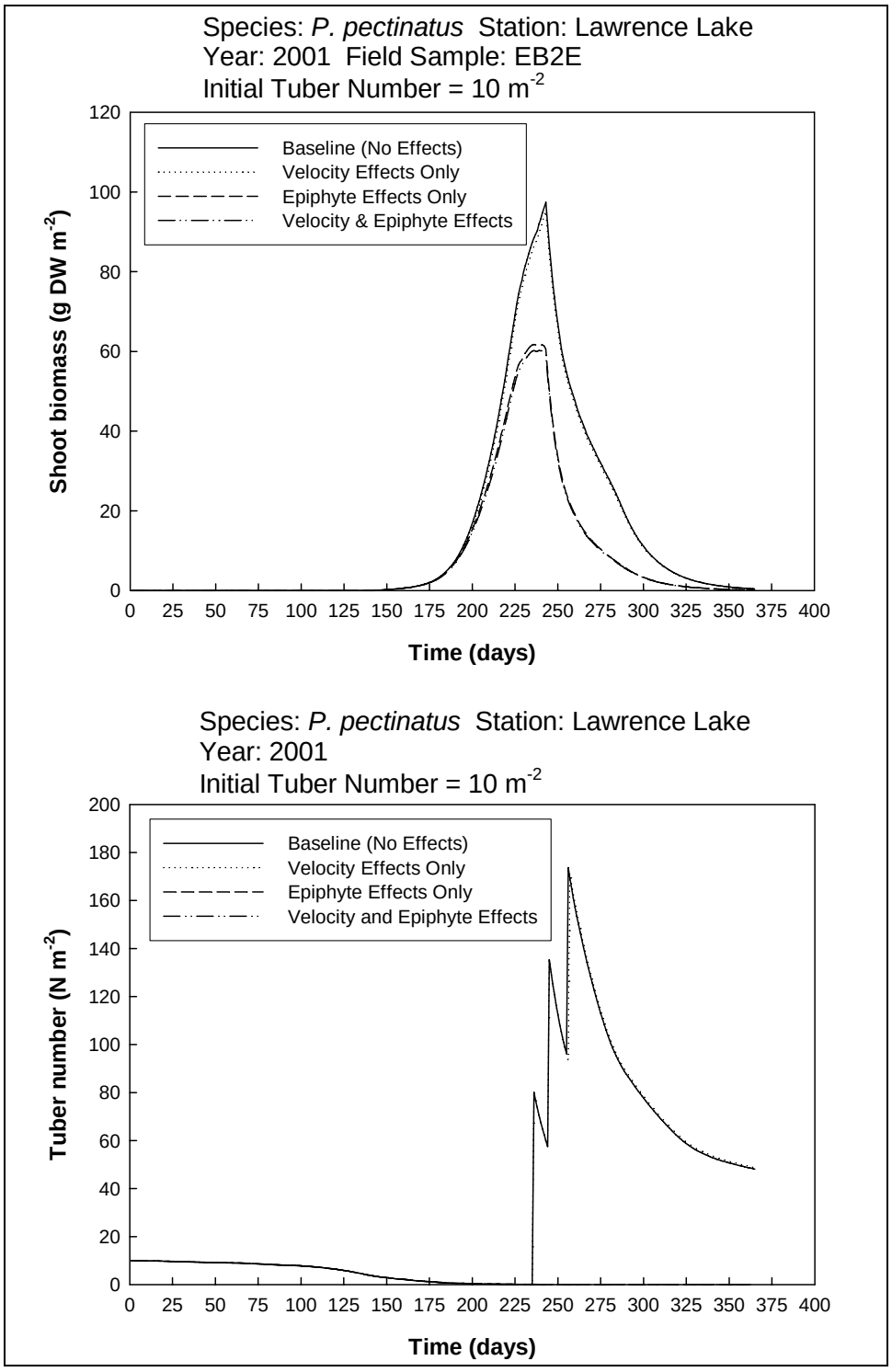

Figure 27. Visual Basic model-simulated biomass of plants and tubers of a sago pondweed community in Upper Mississippi River Pool 8 at Lawrence Lake, in 2001, starting from a low tuber bank density. Simulations were conducted for situations with and without accounting for the effects of current velocity and epiphyte shading. Results are identical to those in Figure 1

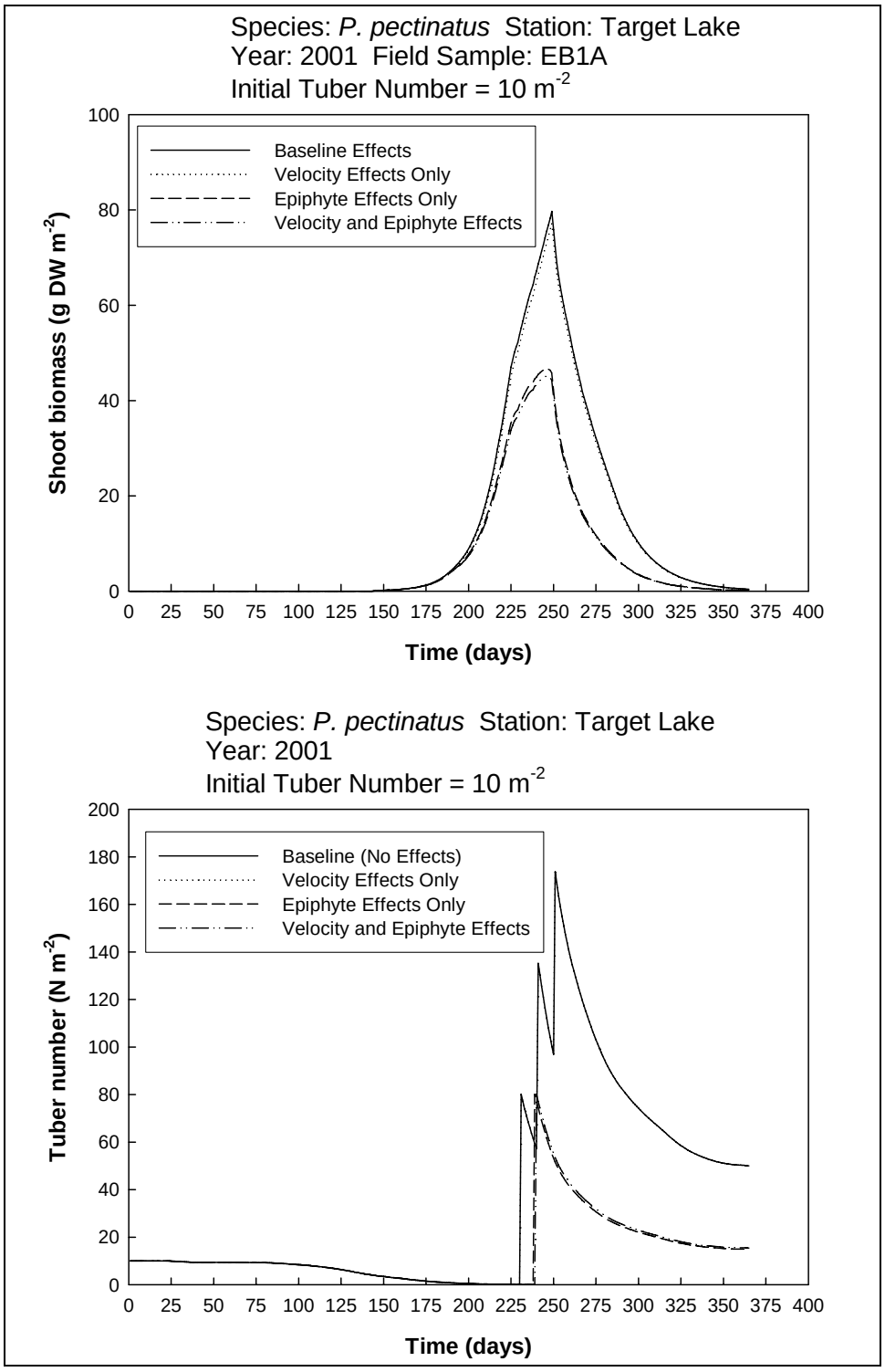

Figure 28. Visual Basic model-simulated biomass of plants and tubers of a sago pondweed community in Upper Mississippi River Pool 8 at Target Lake, in 2001, starting from a low tuber bank density. Simulations were conducted for situations with and without accounting for the effects of current velocity and epiphyte shading. Results are identical to those in Figure 14

References

Bartell, S. M. (1996). "Ecological/environmental risk assessment: principles and practices," In: *Risk Assessment and Management Handbook*, Kolluru, R. V., Bartell, S. M., Pitblado, R. M., and Stricoff, R. S. (eds.), McGraw-Hill, Inc., New York, New York, 10.3-10.59.

Bartell, S. M., Campbell, K. R., Best, E. P. H., and Boyd, W. A. (2000). "Interim Report For The Upper Mississippi River System - Illinois Waterway System Navigation Study. Ecological risk assessment of the effects of incremental increase of commercial navigation traffic (25, 50, 75, and 100% increase of 1992 baseline traffic) on submerged aquatic plants in the main channel borders," *ENV Report 17*. U.S. Army Corps of Engineers, Rock Island District, St. Louis District, St. Paul District.

Best, E. P. H., and Visser, H. W. C. (1987). "Seasonal growth of the submerged macrophyte *Ceratophyllum demersum* L. in mesotrophic Lake vechten in relation to insolation, temperature and reserve carbohydrates," *Hydrobiologia* 148, 231-243.

Best, E. P. H., Woltman, H., and Jacobs, F. H. H. (1996). "Sediment-related growth limitation of *Elodea nuttallii* as indicated by a fertilization experiment," *Freshwater Biology* 36, 33-44.

Best, E. P. H., and Boyd, W. A. (1996). "A simulation model for growth of the submersed aquatic macrophyte hydrilla (*Hydrilla verticillata* (L.F.) Royle," Technical Report A-96-8, U. S. Army Engineer, Waterways Experiment Station, Vicksburg, MS.

_____. (2001a). "A simulation model for growth of the submersed aquatic macrophyte *Vallisneria Americana* Michx," Technical Report ERDC/EL TR-01-5, U.S. Army Engineer Research and Development Center, Environmental Laboratory, MS.

_____. (2001b). "VALLA (version 1.0): a simulation model for growth of American wildcelery," Special Report ERDC/EL SR-01-1, U.S. Army Engineer Research and Development Center, Environmental Laboratory, Vicksburg, MS.

Best, E. P. H., and Boyd, W. A. (2003a). "A simulation model for growth of the submersed aquatic macrophyte *Potamogeton pectinatus* L," Technical Report ERDC/EL TR-03-6, U.S. Army Engineer Research and Development Center, Environmental Laboratory, MS.

Best, E. P. H., and Boyd, W. A. (2003b). "POTAM (version 1.0): a simulation model for growth of sago pondweed," ERDC/EL SR-03-1, U.S. Army Engineer Research and Development Center, Environmental Laboratory, Vicksburg, MS.

Best, E. P. H., Buzzelli, C. P., Bartell, S. M., Wetzel, R. L., Boyd, W. A., Doyle, R. D., and Campbell, K. R. (2001). "Modeling submersed macrophyte growth in relation to underwater light climate: modeling approaches and application potential," *Hydrobiologia* 444, 43-70.

Best, E. P. H., De Vries, D., and Reins, A. (1985). "The macrophytes in the Loosdrecht Lakes: a story of their decline in the course of eutrophication." *Verhaendlungen des Internationalen Vereinigungs Theoretische und Angewandte Limnologie* 22, 868-875.

Best, E. P. H., Nair, S. K., Kenow, K., and Fischer, J. (2002). "Aquatic plant modeling in Pool 8 of the Upper Mississippi River," *Progress Report 2001*. June 28, 2002.

Biggs, B. J. F. (1996). "Hydraulic habitat of plants in streams," *Regulated Rivers: Research and Management* 12, 131-144.

Borman, S., and Schreiber, K. (1992). "The distribution and biomass of aquatic macrophytes in the Red Cedar River near Barron, Wisconsin," *Report Wisconsin Department of Natural Resources Water Resources Management – Western District*, November, 1992: 35 pp.

Bowes, G., Van, T. K., and Haller, W. T. (1977). "Adaptation to low light levels by Hydrilla," *Journal of Aquatic Plant Management* 15, 32-35.

Carlson, B. D., Bartell, S. M., and Campbell, K. R. (2000). "Effects of recreational boating: Recreational traffic forecasting and allocation models," *ENV Report 18.* U.S. Army Corps of Engineers, Rock Island District, St. Louis District, St. Paul District.

Chambers, P. A., Prepas, E. E., Hamilton, H. R., and Bothwell, M. L. (1991). "Current velocity and its effects on aquatic macrophytes in flowing waters," *Ecological Applications* 1, 249-257.

Copeland, R. R., Abraham, D. D., Nail, G. H., Seal, R., and Brown, G. L. (2000). "Interim Report Upper Mississippi River – Illinois Waterway System Navigation Study. Entrainment and transport of sediments by towboats in the Upper Mississippi River and Illinois Waterway, Numerical model study," ENV Report 37, U. S. Army Corps of Engineers, Rock Island District, St. Louis District, St. Paul District.

Donnermeyer, G. N. (1982). "The quantity and nutritive quality of *Vallisneria americana* biomass, in Navigation Pool No. 9 of the Upper Mississippi River," M.S.Thesis, *University of Wisconsin,* La Crosse, WI. 93 pp.

Donnermeyer, G. N., and Smart, M. M. (1985). “The biomass and nutritive potential of *Vallisneria americana* Michx. in Navigation Pool 9 of the Upper Mississippi River.” *Aquatic Botany* 22, 33-44.

Doyle, R. D. (2000). “Interim Report Upper Mississippi River – Illinois Waterway System Navigation Study. Effects of sediment resuspension and deposition on plant growth and reproduction.” ENV Report 28, U. S. Army Corps of Engineers, Rock Island District, St. Louis District, St. Paul District. 64 pp.

Fremling, C. R., and Claflin, T. O. (1984). “Ecological history of the Upper Mississippi River,” In Wiener, J.G., Anderson, R.V., and McConville, D.R., Editors, *Contaminants in the Upper Mississippi River.* Butterworth Publishers, Boston, MA.

Giessen, W. B. J. T., Van Katwijk, M. M., and Den Hartog, C. (1990). “Eelgrass condition and turbidity in the Dutch Wadden Sea,” *Aquatic Botany* 37, 71-85.

Gons, H. J. (1982). “Structural and functional characteristics of epiphyton and epipelon in relation to their distribution in Lake Vechten,” *Hydrobiologia* 95, 79-114.

Goudriaan, J. (1986). “A simple and fast numerical method for the computation of daily totals of crop photosynthesis,” *Agricultural and Forestry Meteorology* 38, 251-255.

Griffin, K. L. (1994). “Caloric estimates of construction cost and their use in ecological studies.” *Functional Ecology* 8, 551-562.

Haller, W. T. (1974). “Photosynthetic characteristics of the submersed aquatic plants *Hydrilla*, southern naiad, and *Vallisneria*,” *Ph.D. Thesis, University of Florida*, Gainesville, FL. 88 p.

Holland, L. E. (1986). “Effects of barge traffic on distribution and survival of ichthyoplankton and small fishes in the Upper Mississippi River,” *Transactions of the American Fisheries Society* 115: 162-165.

Holland-Bartels, L. E., Dewey, M. R., and Zigler, S. J. (1990). “Pilot study of spatial patterns of ichthyoplankton and small fishes in the Upper Mississippi River,” *U.S. Fish and Wildlife Service*, La Crosse, WI.

Hootsmans, M. J. M. (1991). “A growth analysis model for *Potamogeton pectinatus* L.” M. J. M. Hootsmans and J. E. Vermaat. *Macrophytes, a key to understanding changes caused by eutrophication in shallow freshwater ecosystems*. *IHE Report Series* 21, Delft, The Netherlands, 263-311.

Howard-Williams, C. (1981). “Studies on the ability of a *Potamogeton pectinatus* community to remove dissolved nitrogen and phosphorus compounds from lake water,” *Journal of Applied Ecology* 18, 619-637.

Hunt, R. (1982). “Plant growth curves,” Arnold, London.

Kenow, K. P., Nissen, J. M., Drieslein, R., and Thorson, E. M. (2003). “Tundra swan research needs on the Upper Mississippi River,” Proceedings of the 19th Trumpeter Swan Society Conference, 2002. In review.

Korschgen, C. E., George, L. S., and Green, W. L. (1988). “Feeding ecology of Canvasbacks staging on Pool 7 of the Upper Mississippi River,” M. W. Weller (ed). *Waterfowl in Winter*, University of Minnesota Press, Minneapolis, MN, USA, 237-249.

Korschgen, C. E, Green, W. L., and Kenow, K. P. (1997). “Effects of irradiance on growth and winter bud production by *Vallisneria americana* and consequences to its abundance and distribution.” *Aquatic Botany* 58, 1-9.

LTRMP. The Long Term Resource Monitoring Program is being implemented by the U.S. Geological Survey (USGS) in cooperation with the five Upper Mississippi River System states (Illinois, Iowa, Minnesota, Missouri, and Wisconsin), with guidance and overall Program responsibility provided by the U.S. Army Corps of Engineers.

Madsen, T. V., and Sondergaard, M. (1983). “The effects of current velocity on the photosynthesis of *Callitriche stagnalis* Scop,” *Aquatic Botany* 15, 187-193.

Maynord, S. (1999). “Comparison of NAVEFF model to field return velocity and drawdown data,” ENV Report 14, U.S. Army Engineer Waterways Experiment Station, Vicksburg, MS.

Meulemans, J. T. (1989). “Reed and periphyton in Lake Maarsseveen I. Structural and functional aspects,” *Ph.D. Thesis, University of Amsterdam, The Netherlands*. 129 pp.

Ng, E., and Loomis, R. S. (1984). “Simulation of growth and yield of the potato crop.” *Simulation Monographs*, Pudoc, Wageningen: 147 p.

Penning de Vries, F. W. T., and Van Laar, H. H. (1982a). “Simulation of growth processes and the model BACROS.” *Simulation of plant growth and crop production*, Pudoc, Wageningen, 99-102.

Penning de Vries, F. W. T., and Van Laar, H. H. (1982b). “Simulation of growth processes and the model BACROS.” *Simulation of plant growth and crop production*, Pudoc, Wageningen: 114-131.

Roseboom, D. P., Twait, R. M., and Hill, T. E. (1992). “Physical characteristics of sediment and habitat affecting aquatic plant distribution in the Upper Mississippi River System: FY 1990,” *Long Term Resource Monitoring Program Special Report* 92-S011. 85 pp.

Sand-Jensen, K., and Sondergaard, M. (1981). "Phytoplankton and epiphyte development and their effect on submerged macrophytes in lakes of different nutrient status," *Internationale Revue gesamten. Hydrobiologie* 66, 529-552.

Sher-Kaul, S., Oertli, B., Castella, E., and Lachavanne, J. B. (1995). "Relationship between biomass and surface area of six submerged aquatic plant species." *Aquatic Botany* 51: 147-154.

Sommer, U. (1977). "Produktionaanalysen am Periphyton in Schilfgurtel des Neusiedler Sees," *Sitzberichte Osterreichischer Akademie of Wissenschaften Mathematik.-Naturwissenschaften Klassiker Abteilung I.* 186, 219-246.

Spencer, D. F. (1987). Tuber size and planting depth influence growth of *Potamogeton pectinatus* L.," *The American Midland Naturalist* 118, 77-84.

Spencer, D. F., and Anderson, L. W. J. (1987). "Influence of photoperiod on growth, pigment composition and vegetative propagule formation for *Potamogeton nodosus* Poir. and *Potamogeton pectinatus* L," *Aquatic Botany* 28, 102-112.

Spencer, D. F., and Ksander, G. (2003). "Nutrient limitation of *Zannichellia palustris* and *Elodea canadensis* growing in sediments from Fall River, California," *Journal of Freshwater Ecology* 18, 207-213.

Spitters, C. J. T. (1986). "Separating the diffuse and direct component of global radiation and its implications for modeling canopy photosynthesis. II. Calculation of canopy photosynthesis," *Agricultural and Forestry Meteorology* 38, 231-242.

Sullivan, J. F. (2000). "Continuous water quality monitoring in Lower Pool 8 of the Upper Mississippi River during the summer of 1999," *Progress Report on pre-drawdown Studies.* February 2000.

Thornley, J. H. M., and Johnson, I.R. (1990). "Development," In: *Plant and crop modelling. A mathematical approach to plant and crop physiology*, Clarendon Press, Oxford, 74-89; 139-144.

Titus, J., and Adams, M. A. (1979a). "Coexistence and the comparative light relations of the submersed macrophytes *Myriophyllym spicatum* L. and *Vallisneria americana* Michx." *Oecologia* 40, 273-286.

Titus, J. E., and Adams, M. A. (1979b). "Comparative storage utilization patterns in the submersed macrophytes, *Myriophyllum spicatum* and *Vallisneria americana*." *The American Midland Naturalist* 102, 263-272.

Titus, J. E., and Stephens, M. D. (1983). "Neighbor influences and seasonal growth patterns for *Vallisneria americana* in a mesotrophic lake," *Oecologia* 56, 23-29.

Titus, J., Goldstein, R. A., Adams, M. A., Mankin, J. B., O'Neill, R. V., Weiler, P. R., Shugart, H. H., and Booth, R. S. (1975). "A production model for *Myriophyllum spicatum* L," *Ecology* 56, 1129-1138.

Tyser, R. W., Rogers, S. J., Owens, T. W., and Robinson, L. R. (2001). Changes in backwater plant communities from 1975to 1995 in navigation pool 8, Upper Mississippi River," *Regulated River Research and Management* 17, 117-129.

U.S. Environmental Protection Agency (USEPA). (1998). "Guidelines for ecological risk assessment," Risk Assessment Forum, U.S. Environmental Protection Agency, Washington, D.C., EPA/630/R-95/00F.

Van der Bijl, L., Sand-Jensen, K., and Hjermind, A. L. (1989). " Photosynthesis and canopy structure of a submerged plant *Potamogeton pectinatus*, in a Danish lowland stream," *Journal of Ecology* 77, 947-962.

Van Dijk, G. M., Breukelaar, A. W., and Gijlstra, R. (1992). "Impact of light climate history on the seasonal dynamics of a field population of *Potamogeton pectinatus* L. during a three year period (1986-1988)," *Aquatic Botany* 43, 17-41.

Van Duin, E. H. S., Blom, G., Los, F. J., Maffione, R., Zimmerman, R., Cerco, C. F., Dortch, M. S., and Best, E. P. H. (2001). "Modeling under water light climate in relation to sedimentation, resuspension, water quality and autotrophic growth," *Hydrobiologia* 444, 25-42.

Van Keulen, H. (1976). "Evaluation of models," G. W. Arnold and C. T. de Wit, eds, *Critical evaluation of systems analysis in ecosystems research and management*, Simulation Monographs, Pudoc, Wageningen, 22-29.

Van Vooren, A. (1983). "Distribution and relative abundance of Upper Mississippi River fishes," Upper Mississippi Conservation Commission, Fish. Tech. Sect., Rock Island, IL.

Van Wijk, R. J. (1988)."Ecological studies on *Potamogeton pectinatus* L. I. General characteristics, biomass production and life cycles under field conditions," *Aquatic Botany* 31, 211-258.

_____. (1989)."Ecological studies on *Potamogeton pectinatus* L. III. Reproductive strategies and germination ecology," *Aquatic Botany* 33, 271-299.

Van Wijk, R. J., Van Goor, E., and Verkley, J. A. C. (1988). "Ecological studies on *Potamogeton pectinatus* L. II. Autecological characteristics with emphasis on salt tolerance, intraspecific variation and isoenzyme patterns." *Aquatic Botany* 32, 239-260.

Westlake, D. F. (1964). "Light extinction, standing crop and photosynthesis within weed beds," *Verhaendlungen internationaler Vereinigung der Limnologie* 15, 415-425.

Wetzel, R. L., and Neckles, H. A. (1986). “A model of *Zostera marina* L. photosynthesis and growth: simulated effects of selected physical-chemical variables and biological interactions,” *Aquatic Botany* 26, 307-323.

Wiener, J. G., Fremling, C. R., Korschgen, C. E., Kenow, K. P., Kirsch, E. M., Rogers, S. J., Yin, Y., and Sauer, J. S. (1998). “Mississippi River”, M. J. Mac, P. A. Opler, C. E. Puckett Haecker, and P. D. Doran (eds.). *Status and Trends of the Nation's Biological Resources. Biological Resources Division*, U.S. Geological Survey, Reston, Virginia, USA, 351-384.

Yin, Y., Winkelman, J. S., and Langrehr, H. A. (2000). “Long Term Resource Monitoring Program procedures: Aquatic vegetation monitoring,” U.S. Geological Survey, Upper Midwest Environmental Sciences Center, La Crosse, Wisconsin. LTRMP 95-P002-7. 8 p and appendices A-C.

Appendix A
Plant Growth Model Calibration Tables

Table A1
Parameter Values Used in VALLA (Continued)

Parameter	Abbreviation	Value	Reference
Morphology, Phenological Cycle, and Development			
First Julian day number	DAYEM	1	
Base temperature for juvenile plant growth	TBASE	3 °C	calibrated
Development rate as function of temperature	DVRVT* DVRRT	0.015 0.040	calibrated
Fraction of total dry matter increase allocated to leaves	FLVT	0.718	1, 2
Fraction of total dry matter increase allocated to stems	FSTT	0.159	1, 2
Fraction of total dry matter increase allocated to roots	FRTT	0.123	1, 2
Maximum Biomass and Plant Density			
Maximum biomass		496 g DW m^{-1}	2
Plant density	NPL	30 m^{-2}	1
Wintering and Sprouting of Tuber Bank			
(Dormant) tuber density	NDTUB	233 m^{-2}	1
Initial weight per tuber	INTUB	0.090 g DW. $tuber^{-1}$	3, 4
Relative tuber death rate (on number basis)	RDTU	0.018 d^{-1}	1
Initial Growth of Sprouts			
Relative conversion rate of tuber into plant material	ROC	0.0576 g CH2O. g DW-1 d-1	5
Relation coefficient tuber weight-stem length	RCSHST	12 m. g DW^{-1}	5, 6
Critical shoot weight per depth layer	CRIFAC	0.0091g DW. 0.1 m plant layer-1	3, 4
Survival period for sprouts without net photosynthesis	SURPER	23 d	7, 8

(Continued)

1. Titus and Stephens 1983
2. Haller 1974
3. Korschgen and Green 1988
4. Korschgen, Green, and Kenow 1997
5. Bowes et al., 1977
6. Best and Boyd 1996
7. Titus and Adams 1979 b
8. E. P. H. Best unpubl. 1987
9. Titus and Adams 1979 a
10. Penning de Vries and Van Laar, 1982 a, b
11. Titus et al. 1975
12. Donnermeyer 1982
13. Donnermeyer and Smart 1985

*, Calibration function.

Table A1 (Concluded)

Parameter	Abbreviation	Value	Reference
Light, Photosynthesis, Maintenance, Growth, and Assimilate Partitioning			
Water type specific light extinction coefficient	L	0.43-0.80 m^{-1}	1
Plant species specific light extinction coefficient	K	0.0235m^2 g DW^{-1}	9
Potential CO_2 assimilation rate at light saturation for shoots	AMX	0.0165 g CO_2. g DW-1 h-1	9
Initial light use efficiency for shoots	EE	0.000011 g CO_2 J^{-1}	10
Reduction factor for AMX to account for senescence plant parts	REDF	1.0	User def.
Daytime temperature effect on AMX as function of DVS	AMTMPT*	0 - 1	
Reduction factor to relate AMX to water pH	REDAM	1.0	
Parameter	Abbreviation	Value	Reference
Water type specific light extinction coefficient	L	0.43-0.80 m^{-1}	1
Plant species specific light extinction coefficient	K	0.0235m^2 g DW^{-1}	9
Potential CO_2 assimilation rate at light saturation for shoots	AMX	0.0165 g CO_2. g DW-1 h-1	9
Initial light use efficiency for shoots	EE	0.000011 g CO_2 J^{-1}	10
Reduction factor for AMX to account for senescence plant parts	REDF	1.0	User def.
Daytime temperature effect on AMX as function of DVS	AMTMPT*	0 - 1	
Reduction factor to relate AMX to water pH	REDAM	1.0	
Conversion factor for translocated dry matter into CH_2O	CVT	1.05	10
Dry matter allocation to each plant layer	DMPC*	0-1	9
Thickness per plant layer	TL	0.1 m	11
Water depth	DEPTH	1.4 m	User def.
Daily water temperature (field site)	WTMPT	-, °C	User def.
Total live dry weight measured (field site)	TGWMT	-, g DM m^{-2}	User def.
Induction and Formation of New Tubers			
Translocation (part of net photosynthetic rate)	RTR	0.247	4, 12,13
Tuber number concurrently initiated per plant	NINTUB	5.5 $plant^{-1}$	13
Critical tuber weight	TWCTUB	14.85 g DW m^{-2}	1, 3,13
Tuber density measured (field site)	NTMT	233 m^{-2}	1
Flowering and Senescence			
Relative death rate of leaves (on DW basis; Q10 =2)	RDRT	0.021 d^{-1}	1
Relative death rate of stems and roots (on DW basis; Q10=2)	RDST	0.021 d^{-1}	1
Harvesting			
Harvesting	HAR	0 or 1	User def.
Harvesting day number	HARDAY	1-365	User def.
Harvesting depth (measured from water surface; 1-5 m)	HARDEP	0.1m<DEPTH	User def.

Table A2
Parameter Values Used in POTAM

Parameter	Abbreviation	Value	Reference
Morphology, Phenological Cycle, and Development			
First Julian day number	DAYEM	1	
Base temperature for juvenile plant growth	TBASE	3 °C	calibrated
Development rate as function of temperature DVR prior to flowering (DVRVT), DVR subsequently (DVRRT)	DVRVT* DVRRT	0.015 0.040	calibrated
Fraction of total dry matter increase allocated to leaves	FLVT	0.731	1, 2
Fraction of total dry matter increase allocated to stems	FSTT	0.183	1, 2
Fraction of total dry matter increase allocated to roots	FRTT	0.086	1
Maximum Biomass and Plant Density			
Maximum biomass		1,952 g DW m^{-2}	3
Plant density	NPL	30 m^{-2}	1, 4
Wintering and Sprouting of Tuber Bank			
(Dormant) tuber density	NDTUB	240 m^{-2}	1
Initial dry weight per tuber	INTUB	0.083 g DW. $tuber^{-1}$	1
Relative tuber death rate (on number basis)	RDTU	0.026 d^{-1}	5
Initial Growth of Sprouts			
Relative conversion rate of tuber into plant material	ROC	0.0576 g CH_2O. g DW^{-1} d^{-1}	6
Relation coefficient tuber weight-stem length	RCSHST	12 m. g DW^{-1}	6, 7, 8
Critical shoot weight per depth layer	CRIFAC	0.0076 g DW. 0.1 m plant layer-1	7, 8
Survival period for sprouts without net photosynthesis	SURPER	27 d	1
Light, photosynthesis, maintenance, growth and assimilate partitioning			
Water type specific light extinction coefficient	L	1.07 m^{-1}	1
Plant species specific light extinction coefficient	K	0.095m^2 g DW^{-1}	1
Potential CO_2 assimilation rate at light saturation for shoot tips	AMX	0.019 g CO_2. g DW-1 h-1	9
Initial light use efficiency for shoot tips	EE	0.000011 g CO_2 J^{-1}	10
Reduction factor for AMX to account for senescence plant parts over vertical vegetation axis	REDF	1.0	user def.
Daytime temperature effect on AMX as function of DVS	AMTMPT*	0-1	1
Reduction factor to relate AMX to water pH	REDAM	1	1
Conversion factor for translocated dry matter into CH_2O	CVT	1.05	10
Dry matter allocation to each plant layer	DMPC*	0-1	1
Thickness per plant layer	TL	0.1 m	11

(Continued)

1.Best and Boyd 2003a
2. Sher-Kaul et al. 1995
3. Howard-Williams 1978
4. Van Wijk 1989
5. Van Wijk 1988
6. Best and Boyd 1996
7. Spencer 1987
8. Spencer and Anderson 1987
9. Van der Bijl et al. 1989
10. Penning de Vries and Van Laar, 1982 a, b
11. Titus et al. 1975
12. Van Wijk et al. 1988
* Calibration function

Table A2 (Concluded)

Parameter	Abbreviation	Value	Reference
Light, Photosynthesis, Maintenance, Growth and Assimilate Partitioning (cont.)			
Water depth	DEPTH	1.3 m	user def.
Daily water temperature (field site)	WTMPT	-, °C	user def.
Total live dry weight measured (field site)	TGWMT	-, g DM m^{-2}	user def.
Induction and Formation of New Tubers			
Translocation (part of net photosynthetic rate)	RTR	0.19	1, 12
Tuber number concurrently initiated per plant	NINTUB	8 $plant^{-1}$	1, 8
Critical tuber weight	TWCTUB	19.92 g DW m^{-2}	1, 4
Tuber density measured (field site)	NTMT	440 m^{-2}	4
Flowering and Senescence			
Relative death rate of leaves (on DW basis; Q10 =2)	RDRT	0.047 d^{-1}	1
Relative death rate of stems and roots (on DW basis; Q10=2)	RDST	0.047 d^{-1}	1
Harvesting			
Harvesting	HAR	0 or 1	user def.
Harvesting day number	HARDAY	1-365	user def.
Harvesting depth (measured from water surface; 1-5 m)	HARDEP	0.1m<DEPTH	user def.

Table A3
Relationship Between DVS of Wildcelery, Day of Year and 3 °C Day-Degree Sum in a Temperate Climate (DVR prior to flowering period, DVRVT= 0.015; DVR from flowering period onwards, DVRRT= 0.040)

Developmental Phase/Description	DVS Value	Day Number	3 °C Day-Degree Sum
First Julian day number → tuber sprouting and initiation elongation	0 -> 0.291	0 -> 105	1 -> 270
Tuber sprouting and initial elongation → leaf expansion	0.292 -> 0.875	106 -> 180	271 ->1215
Leaf expansion → floral initiation and anthesis	0.876 ->1.000	181 ->191	1216 -> 1415
Floral initiation and anthesis →induction of tuber formation, tuber formation and senescence	1.001 -> 2.000	192 -> 227	1416 -> 2072
Tuber formation and senescence → senesced	2.001 -> 4.008	228 -> 365	2073 -> 3167
Senesced	4.008	365	3167

Note: Calibration was on field data on biomass and water transparency from Chenango Lake, New York, 1978 (Titus and Stephens 1983) and climatological data from Binghamton (air temperatures) and Ithaca (irradiance), New York, 1978.

Table A4
Relationship between DVS of Sago Pondweed, Day of Year and 3 °C Day-Degree Sum in a Temperate Climate (DVR prior to flowering period, DVRVT= 0.015; DVR from flowering period onwards, DVRRT= 0.040)

Developmental Phase/Description	DVS Value	Day Number	3 °C Day-Degree Sum
First Julian day number → tuber sprouting and initiation elongation	0 -> 0.210	0 -> 77	1 -> 193
Tuber sprouting and initial elongation →leaf expansion	0.211 -> 0.929	78 -> 187	194 -> 1301
Leaf expansion → floral initiation and anthesis	0.930 ->1.000	188 ->195	1302 -> 1434
Floral initiation and anthesis-→ induction of tuber formation, tuber formation and senescence	1.001 -> 2.000	196 -> 233	1435 -> 2077
Tuber formation and senescence → senesced	2.001 -> 4.033	234 -> 365	2078 -> 3193
Senesced	4.033	365	3193

Note: Calibration was on field data on biomass and water transparency from the Western Canal near Zandvoort, The Netherlands, 1987 (Best, Jacobs, and Van de Hagen unpublished.; In Best and Boyd 2003a) and climatological data from De Bilt, The Netherlands, 1987.

Appendix B
Variable Listing and Output Parameters Plant Growth Models Available

Variable Listing. Output Parameters Marked with an *

Abbreviation	Explanation	Dimension
AH(i)	Absolute height of vegetation on top of stratum I, measured from the plant top	m
AMAX	Actual CO_2 assimilation rate at light saturation for individual shoots	g CO_2.g DW^{-1}.h^{-1}
AMTMP	Daytime temperature effect on AMX (relative)	-
AMTMPT	Table of AMX as function of DVS	-, -
AMX	Potential CO_2 assimilation rate at light saturation for shoot tips	g CO_2.g DW^{-1}.h^{-1}
ASRQ	Assimilate requirement for plant dry matter production	g CH_2O.g DW^{-1}
ATMTR	Atmospheric transmission coefficient	-
COSLD	Intermediate variable in calculating solar height	-
CRIFAC	Critical weight per 0.1 m vegetation layer	g DW per 0.1 m plnt ht^{-1}. $plnt^{-1}$
CRIGWT	Critical weight per 0.1 m vegetation layer	g DW per 0.1 m plnt ht^{-1}. m^{-2}
CVT	Conversion factor of translocated dry matter into CH_2O	-
DAVTMP*	Daily average temperature	°C
DAY	Day number (January 1=1)	d
DAYEM	First Julian day number	d
DAYL*	Day length	h
DDELAY	Integer value of DELAY	-
DDTMP*	Daily average daytime temperature	°C
DEC	Declination of the sun	radians
DELAY	Lag period chosen to relate water temperature to air temp., in cases where water temp. has not been measured	d
DEPTH	Water depth	m
DLV	Death rate of leaves	g DW. m^{-2}.d^{-1}
DMPC(i)	Dry matter allocation to each plant layer (relative)	-
DMPCT	Table to read DMPC(i) as function of depth layer (relative)	-
DPTT*	Table to read water depth as a function of day no	m, d
DRT	Death rate of roots	g DW. m^{-2}.d^{-1}
DSINB	Integral of SINB over the day	s.d^{-1}
DSINBE	Daily total of effective solar height	s.d^{-1}
DSO	Daily extra-terrestrial radiation	J.m^{-2} .d^{-1}
DST	Death rate of stems	g DW.m^{-2}.d^{-1}
DTEFF*	Daily effective temperature	°C
DTGA*	Daily total gross CO_2 assimilation of the vegetation	g CO_2.m^{-2}.d^{-1}
DTR	Measured daily total global radiation	J.m^{-2}.d^{-1}
DVR	Development rate as function of temperature sum	d^{-1}
DVRRT	Table of post-anthesis development rate as function of temperature sum	d^{-1}, °C
DVRVT	Table of pre-anthesis development rate as function of temperature sum	d^{-1}, °C
DVRVT	Development rate pre-anthesis	d^{-1}
DVS*	Development phase of the plant	-

Abbreviation	Explanation	Dimension
EE	Initial light use efficiency for shoots	g CO_2. J^{-1}
EPHSWT	On/off switch effect epiphyte shading on photosynthesis	-
EPISHD	Epiphyte shading effect on light interception on light interception by the plant as function of DVS	-,-
EPHY	Epiphyte shading effect on light interception by the plant as function of DVS	-,-
FGROS*	Instantaneous CO_2 assimilation rate of the vegetation	g $CO_2.m^{-2}.h^{-1}$
FGL	Instantaneous CO_2 assimilation rate per vegetation layer	g $CO_2.m^{-2}.h^{-1}$
FL	Leaf dry matter allocation to each layer of shoot (relative)	-
FLT	Table to read FL as function of DVS	-, -
FLV	Fraction of total dry matter increase allocated to leaves	-
FLVT	Table to read FLV as function of DVS	-
FRDIF	Diffuse radiation as a fraction of total solar radiation	-
FRT	Fraction of total dry matter increase allocated to roots	-
FRTT	Table to read FRT as function of DVS	-, -
FST	Fraction of total dry matter increase allocated to stems	-
FSTT	Table to read FST as function of DVS	-, -
GLV	Dry matter growth rate of leaves	g $DW.m^{-2}.d^{-1}$
GPHOT*	Daily total gross assimilation rate of the vegetation	g $CH_2O.m^{-2}.d^{-1}$
GRT	Dry matter growth rate of roots	g $DW.m^{-2}.d^{-1}$
GST	Dry matter growth rate of stems	g $DW.m^{-2}.d^{-1}$
GTW	Dry matter growth rate of the vegetation (plant excluding Tubers)	g $DW.m^{-2}.d^{-1}$
HAR	Harvesting (0=no harvesting, 1=harvesting)	-
HARDAY	Harvesting day number	d
HARDEP	Harvesting depth (measured from water surface)	m
HIG(i)	Height on top of stratum I (measured from water surface)	m
HOUR	Selected hour during the day	h
I	Counter in DO LOOP	-
IABS(i)	Total irradiance absorbed per depth layer	$J.m^{-2}.s^{-1}$
IABSL(i)	Total irradiance absorbed per depth layer	$J.m^{-2}.s^{-1}$
IDAY	Integer equivalent of variable DAY	d
INTUB	Initial dry weight of a tuber	g $DW.tuber^{-1}$
IREMOB	Initial value remobilization	g $CH_2O.m^{-2}$
IRS*	Total irradiance just under the water surface	$J.m^{-2}.s^{-1}$
IRZ(i)	Total irradiance on top of depth layer I	$J.m^{-2}.s^{-1}$
IWLVD	Initial dry matter of dead leaves	g $DW.m^{-2}$
IWLVG	Initial dry matter of green (live) leaves	g $DW.m^{-2}$
IWRTD	Initial dry matter of dead roots	g $DW.m^{-2}$
IWRTG	Initial dry matter of green (live) roots	g $DW.m^{-2}$
IWSTD	Initial dry matter of dead stems	g $DW.m^{-2}$
IWSTG	Initial dry matter of green (live) stems	g $DW.m^{-2}$
K	Plant species specific light extinction coefficient	$m^2.g\ DW^{-1}$, -
KCOUNT	Counter used to calculate number of consecutive days in which seedlings have a negative net photosynthesis	-
KT	Table to read K as function of DVS	-

Abbreviation	Explanation	Dimension
L	Water type specific light extinction coefficient	m^{-1}
LAT	Latitude of the site	degrees
LT	Table to read L as function of day number	d, m-1
MAINT*	Maintenance respiration rate of the vegetation	g CH_2O.m-2.d-1
MAINTS	Maintenance respiration rate of the vegetation at reference temperature	g CH_2O.m-2.d-1
NDTUB*	Dormant tuber number	dormant tubers.m^{-2}
NGLV	Net growth rate of leaves	g DW.m^{-2}.d^{-1}
NGRT	Net growth rate of roots	g DW.m^{-2}.d^{-1}
NGST	Net growth rate of stems	g DW.m^{-2}.d^{-1}
NGTUB*	Sprouting tuber number	spr. tubers.m^{-2}
NINTUB	Tuber number concurrently initiated per plant	conc.in.tubers .$plnt^{-1}$
NNTUB*	New tuber number	new tubers .m^{-2}
NPL	Plant density	plants .m^{-2}
NTM*	Tuber density measured (field site)	tubers.m^{-2}
NTMT	Table to read NTM as function of day number	tubers.m^{-2}, d
NTUBD*	Dead tuber number	dead tubers.m^{-2}
NUL	Zero (0)	-
NTUBPD	Dead tuber number previous day	dead p.d.tubers.m^{-2}
PAR	Instantaneous flux of photosynthetically active radiation	J.m^{-2}.s^{-1}
PARDIF	Instantaneous flux of diffuse PAR	J.m^{-2}.s^{-1}
PARDIR	Instantaneous flux of direct PAR	J.m^{-2}.s^{-1}
PI	Ratio of circumference to diameter of circle	-
RAD	Factor to convert degrees to radians	radians.$degree^{-1}$
RC	Reflection coefficient of irradiance at water surface (relative)	-
RCSHST	Relation coefficient tuber weight-stem length	m.g DW^{-1}
RDR	Relative death rate of leaves (on DW basis)	d^{-1}
RDRT	Table to read RDR as function of DAVTMP	d^{-1}, °C
RDS	Relative death rate of stems and roots (on DW basis)	d^{-1}
RDST	Table to read RDS as function of DAVTMP	d^{-1}, °C
RDTU	Relative death rate of tubers (on number basis)	d^{-1}
REDAM	Reduction factor to relate AMX to pH and oxygen levels of the water (relative)	-
REDAM1	Reduction factor for AMAX to account for effects of current velocity (relative)	-, cm s-1
REDAM2	Reduction factor for AMAX to account for effects of current velocity, table (relative)	-, cm s-1
REDF(i)	Reduction factor for AMX to account for senescence plant parts over vertical axis of vegetation (relative)	-
REMOB*	Remobilization rate of carbohydrates	g DW.m^{-2}.d^{-1}
ROC	Relative conversion rate of tuber into plant material	g CH_2O.g DW^{-1}.d^{-1}
RTR	Maximum relative tuber growth rate at 20 °C	g DW.$tuber^{-1}$.d^{-1}
RTRL	Relative tuber growth rate at ambient temperature	g DW.$tuber^{-1}$.d^{-1}

Abbreviation	Explanation	Dimension
SC	Solar constant corrected for varying distance sun-earth	$J.m^{-2}.s^{-1}$
SC(i)	Shoot dry matter in depth layer i	$g\ DW.m^{-2}.layer^{-1}$
SHTBIO	Shoot biomass; one term for sum WLV + WST	$g\ DW.\ m^{-2}$
SINB	Sine of solar elevation	-
SINLD	Intermediate variable in calculating solar declination	-
STEMLE	Stem length	m
SURFAC	Expression of warning that plant canopy is not at water And tuber class has died	-
SSURPR	Integer value of SURPER	-
SURPER	Survival period sprouting tubers	d
TBASE	Base temperature for juvenile plant growth	°C
TEFF*	Factor accounting for effect of temperature on maintenance respiration, remobilization, relative tuber growth and death rates	-
TEFFT	Table to read TEFF as function of temperature (Q10 of 2, up to 45 °C)	-, °C
TGW*	Total live plant dry weight (excluding tubers)	$g\ DW.m^{-2}$
TGWM*	Total live plant dry weight measured (field site)	$g\ DW.m^{-2}$
TGWMT	Table to read TGWM as function of day number	$g\ DW.m^{-2}$, d
TL	Thickness per depth layer	m
TMAX	Daily maximum temperature	°C
TMIN	Daily minimum temperature	°C
TMPSUM*	Temperature sum after 1 January	°C
TRANS*	Translocation rate of carbohydrates	$g\ CH_2O.m^{-2}.d^{-1}$
TREMOB*	Total remobilization	$g\ DW.m^{-2}$
TW*	Total live + dead plant dry weight (excluding tubers)	$g\ DW.m^{-2}$
TWCTUB	Total critical dry weight of new tubers	$g\ DW.m^{-2}$
TWGTUB*	Total dry weight of sprouting tubers	$g\ DW.m^{-2}$
TWLVD*	Total dry weight of dead leaves	$g\ DW.m^{-2}$
TWLVG*	Total dry weight of live leaves	$g\ DW.m^{-2}$
TWNTUB*	Total dry weight of new tubers	$g\ DW.m^{-2}$
TWRTD*	Total dry weight of dead roots	$g\ DW.m^{-2}$
TWRTG*	Total dry weight of live roots	$g\ DW.m^{-2}$
TWSTD*	Total dry weight of dead stems	$g\ DW.m^{-2}$
TWSTG*	Total dry weight of live stems	$g\ DW.m^{-2}$
TWTUB*	Total dry weight of tubers	$g\ DW.m^{-2}$
TWTUBD	Total dry weight of dead tubers	$g\ DW.m^{-2}$
VEL	Current velocity as function of day number	$cm\ s^{-1}$, d
VELSWT	On/off switch for effect current velocity on photosynthesis	-
WLV	Dry weight of leaves (live + dead)	$g\ DW.m^{-2}$
WRT	Dry weight of roots (live + dead)	$g\ DW.m^{-2}$
WST	Dry weight of stems (live + dead)	$g\ DW.m^{-2}$
WTMP*	Daily water temperature	°C
WTMPT	Table to read WTMP as function of day number	°C, d
WVEL	Current velocity as function of day number	$cm\ s^{-1}$
YRNUM	Year number simulation (1-5)	y

Appendix C
Input Files VALLA v2.0 and POTAM v2.0

MODEL.DAT File Used as Input for VALLA V2.0

```
*-------------------------------------------------------------------*
* Model data file generated by FST translator version 1.15 TEST    *
* - Initial constants as far as specified with INCON statements,   *
* - Model parameters,                                               *
* - AFGEN functions,                                                *
* - A SCALE array in case of a general translation                  *
*                                                                   *
* File name: MOD_P08_M686_6J_2.DAT; input MODEL.DAT file for run    *
* of VALLA for Upper Mississippi River Pool 8, 2001 conditions,     *
* with velocity-corrected photosynthesis, for SITE_ID M686.6J       *
* using La Crosse weather data usa4.001, Daily values used for      *
* wtemp, wdepth, velocity, and LT; the wdepth was modified to       *
* match measured data at site EB5B on Julian Day 213.              *
* Date: 10 Dec. 2001                                                *
* Time: 08:45:00                                                    *
*-------------------------------------------------------------------*
```

* Initial constants
* ----------

INTUB	= 0.09	! Initial dry weight of a tuber (g DW. tuber^{-1})
IREMOB	= 0.	! Initial value remobilization (g $CH_2O.m^{-2}$)
IWLVD	= 0.	! Initial dry matter of dead leaves (g DW. m^{-2})
IWLVG	= 0.	! Initial dry weight of live leaves (g DW. m^{-2})
IWRTD	= 0.	! Initial dry weight of dead roots (g DW. m^{-2})
IWRTG	= 0.	! Initial dry weight of live roots (g DW. m^{-2})
IWSTD	= 0.	! Initial dry weight of dead stems (g DW. m^{-2})
IWSTG	= 0.	! Initial dry weight of live stems (g DW. m^{-2})
NUL	= 0.	! Zero (0)
REMOB	= 0.0	! Remobilization rate of carbohydrates (g $CH_2O.m^{-2}$)

* Model parameters
* ----------

YRNUM	= 1.	! Year number simulation (1-5) (y)
AMX	= 0.0165	! Potential CO_2 assimilation rate at light ! saturation for shoot tips (g CO_2. g $DW^{-1}.h^{-1}$)
CRIFAC	= 0.0091	! Critical weight per 0.1 m vegetation layer ! (g DW per 0.1 m plnt ht^{-1}. m^{-2})
CVT	= 1.05	! Conversion factor of translocated dry matter into CH_2O (-)
DAYEM	= 1.	! First Julian day number (d)
DELAY	= 1.	! Lag period chosen to relate water temperature to air ! temperature, in cases where water temp. has not been ! measured (d)
EE	= 0.000011	!Initial light use efficiency for shoots (g CO_2. J^{-1})
EPHSWT	= 1.	! On/off switch effect epiphyte shading on photosynthesis
HAR	= 0.	! Harvesting (0 = no harvesting, 1 = harvesting)
HARDAY	= 304.	! Harvesting day number (d)
HARDEP	= 0.8	! Harvesting depth (measured from water surface; m)
NDTUB	= 233.	! Dormant tuber number (dormant tubers.m^{-2})
NINTUB	= 5.5	! Tuber number concurrently initiated per plant ! (conc.in.tubers.$plnt^{-1}$
NPL	= 30.	! Plant density (plants.m^{-2})

RC	= 0.06	! Reflection coefficient of irradiance at water surface ! (relative; -)
RCSHST	= 12.0	! Relation coefficient tuber weight- stem length (m g DW^{-1})
RDTU	= 0.018	! Relative death rate of tubers (on number basis; d^{-1})
REDAM	= 1.	! Reduction factor to relate AMX to pH and oxygen levels of ! the water (relative; -)
ROC	= 0.0576	! Relative conversion rate of tuber into plant material ! (g CH_2O g $DW^{-1}.d^{-1}$)
RTR	= .247	! Maximum relative tuber growth rate at 20 °C ! (g $DW.tuber^{-1}.d^{-1}$)
SURPER	= 23.	! Survival period sprouting tubers (d)
TBASE	= 3.	! Base temperature for juvenile plant growth (°C)
TL	= 0.1	! Thickness per depth layer (m)
TWCTUB	= 14.85	! Total critical dry weight of new tubers (g DW. m^{-2})
VELSWT	= 1.	! On/off switch for effect current velocity on photosynthesis

* AFGEN functions
* ----------

```
        ! Daytime temperature effect on AMX as function of DVS (-,-)
AMTMPT =
   -30., 0.00001, 0., 0.00001, 5., 0.12, 15., 0.424, 20., 0.568, 25., 0.735, 30., 0.879,
    35., 1.0, 50., 0.00001

        ! Dry matter allocation to each plant layer (relative; - , layer number)
DMPCT  =
   1.0, .184, 2.0, .184, 3.0, .184, 4.0, .114, 5.0, .114

        ! Water depth as function of day number (m, d)
DPTT =
    1., 0.23, 151., 0.23, 164., 0.23, 178., 0.23, 192., 0.23, 205., 0.23, 221., 0.23, 235., 0.23,
    365., 0.23

        ! Development rate prior to flowering period as function of temperature (-,°C)
DVRVT = -15., 0., 0., 0., 30., 0.015

        ! Development rate from flowering period onwards as function of temperature (-, °C)
DVRRT = -15., 0., 0., 0., 30., 0.040

        ! Epiphyte shading effect on light interception by the plant as function of DVS (-, -)
EPHY = 0., 0.0, 2.0, 0.43, 20., 0.0

        ! Leaf dry matter allocation to each layer of the plant as function of DVS (-,-)
FLT    =
   0., 0.82, 3.5, 0.82, 20.0, 0.82

        ! Fraction of total dry matter increase allocated to leaves as function of DVS (-,-)
FLVT   =
   0., 0.718, 3.5, 0.718, 20.0, 0.718

        ! Fraction of total dry matter increase allocated to roots as function of DVS (-,-)
FRTT   =
   0., 0.123, 3.5, 0.123, 20.0, 0.123
```

```
        ! Fraction of total dry matter increase allocated to stems as function of DVS (-,-)
FSTT   =
   0., 0.159, 3.5, 0.159, 20.0, 0.159

        ! Plant species specific light extinction coefficient as function of DVS (m2.g DW-1, -)
KT     =
   0., 0.0235, 3.5, 0.0235, 20.0, 0.0235

        ! Water type specific light extinction coefficient as function of day number (m-1, d)
LT     =
   1., 3.00, 151., 3.00, 164., 4.23, 178., 3.75, 192., 3.00, 205., 4.13, 221., 3.44, 235., 3.00,
    365., 3.00

        ! Relative death rate of roots as function of daily average temperature
         ! (g DW. g DW.d-1, °C)
RDRT   =
   0., 0.021, 19., 0.021, 30., 0.042, 40., 0.084, 50., 1.

        ! Relative death rate of shoots as function of daily average temperature
         ! ( g DW. g DW.d-1, °C)
RDST   =
   0., 0.021, 19., 0.021, 30., 0.042, 40., 0.084, 50., 1.

        ! Reduction factor for AMAX to account for effects of current velocity, read from input file
    ! (-, cm s-1)
REDAM1 = 0., 1.0, 3.82, 1.0, 7.636, 0.989734, 82., 0.0, 120., 0.0

        ! Reduction factor for AMX to account for senescence plant parts over vertical axis
         ! of vegetation (relative; -,-)
REDFT  =
   0.0, 1.0, 1.0, 1.0, 20.0, 1.0

        ! Factor accounting for effect of temperature on maintenance respiration,
         !  remobilization, and relative tuber growth rate (relative; -, °C)
TEFFT  =
   0.0, 0.0001, 10., 0.5, 20., 1., 30., 2., 40., 4., 45., 6., 50., 0.0001

        ! Daily water temperature as function of day number (°C, day)
WTMPT  =
   1.,  0.20, 11., 0.20., 24., 0.20, 37., 0.20, 53., 0.20, 67., 0.10, 79., 0.10, 95., 5.80, 122., 13.30,
   136., 20.40, 151., 17.30, 165., 22.20, 178., 25.90, 192., 26.40, 204., 25.90, 221., 29.20, 235.,
   25.20, 247., 24.00, 261., 17.90, 277., 15.90, 289., 10.50, 309., 9.10, 317., 8.30, 333., 5.80,
   347., 2.60, 365., 2.60

        ! Current velocity as function of day number (cm s-1, d)
WVEL =
   1., 36.00, 151., 36.00, 164., 11.00, 178., 37.00, 192., 29.00, 205., 6.00, 221., 25.00, 235., 3.00,
   365., 3.00

        ! Tuber density measured (field site) as function of day number (tubers.m-2, d)
NTMT   =
   1., 233., 98., 233., 134., 233., 162., 233., 190., 233., 233., 233., 260., 233., 289.,
   233.,  365., 233.
```

! Total live dry weight measured (field site) as function of day number (g DW.m^{-2}, d)

TGWMT =

1., 0., 153., 2.4, 166., 3.8, 178., 7.1, 199., 17.3, 220., 50.1, 243., 41.0, 266., 25.3,
365., 0.

MODEL.DAT File Used as Input for POTAM V2.0

```
*-------------------------------------------------------------------*
* Model data file generated by FST translator version 1.15 TEST    *
* - Initial constants as far as specified with INCON statements,   *
* - Model parameters,                                              *
* - AFGEN functions,                                               *
* - A SCALE array in case of a general translation                 *
*                                                                  *
* File name: MOD_P08_POT_M696_5D_1.DAT;input MODEL.DAT file for    *
* run of POTAM for Upper Mississippi River Pool8,2001 conditions,  *
* without velocity-corrected photosynthesis, for Site_ID M696.5D   *
* using La Crosse weather data usa4.001, daily values used for     *
* wtemp, wdepth, velocity, and LT; DPTT used from EB1A.            *
* Date: 25 April 2001                                              *
* Time: 14:00:00                                                   *
*-------------------------------------------------------------------*
```

* Initial constants
* ----------

INTUB	= 0.083	! Initial dry weight of a tuber (g DW. tuber^{-1})
IREMOB	= 0.	! Initial value remobilization (g $CH_2O.m^{-2}$)
IWLVD	= 0.	! Initial dry matter of dead leaves (g DW. m^{-2})
IWLVG	= 0.	! Initial dry weight of live leaves (g DW. m^{-2})
IWRTD	= 0.	! Initial dry weight of dead roots (g DW. m^{-2})
IWRTG	= 0.	! Initial dry weight of live roots (g DW. m^{-2})
IWSTD	= 0.	! Initial dry weight of dead stems (g DW. m^{-2})
IWSTG	= 0.	! Initial dry weight of live stems (g DW. m^{-2})
NUL	= 0.	! Zero (0)
REMOB	= 0.0	! Remobilization rate of carbohydrates (g $CH_2O.m^{-2}$)

* Model parameters
* ----------

YRNUM	= 1.	! Year number simulation (1-5) (y)
AMX	= 0.019	! Potential CO_2 assimilation rate at light ! saturation for shoot tips (g CO_2. g $DW^{-1}.h^{-}$
CRIFAC	= 0.0076	! Critical weight per 0.1 m vegetation layer ! (g DW per 0.1 m plnt ht^{-1}. m^{-2})
CVT	= 1.05	! Conversion factor of translocated dry matter into CH_2O (-)
DAYEM	= 1.	! First Julian day number (d)
DELAY	= 7.	! Lag period chosen to relate water temperature to air ! temperature, in cases where water temp. has not been ! measured (d)
EE	= 0.000011	! Initial light use efficiency for shoots (g CO_2. J^{-1})
EPHSWT	= 1.	! On/off switch effect epiphyte shading on photosynthesis
HAR	= 0.	! Harvesting (0 = no harvesting, 1 = harvesting
HARDAY	= 304.	! Harvesting day number (d)
HARDEP	= 0.8	! Harvesting depth (measured from water surface; m)
NDTUB	= 240.	! Dormant tuber number (dormant tubers.m^{-2})
NINTUB	= 8.	! Tuber number concurrently initiated per plant ! (conc.in.tubers.$plnt^{--1}$
NPL	= 30.	! Plant density (plants.m^{-2})
RC	= 0.06	! Reflection coefficient of irradiance at water surface ! (relative; -)
RCSHST	= 12.0	! Relation coefficient tuber weight- stem length (m g DW^{-1})

RDTU	= 0.026	! Relative death rate of tubers (on number basis; d^{-1}) .
REDAM	= 1.	! Reduction factor to relate AMX to pH and oxygen levels of ! the water (relative; -)
ROC	= 0.0576	! Relative conversion rate of tuber into plant material ! (g CH_2O g $DW^{-1}.d^{-1}$)
RTR	= .19	! Maximum relative tuber growth rate at 20 °C ! (g $DW.tuber^{-1}.d^{-1}$)
SURPER	= 27.	! Survival period sprouting tubers (d)
TBASE	= 3.	! Base temperature for juvenile plant growth (°C)
TL	= 0.1	! Thickness per depth layer (m)
TWCTUB	= 19.92	! Total critical dry weight of new tubers (g DW. m^{-2})
VELSWT	= 1.	! On'off switch for effect current velocity on photosynthesis

```
* AFGEN functions
* ----------------------

        ! Daytime temperature effect on AMX as function of DVS (-,-)
AMTMPT =
   -30., 0.00001, 0., 0.00001, 10., 0.027, 18., 0.51, 20., 0.53, 23., 0.71, 28., 0.91,
    30., 1.0, 50., 0.00001

        ! Dry matter allocation to each plant layer (relative; - , layer number)
DMPCT  =
    1.0, .043, 2.0, .043, 3.0, .231, 4.0, .254, 5.0, .213

        ! Water depth as function of day number (m, d)
DPTT =
    1., 0.55, 11., 0.55, 23., 0.55, 37., 0.48, 53., 0.50, 67., 0.43, 79., 0.42, 95., 1.00, 108., 0.55, 123., 0.55,
    136., 1.68, 151., 2.00, 164., 1.14, 178., 1.59, 192., 0.90, 206., 0.65, 221., 0.71, 235., 0.69, 247., 0.55,
    261., 0.66, 365., 0.66

        ! Development rate prior to flowering period as function of temperature (-,°C)
DVRVT = -15., 0., 0., 0., 30., 0.015

        ! Development rate from flowering period onwards as function of temperature (-,°C)
DVRRT = -15., 0., 0., 0., 30., 0.040

        ! Epiphyte shading effect on light interception by the plant as function of DVS (-, -)
EPHY = 0., 0.0, 2.0, 1.0, 20., 0.0

        ! Leaf dry matter allocation to each layer of the plant as function of DVS (-,-)
FLT    =
   0., 0.8, 3.5, 0.8, 20.0, 0.8

        ! Fraction of total dry matter increase allocated to leaves as function of DVS (-,-)
FLVT   =
   0., 0.731, 3.5, 0.731, 20.0, 0.731

        ! Fraction of total dry matter increase allocated to roots as function of DVS (-,-)
FRTT   =
   0., 0.086, 3.5, 0.086, 20.0, 0.086

        ! Fraction of total dry matter increase allocated to stems as function of DVS (-,-)
FSTT   =
   0., 0.183, 3.5, 0.183, 20.0, 0.183
```

```
        ! Plant species specific light extinction coefficient as function of DVS (m2.g DW-1, -)
KT    =
   0., 0.095, 3.5, 0.095, 20.0, 0.095

        ! Water type specific light extinction coefficient as function of day number (m-1, d)
LT    =
   1., 2.54, 11., 2.54, 23., 3.75, 37., 2.70, 53., 2.89, 67., 3.17, 79., 5.00, 95., 1.92, 108., 4.58,
   123., 2.39, 136., 1.68, 151., 2.43, 164., 3.06, 178., 0.77, 192., 5.50, 206., 3.37, 221., 2.62,
    235., 2.43, 247., 3.30, 261., 2.70, 365., 2.70

        ! Relative death rate of roots as function of daily average temperature
        ! (g DW. g DW.d-1, °C)
RDRT  =
   0., 0.047, 19., 0.047, 30., 0.094, 40., 0.188, 50., 1.

        ! Relative death rate of shoots as function of daily average temperature
        ! ( g DW. g DW.d-1, °C)
RDST  =
   0., 0.047, 19., 0.047, 30., 0.094, 40., 0.188, 50., 1.

        ! Reduction factor for AMAX to account for effects of current velocity, read from input file
        ! (-, cm s-1)
REDAM1 = 0., 0.98469, 3.82, 1., 7.6, 1., 93.33, 0.0, 120., 0.0

        ! Reduction factor for AMX to account for senescence plant parts over vertical axis
        ! of vegetation (relative; -,-)
REDFT  =
   0.0, 1.0, 1.0, 1.0, 5.0, 1.0

        ! Factor accounting for effect of temperature on maintenance respiration,
        !  remobilization, and relative tuber growth rate (relative; -, °C)
TEFFT  =
   0.0, 0.0001, 10., 0.5, 20., 1., 30., 2., 40., 4., 45., 6., 50., 0.0001

        ! Daily water temperature as function of day number (°C, day)
WTMPT  =
   1.,  0.20, 11., 0.20., 23., 0.0, 37., 0.00, 53., 0.10, 67., 0.30, 79., 1.60, 95., 4.80, 108., 6.40, 123.,
   13.10, 136., 21.10, 151., 17.80, 164., 24.20, 178., 26.80, 192., 28.20, 206., 27.10, 221., 29.30,
   235.,  23.60, 247., 24.30, 261., 15.60, 277., 13.10, 289., 8.70, 309., 6.80, 317., 8.00, 333., 4.70,
   347., 2.50, 362., 0.0, 365., 1.60

        ! Current velocity as function of day number (cm s-1, d)
WVEL =
   1., 0.0, 11., 0.0, 23., 0.0, 37., 0.0, 53., 2.0, 67., 0.0, 79., 0.0, 95., 2.0, 108., 7.0, 123., 10.0,
    136., 2.0, 151., 0.0, 164., 0.0, 178., 0.0, 192., 0.0, 205., 1.0, 221., 0.0, 235., 0.0, 247., 0.0,
    365., 0.0

        ! Tuber density measured (field site) as function of day number (tubers.m-2, d)
NTMT  =
   1., 400., 98., 400., 134., 400., 190., 400., 233., 400., 260., 400., 289., 400.,
   365., 400.

        ! Total live dry weight measured (field site) as function of day number (g DW.m-2, d)
TGWMT  =
   1., 0., 98., 0.64, 134., 8., 190., 50.0, 233., 78.5, 260., 52.0, 289., 29.5, 365., 0.
```

Appendix D
Example Illustrating Calculations Needed for Runs with Changed Default Values

Details on changing input streams for model runs, and handling and rapid visualizing output are presented in Best and Boyd, 2001a, and -------, 2003a. In all examples, almost identical MODEL.DAT files are used as for the nominal runs of VALLA V2.0 and POTAM V2.0, and only small changes have to be made. Such changes are illustrated for examples regarding POTAM below. It is recommended to save the default MODEL.DAT file in its original form under a different name on a safe place on your PC to avoid the occurrence of unintended changes in the default MODEL.DAT file. Before reuse of the default MODEL.DAT file, the latter file has to be saved again as MODEL.DAT, to be recognized by the (executable of the) source code.

EXAMPLE 1: Changes in tuber bank density, individual tuber weight, tuber number concurrently initiated, of sago pondweed

This run is started from tubers alone; i.e. no green plant weight, a low tuber bank density (i.e. 10 tubers m^{-2}), and a smaller tuber size (of 0.070 g DW $tuber^{-1}$) than in the nominal run on day 1 of the simulation.

Wintering in the form of tubers alone, without remaining plant biomass, is typical under temperate climatological conditions.

This requires the following entries in the MODEL.DAT file used as Input for POTAMv 2.0
Under the 'Initial constants' section:

IWLVD = 0.
IWLVG = 0.
IWRTD = 0.
IWRTG = 0.
IWSTD = 0.
IWSTG = 0.

Low tuber bank densities typically occur under a high grazing pressure by waterfowl.

A. Tuber bank density $\geq$ than the typical plant density of 30 plants m^{-2} This requires the following entries in the MODEL.DAT file used as Input for POTAMv 2.0:

Under the 'Model parameters' section:

NDTUB = 30. (or higher)

B. Tuber bank density < than the typical plant density of 30 plants m^{-2} This requires the following entries in the MODEL.DAT file used as Input for POTAMv 2.0:

Under the 'Model parameters' section:

NDTUB = 10. (or lower)
NPL = 10. (same number as NDTUB)
TWCTUB = 6.64 (0.083 (INTUB) x 8. (NINTUB) x 10 (NPL))

A smaller than nominal tuber size may occur in shallow water bodies in relatively warm, temperate climates. Individual tuber weight and tuber number concurrently initiated by each plant depend on the light level at which the plant grows. Both tuber weight and number decrease with light level according to the relationship shown in Figure 4 of this report. The tuber weight used in the nominal run is representative for the light level in the calibration situation. However, light levels experienced by a sago pondweed vegetation at other sites can be higher or lower; consequently tuber behavior has to be modified to apply to those situations.

This requires the following entries in the MODEL.DAT file used as Input for POTAMv 2.0:

Under the 'Initial constants' section:

INTUB = 0.070

Under the 'Model parameters' section:

NINTUB = 6.
SURPER = 22.8 (0.07 (INTUB) x 6 (NINTUB) x 27 (nominal SURPER-value)
TWCTUB = 12.6 (0.07 (INTUB) x 6 (NINTUB) x 30 (NPL, nominal value)

A smaller than nominal tuber number concurrently initiated . In several cases, plant density and tuber number concurrently formed by a sago pondweed population is known, but tuber size is not. For example, tuber number concurrently formed is 10. According to Figure 4, tuber size would be 0.12 g DW tuber^{-1}.

This requires the following entries in the MODEL.DAT file used as Input for POTAMv 2.0:

Under the 'Initial constants' section:

INTUB = 0.12

Under the 'Model parameters' section:

NINTUB = 10.
SURPER = 32.4 (0.12 (INTUB) x 10 (NINTUB) x 27 (nominal SURPER-value)
TWCTUB = 36. (0.12 (INTUB) x 10 (NINTUB) x 30 (NPL, nominal value)

EXAMPLE 2: Changes in anchorage depth of sago pondweed populations

Sago pondweed populations occur in a wide variety of water bodies and anchorage depths. Moreover, water levels may change annually, seasonally, or daily, considerably changing the available space as well as the physical (light, current velocity) and chemical (carbon) environment for the plants. The versions 2.0 of POTAM and VALLA accommodate daily changes in water level.

This run is started from tubers alone; i.e. no green plant weight, a default tuber bank density (i.e. 240 tubers m^{-2}), and a default tuber size (of 0.083 g DW tuber^{-1}). However, the values for measured water depths (DPTT) under the section 'AFGEN functions' have to be changed (1.3 m is default).

This requires the following entries in the MODEL.DAT file used as Input for POTAMv 2.0:

Under the 'AFGEN functions' section:

A. In a water body with an annually changing water depth of 0.2 m

DPTT = 1., 0.2, 365., 0.2

B. In a water body with a seasonally changing water depth (important for reservoirs and flood-prone, riverine, environments).

DPTT = 1., 0.2, 3., 0.5, 10., 1.0, 365., 0.2

Data pairs have to be entered, by giving first the Julian day no followed by '.,' and subsequently the value of the water depth at that day followed by ','.

EXAMPLE 3: Changes in water transparency within sago pondweed populations

Sago pondweed populations occur in a wide variety of water bodies with their typical water transparency patterns. Water transparency in these waters may change considerably annually, seasonally, or daily, changing the available light for the plants. The versions 2.0 of POTAM and VALLA accommodate daily changes in water transparency.

This run is started from tubers alone; i.e. no green plant weight, a default tuber bank density (i.e. 240 tubers m^{-2}), and a default tuber size (of 0.083 g DW $tuber^{-1}$); however, the values for measured water transparency expressed as light extinction coefficients (LT) under the section 'AFGEN functions' have to be changed (range 0.77 to 5.00 m^{-1} is default).

This requires the following entries in the MODEL.DAT file used as Input for POTAMv 2.0:

Under the 'AFGEN functions' section:

LT = 1., 2.0, 10., 2.5, 150., 3.0, 365., 2.0

Data pairs have to be entered, by giving first the Julian day no followed by '.,' and subsequently the value of the water depth at that day followed by ','.

Appendix E
Additional Data on Environmental Variables at Monitoring Stations Used to Complete Input Files for the Aquatic Plant Growth Simulations

Day No.	Water Temperature °C	Water Depth ms	Current Velocity m s^{-1}	Secchi Disk Depth m	Light Extinction Coefficient Water Column m^{-1}
Lawrence Lake					
2002					
14	0.8	1.63	0	1.63	1.01
22	0.4	1.58	0	1.58	1.04
36	0.6	1.55	0.02	1.55	1.06
52	0.7	1.68	0.03	0.80	2.06
77	3.8	1.74	0	0.97	1.70
94	4.5	1.82	0	0.89	1.85
108	18.3	2.59	0	0.73	2.26
123	13.7	1.96	0	1.26	1.31
136	16.1	2.17	0	1.23	1.34
149	24.0	1.70	0	1.70	0.97
157	22.3	1.84	0.02	0.94	1.76
Point of Inflow Pool 8 (used for Turtle Island)					
2001					
11	0.2	6.0	0.23	1.96	0.84
37	0.2	5.9	0.22	1.91	0.86
67	0.2	5.9	0.21	1.98	0.83
95	5.1	6.5	0.68	0.67	2.46
108	5.9	9.8	-	0.36	4.58
123	12.8	8.8	1.34	0.57	2.89
151	17.4	7.6	0.98	0.62	2.66

(Continued)

Day No.	Water Temperature °C	Water Depth ms	Current Velocity m s^{-1}	Secchi Disk Depth m	Light Extinction Coefficient Water Column m^{-1}
Point of Inflow Pool 8 (used for Turtle Island) (cont.)					
2001					
178	24.4	6.7	1.10	0.50	3.30
204	27.0	4.5	0.54	0.85	1.94
235	23.8	5.7	0.47	0.88	1.87
261	18.4	4.9	0.37	0.80	2.06
289	-	4.9	0.35	0.75	2.20
317	8.1	5.2	0.38	0.85	1.94
347	2.9	6.2	0.68	0.83	1.99
Channel Border Pool 13					
2001					
11	0.1	1.10	0.14	1.10	1.50
24	0.1	1.08	0.13	1.08	1.53
38	0.1	1.06	0.11	1.06	1.56
50	0.1	0.98	0.10	0.98	1.68
65	0.1	1.00	0.12	1.00	1.65
81	2.7	1.15	0.15	1.15	1.43
94	5.7	1.08	0.16	0.45	3.67
108	8.2	2.70	0.38	0.30	5.50
123	16.1	3.30	0.47	0.40	4.13
135	17.0	3.01	0.48	0.42	3.93
148	16.9	1.00	0.41	0.36	4.58
166	23.6	1.18	0.31	0.40	4.13
178	24.8	1.12	0.29	0.38	4.34
192	27.9	0.85	0.17	0.50	3.30
208	25.8	1.07	0.18	0.55	3.00
189	29.8	1.14	0.10	0.42	3.93
202	23.1	1.02	0.11	0.34	4.85
247	24.3	1.08	0.13	0.34	4.85
263	19.5	1.08	0.04	0.30	5.50
274	16.5	1.05	0.11	0.36	4.58
289	12.2	1.08	0.10	0.40	4.13
302	7.6	0.96	0.04	0.42	3.93
319	10.0	1.08	0.08	0.48	3.44
332	7.2	1.08	0.15	0.68	2.43
346	5.5	1.08	0.19	0.58	2.84